Universidade de Aveiro Departamento de Engenharia Cerâmica e do Vidro
Ano 2012

CLARA PICCIRILLO

DEPOSIÇÃO QUÍMICA EM FASE VAPOR DE FILMES FINOS DE VO_2 TERMOCRÓMICOS

CHEMICAL VAPOUR DEPOSITION OF VANADIUM OXIDES THERMOCHROMIC THIN FILMS

Universidade de Aveiro Departamento de Engenharia Cerâmica e do Vidro
Ano 2012

CLARA PICCIRILLO

DEPOSIÇÃO QUÍMICA EM FASE VAPOR DE FILMES FINOS DE VO_2 TERMOCRÓMICOS

CHEMICAL VAPOUR DEPOSITION OF VANADIUM OXIDE THERMOCHROMIC THIN FILMS

Tese apresentada à Universidade de Aveiro para cumprimento dos requisitos necessários à obtenção do grau de Doutor em Ciência e Engenharia de Materiais.

I dedicate this work to all my family and to Rob, for all the support they gave me in all these years.

o júri

presidente

Prof. Doutor Maria Celeste Silva do Carmo
Professora Catedrática do Departamento de Física da Universidade de Aveiro

Prof. Doutor Joaquim Manuel Vieira
Professor Catedrático do Departamento de Engenharia Cerâmica e do Vidro da Universidade de Aveiro

Prof. Doutor Vasco Manuel Pinto Teixeira
Professor Associado da Escola de Ciências da Universidade do Minho

Prof. Doutor Pedro Manuel de Melo Bandiera Tavares
Professor Associado da Universidade de Trás-Os-Montes e Alto Douro

Prof. Doutor Isabel Maria das Mercês Ferreira
Professora Auxiliar da Faculdade de Ciências e Tecnologia da Universidade Nova de Lisboa

Doutor Filipe José Alves de Oliveira
Investigador Axiliar da Universidade de Aveiro

agradecimentos

I would like to thank Prof. Ivan Parkin, Dr. Russell Binions, Dr. Cristopher Blackman and Dr. Robert Palgrave for their help and support in the this work.

palavras-chave

Óxido de vanâdio, Termocrómico, Filmes finos, Deposição Quimica em fase Vapor (CVD).

resumo

Os materiais termocrómicos exibem alterações das suas propriedades ópticas, tais como a transmitância ou a reflectância, com a variação da temperatura. Um material inteligente ideal permite a passagem da radiação solar através uma janela quando está frio, mas reflecte a mesma radiação quando está calor. A variação destas propriedades é frequentemente associada a uma transição de fase, a qual ocorre a uma temperatura definida e que, normalmente, é reversível. Estes materiais são geralmente utilizados como filmes finos em vidros de janelas.

Nesta tese apresenta-se o desenvolvimento de filmes finos de óxido de vanâdio (IV) (VO_2) termocrómicos – não dopados e dopados com tungsténio, nióbio e nanopartículas de ouro – que podem ser utilizados como revestimentos para o controle da passagem da radiação solar. Os filmes foram processados recorrendo à deposição química em fase vapor (CVD), com a técnica “atmospheric pressure” (APCVD) melhorada, e as novas tecnicas “aerosol assisted” (AACVD) e híbrida (AP/AACVD).

Foram também estudados os efeitos dos dopantes na temperatura de transição metal – semiconductor, e na transmitância e reflectância dos filmes. O desenvolvimento de materiais termocrómicos baseados em VO_2 com propriedades optimizadas aumentou significativamente a compreensão dos mecanismos associados ao comportamento termocrómico.

keywords

Vanadium (IV) oxide, Thermochromic, Thin Films, Chemical Vapour Deposition.

abstract

Thermochromic materials change optical properties, such as transmittance or reflectance, with a variation in temperature. An ideal intelligent (smart) material will allow solar radiation in through a window in cold conditions, but reflect that radiation in warmer conditions. The variation in the properties is often associated with a phase change, which takes place at a definite temperature, and is normally reversible. Such materials are usually applied to window glass as thin films.

This thesis presents the work on the development of thermochromic vanadium (IV) oxide (VO_2) thin films – both undoped and doped with tungsten, niobium and gold nanoparticles – which could be employed as solar control coatings. The films were deposited using Chemical Vapour Deposition (CVD), using improved Atmospheric Pressure (APCVD), novel Aerosol Assisted (AACVD) and novel hybrid AP/AACVD techniques. The effects of dopants on the metal-to-semiconductor transition temperature and transmittance/reflectance characteristics were also investigated.

This work significantly increased the understanding of the mechanisms behind thermochromic behaviour, and resulted in thermochromic materials based on VO_2 with greatly improved properties.

Index

List of Figures.

Summary

The work presented here is on the deposition of vanadium (IV) oxide (VO_2) thin films – undoped and doped – which could be employed as solar control coatings. The films were deposited using Chemical Vapour Deposition (CVD) methodology.

In section 1, a brief review of the state of the art at the time this work was carried out is given. Firstly, the topic of solar control coatings is introduced, with particular attention given to thermochromic coatings. Subsequently, vanadium (IV) oxide and its properties are described, mainly in relation to its possible use as a solar control coating. Details are given about its metal-to-semiconductor transition, and how the temperature of this transition can be changed (presence of dopants or strained microstructure). Then a description of the work previously done with vanadium (IV) oxide is given, especially with Chemical Vapour Deposition (CVD). More details about CVD – the principles, how it works and some examples of applications – will be described. Finally, some background will be given about gold nanoparticles and their optical properties.

In section 2, some of the issues still affecting the use of vanadium (IV) oxide as solar control coatings will be discussed.

In section 3, the work performed by Clara Piccirillo will be presented. Firstly, an outline of the research will be given, specifying the role of Clara Piccirillo. Then, each of the published articles will be described, highlighting the most important findings.

In section 4, a summary of the results achieved is presented.

In section 5, a description of how the work was successively continued is given, with particular attention to the contribution given by the research of Clara Piccirillo.

1. State of the art: vanadium (IV) oxide, its properties, and the work done so far

1.1 Solar control coatings

Solar control coatings are thin films applied on windows to control the amount of heat getting into a room, or escaping from it; as a consequence, the room's temperature will be controlled. With the use of an appropriate coating on window glazing, we can have a more comfortable environment, neither too hot nor too cold. At the same time, there will also be a reduction in energy consumption associated with the heating or the cooling of the environment itself.

The simplest solar control coatings are based on a material suitable for only one kind of climate. In climates that are cold for the majority of the time, for instance, one or more transparent insulating layers can be applied on a window, to minimise the heat exchange between the inside and the outside environment. This will limit the dispersion of the heat generated inside by artificial heating or by black body radiation; there will be, therefore, a reduction the energy used for heating the place. In a mainly hot environment, on the contrary, thin films with very high infrared reflectance can be applied to the glass of a window; in this way, most of the energy from the sun will be reflected, keeping the room temperature cool. This will minimise the use of air conditioning, thus reducing the energy consumption associated with it (Granqvist, 2003 and reference therein).

This approach, however, is not suitable for many locations such as central Europe or North America; in these cases, very cold winters and very hot summers require a different coating, capable of performing both of the functions described above. Window coatings made with thermochromic materials are the ones which can fulfil these requirements.

Thermochromic materials are part of the larger class of "smart" or intelligent materials. A material is defined smart when it changes its properties depending on the external conditions. In the specific case of thermochromism, the material behaviour changes with a different temperature; optical properties such as transmittance or reflectance, for instance, can vary remarkably at higher or lower temperatures. The variation in the properties is normally associated with a phase change, which takes place at a definite temperature; the phase change is normally reversible.

Figure 1 (Jin, 2000) shows the behaviour of a thermochromic coating, when applied on a window. At temperature values lower than the transition temperature (Tc) the material shows a low reflectance; therefore the solar radiation and the heat associated will not be reflected, but will reach the inside environment. Above the transition temperature, however, the reflectance will be higher; therefore, part of the energy from the sun will be reflected. With this behaviour, the heat gain from the sun and the black body radiation inside the building will be maximised in winter; in summer, on the contrary, the solar heat gain will be dramatically reduced. The use of these coatings will provide a comfortable temperature all year around, and at the same time, substantial energy savings can be achieved.

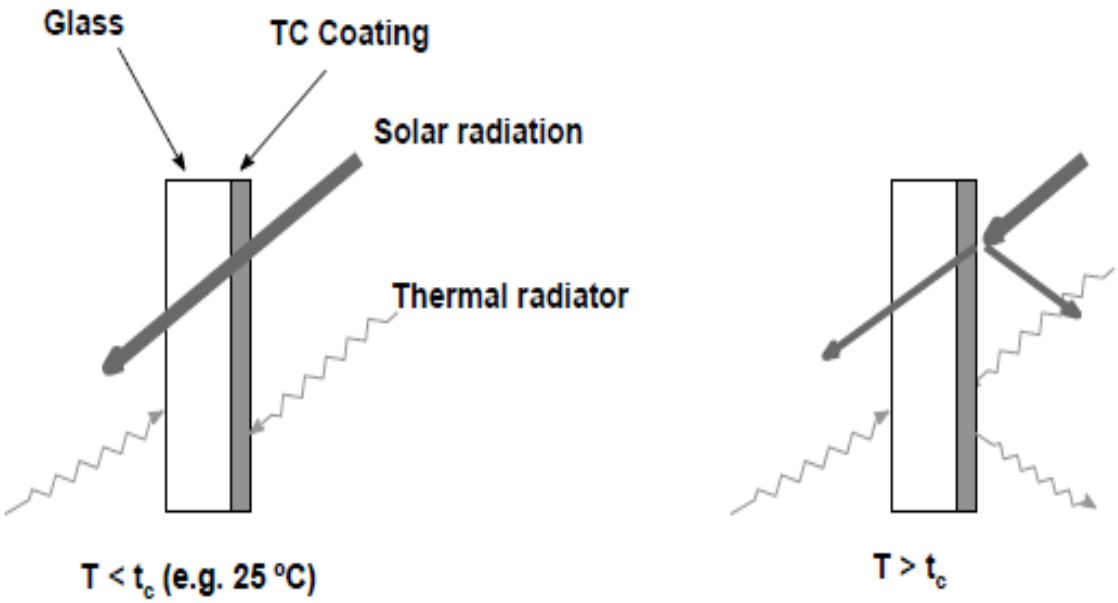

Figure 1. Behaviour of a thermochromic coating on a window. Note: the drawing is not to scale.

An ideal thermochromic coating should be highly transparent in the visible region; in this way all the visible light from the sun can enter the building, without any reduction in visibility, and reducing the necessity for artificial lighting.

Additionally, the variation in its optical properties in the infrared region associated with the phase change should be as high as possible. A great increase in its reflectance above the transition temperature, for instance, will lead to a substantial decrease in the

solar energy entering the building, keeping the inside temperature lower. If the change in the reflectance is smaller, however, the whole process will be less effective.

Another important parameter for a thermochromic coating is the value of its transition temperature: for the film to be employed as a solar controller on window, the transition should take place for values close to room temperature, preferably between 20 and 25°C.

For some of its characteristics, vanadium (IV) oxide could be used as solar control coating; in the next section this material and its properties will be described in detail.

1.2 Vanadium (IV) oxide and its phase transition

Vanadium is a transition metal showing different possible oxidation states; the most common ones are (III), (IV) and (V), whose corresponding oxides are V_2O_3, VO_2 and V_2O_5 respectively.

In recent years, there has been an increasing interest in studying vanadium (IV) oxide: in fact, because of its properties, it has several technological applications in fields such as optics and electronics. The most important characteristic of vanadium (IV) oxide is its thermochromic behaviour, as its optical and electrical characteristics are different depending on the value of the temperature.

The change in these properties is associated with a phase transition in the vanadium (IV) oxide structure, more exactly a Metal-to-Semiconductor Transition (MST). At room temperature, vanadium (IV) oxide is stable in the monoclinic structure (M), which has the characteristics of a semiconductor. At high temperature, on the contrary, the rutile structure (R) is more favoured; this structure behaves as a semimetal. This transition takes place at 68°C, and it is completely reversible (Morin, 1959; Manning, 2002).

The two structures are shown in Figures 2 (a) and (b) below.

In the monoclinic structure, the V^{4+}–V^{4+} pairing alternates at shorter (0.265 nm) and longer (0.312 nm) distances along the monoclinic *a* axis. The cell parameters are a = 5.75 Å, b = 4.52 Å, c = 5.38 Å and β = 122.60º. The rutile phase has a tetragonal structure, with equidistant vanadium atoms (0.288 nm) in chains of edge sharing [VO_6] octahedra; the cell parameters are a = 4.55 Å and c = 2.85 Å. On passing through the MST, the (100) planes of vanadium atoms in the monoclinic phase shift by 0.043 nm parallel to (001). This shift causes the breaking of the V^{4+}–V^{4+} pairs to form a tetragonal phase, allowing metallic conductivity. In the diagram of the monoclinic phase (Figure 2a), the V^{4+}-V^{4+} alternate

spacing can be observed, together with the structure distortion along the *a* axis (Roger, 1993).

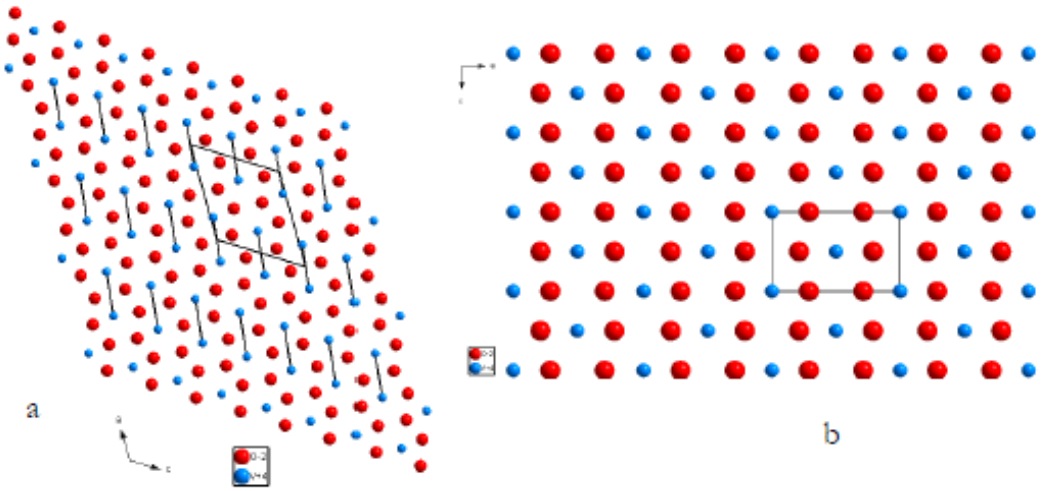

Figure 2. Monoclinic (a) and rutile (b) structures for vanadium (IV) oxide viewed along the *b* axis. The oxygen atoms are the red dots; in the monoclinic structure, the V-V pairs are indicated.

The monoclinic structure behaves as a wide band gap semiconductor, showing very high resistivity and a very low reflectance. The rutile structure, on the contrary, is an electrical conductor, with much higher reflectance, especially in the infrared. In the visible region, however, the difference is much smaller - in some cases there is almost no change at all. Both below and above the transition temperature, vanadium (IV) oxide absorbs in the visible; this gives the material a brown-yellow colour.

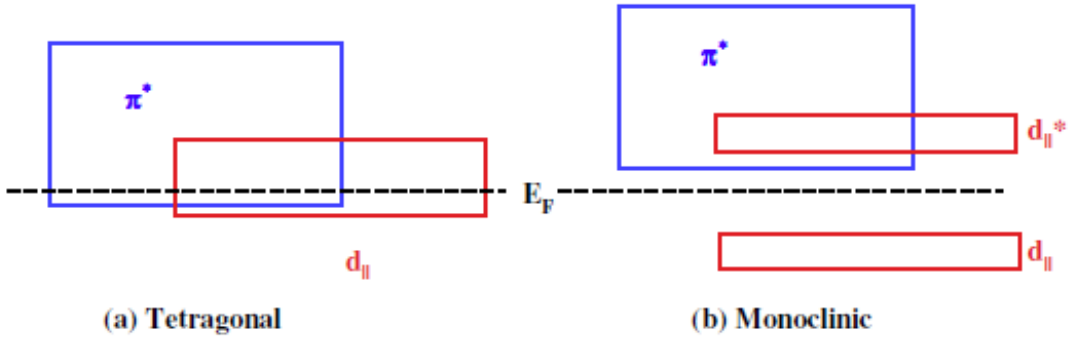

Figure 3. Band structure scheme for (a) tetragonal and (b) monoclinic vanadium (IV) oxide. E_F indicates the Fermi level.

The nature of the MST for vanadium (IV) is not completely understood. The most accepted explanation is based on models using the molecular orbitals theory (Goodenough, 1971); Figure 3 shows the band structure scheme for the two vanadium (IV) oxide forms (Adler, 1967). It can be seen how, for the monoclinic structure, there is an energy gap between the d|| orbitals, due to V-V pairs resulting from overlap of dx2- y2 atomic orbitals. This feature is not present in the rutile structure, due to the absence of the V-V pairing.

According to this theory, vanadium (IV) oxide has two transition temperatures, T_c and T_c'; the first one is due to an anti-ferroelectric distortion, while the second is caused by crystallographic distortion. The values of these two temperatures are coincident. The theory was confirmed later (Eyert, 2002), with calculations made using density functional theory.

When going from low to high temperature, and vice versa, cycled from one phase to the other, vanadium (IV) oxide shows a hysteresis behaviour. This happens for phase transitions where some regions of the material have already undergone to the complete transition while others have not. These are first-order transitions, where a latent heat is necessary for the transition to happen, which cannot be transferred immediately from the materials to the surroundings and vice versa.

More recently, it has been reported that the MST for vanadium (IV) oxide thin films can also be induced by applying an electric field (Lappaleinen, 2008 and reference therein). These characteristics make vanadium (IV) oxide a suitable material not only for solar control coatings, but also as optical shutters, switches for optical communication systems and electrical switches for electronics.

1.3 Change in the value of the transition temperature

As mentioned above in section 1.1, for a material to have a practical use as a solar control coating, the MST has to take place at a temperature lower than 68^{o}C, the value for vanadium (IV) oxide. Studies performed on this material showed that it is possible to change its Tc value by doping the material. With the use of appropriate elements, the temperature at which the MST takes place can either be increased or lowered.

Experimental data showed that metals with a valence lower than V(IV) cause an increase in the transition temperature; examples of this are trivalent ions such as Cr(III) or

Al(III). Using metals with a higher valence, on the contrary, causes a decrease in the Tc value; this can be achieved with metals such as W(IV) and Nb(V) (MacChesney, 1967).

Although these data were confirmed, the way doping causes the change in the value of the transition temperature it is still not completely clear. One hypothesis is that, in the presence of the dopant, the material has a second semiconducting phase between the two monoclinic and tetragonal phases. The additional semiconducting phase has a different structure, depending on the valence of the dopant ion: it has either an orthorhombic or a rutile structure, for low- and high-valence ions, respectively (Goodenough, 1971). According to this theory, ions such as tungsten (VI), niobium (V) or F^- destabilise the anti-ferroelectric state with the introduction of extra π^* electrons; this causes a decrease in the anti-ferroelectric transition temperature, Tc. The opposite happens with low-valence ions, which stabilise this state and, therefore, increase the Tc value. For elements like titanium (IV) d0, the mechanism is different, as they can cause a decrease in the crystallographic transition temperature, Tc´. These hypotheses were confirmed by subsequent work (Tang, 1985; Netsianda, 2008).

In the next paragraphs, some published results about the effect of dopants on the transition temperature are given. They are limited to a period up to the year 2008, when Clara Piccirillo completed her research in this field.

Considering the decrease in the transition temperature, the best results were achieved employing W(VI) as dopant. Published data showed that W(VI) caused the greatest reduction in the temperature per atom % present in the vanadium (IV) oxide lattice, in the order of between 20 and 25^{o}C. This was observed for films prepared with different methodologies, such as sol-gel, Physical Vapour Deposition (PVD) and Chemical Vapour Deposition (CVD) (Béteille, 1998; Burkhardt, 1999; Jin, 1998; Manning, 2004c).

Other elements were also used, even if they were less effective in terms of temperature decrease; molybdenum, iron and fluorine, for instance, were employed for films deposited with the PVD method. Co-doping of tungsten and fluorine was also performed with this technology (Burkhardt, 2002); these results were particularly interesting, as an increase in the visible transmittance was observed together with a decrease in the transition temperature. As for the sol-gel technique, vanadium (IV) oxide thin films were deposited with gold, niobium and molybdenum as dopants; co-doping of

molybdenum and tungsten was also reported (Cavanna, 1999; Greenberg, 1983; Hanlon, 2003; Takahashi, 2001; Jiazhen, 2008).

In some cases the presence of the dopant into the lattice did not affect just the Tc value, but also the width of the hysteresis loop. This happened, for instance, for vanadium (IV) oxide deposited by the sol-gel method, co-doped with tungsten and titanium; these thin films showed almost no hysteresis loop (Takahashi, 2001). Doping with fluorine, on the other hand, had the opposite effect, broadening the width of the loop (Phillips, 1998).

A decrease in the transition temperature was also observed for some undoped vanadium (IV) oxide thin films. Films prepared with different techniques, with thickness of less than 200 nm, showed lower Tc values (Cavanna, 1999; Maruyama, 1993). A possible explanation for this decrease is that intrinsic stresses in the film crystallites cause the reduction in the temperature (Case, 1984); this could be due to the mismatch with the substrate. The stress induced by the substrate will be more important for thinner films, while it will not have much influence on a thicker coating. When stress was induced with low-energy ion bombardment, vanadium (IV) oxide thin films showed a lower transition temperature. According to Rakotoniaina (Rakotoniaina, 1993), the presence of tungsten caused strain in the lattice of vanadium (IV) oxide thin films, and this led to a decrease in the transition temperature.

The strain in the lattice structure, and its effect on the value of the thermochromic transition, is not a well-understood phenomenon, and it needs a more complete and systematic investigation.

1.4 Techniques to produce vanadium (IV) oxide thin films

The most common methodologies to prepare vanadium (IV) thin films are sol-gel, Physical Vapour Deposition (PVD) and Chemical Vapour Deposition (CVD). In this section, literature data is given for both sol-gel and PVD techniques; as above, the reported results are limited to a period up to the year 2008. The CVD methodology, on the other hand, is described in more detail in the next section, as it is the technique used by Clara Piccirillo during her research.

The sol-gel method has been successfully used to prepare undoped and doped vanadium (IV) oxide thin films (Lu, 1999; Livage, 1999; Hanlon, 2002; Zhao, 1999; Takahashi, 1996 and 2001; Pan, 2004; Jiazhen, 2008). With this technique, a substrate is dip- or spin-coated with a solution of a suitable vanadium precursor (alkoxides or

polyvanadates); subsequently the covered substrate undergoes a treatment to form the film – generally a partial hydrolysis of the coating and heating in a reduced atmosphere. The main advantage of the sol-gel method is its simplicity; furthermore, it is easy to obtain films with uniform thickness. The exact stoichiometry of doped or multi-component films is also easily achieved, by controlling the composition of the depositing solutions. Deposition precursors, however, may be expensive; furthermore, the use of this technique for large areas of glass is not always easy, adding additional costs to the process.

Physical Vapour Deposition (PVD) methodology was also widely employed to deposit vanadium (IV) oxide thin films. In PVD, atoms or molecules are vaporised and removed from a target in vacuum conditions. The vaporised species are then transported inside a chamber and deposited by condensation on an appropriate substrate. The deposition of multi-component or doped films can be performed by using more than one target; the relative composition of each component can be controlled with the use of targets of different sizes. The removal of the atoms from the target can be performed in different ways, such as laser ablation, plasma, DC and RF magnetron sputtering, or ion beam sputtering. Literature reports several vanadium (IV) oxide films deposited with these methods, both pure and doped (Saitzek, 2007; Cui, 2008; Kana, 2008a; Kana, 2008b; Nihei, 2008; Burkhardt, 2002; Aliev, 2004; Maaza, 2005). The films deposited with PVD normally show good characteristics and properties; it is, however, not practical to use it in an industrial application. In fact, the deposition equipment is very expensive, and performing the process has high costs too, due to the use of low pressure. Furthermore, the deposition rates are always slow; another problem is also that only a limited area of the glass that can be coated, due to the dimensions of the chamber. All these issues make the process unsuitable for an industrial application.

1.5 Chemical Vapour Deposition

Chemical Vapour Deposition (CVD) is a methodology to deposit a solid thin film with a chemical reaction on a substrate from gas phase precursors. The CVD technique is widely used at an industrial level for the production of many important products. Thin films of silicon for the micro electronic industries or synthetic diamonds, for instance, are all produced by CVD. It is also already extensively used in the glass industry, for glass coatings; Activ and K-Glass are examples of coated glass produced by CVD.

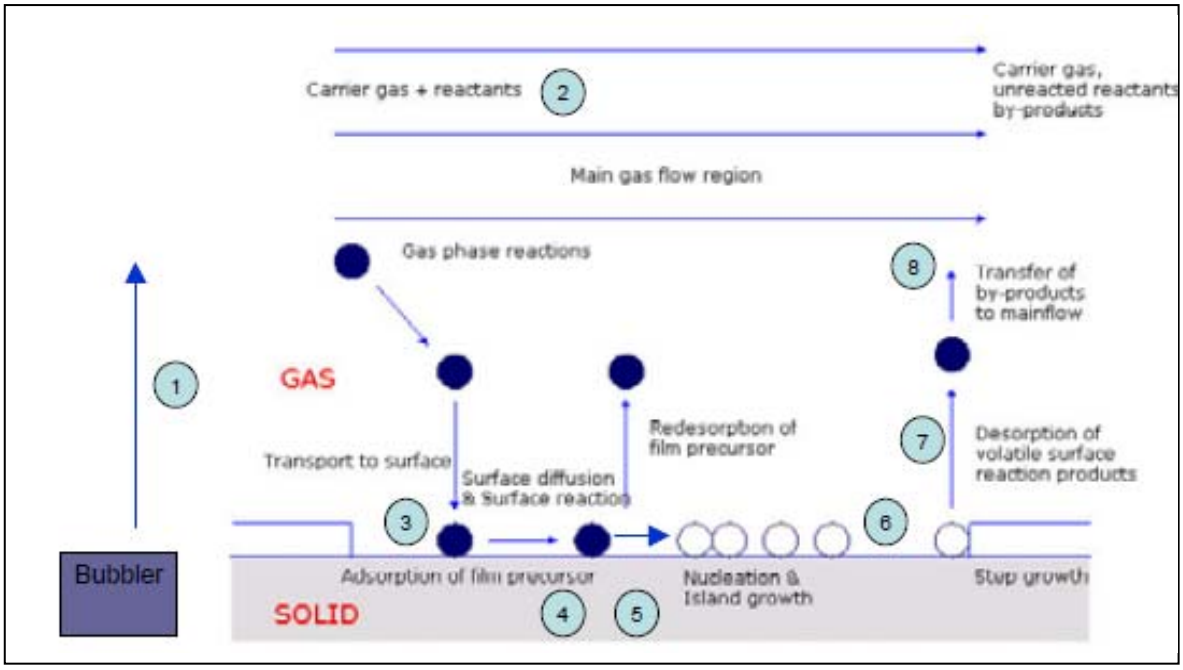

Figure 4. Schematic of the steps taking place during CVD deposition. (1) Generation of active gaseous species of suitable precursor(s); (2) Transport of the precursor(s) into the reaction chamber; (3) Adsorption on the hot solid surface; (4) Decomposition of the precursor to give the atom needed for the film, and waste; (5) Migration of atoms to a strong binding site; (6) Nucleation that leads to the growth of the thin film; (7) Desorption of unwanted side products; (8) Removal of unwanted products.

For a reaction to happen in a CVD process, suitable precursors have to be used; the characteristics/limitations of the precursors depend on the type of CVD technique employed (more details will be given below). The deposition takes place on a substrate made of an appropriate material, which is normally placed inside a reaction chamber (or reactor); Figure 4 shows the most important steps taking place during a CVD deposition process (Hitchman, 1993).

The precursors are carried into the reactor by one or more gas flows; in many cases this gas functions only as a carrier, without taking part in the reaction. In such situations, nitrogen is the most common choice, as it is inert, safe to use and inexpensive. In other cases, however, a different and reactive gas can be used, to react with the precursors; an example of this can be the use of a nitrogen–oxygen mixture, if a more oxidative environment is necessary for the reaction to happen, or hydrogen, for a more reducing one.

Inside the reactor, the gaseous precursors come into contact with the substrate; the application of a form of energy (e.g., heat) triggers the chemical reaction(s).

The reaction to form the product can take place in the gaseous phase; there will be, subsequently, an adsorption of the formed solid on the substrate to form the film. Alternatively, the reaction can be heterogeneous and take place directly on the surface of the substrate, with a direct formation of the film.

Often many different processes can take place at the same time, sometimes with the formation of by-products. If they are in the gaseous phase or not adsorbed on the surface of the substrate, they can be transported out of the reactor with the exhaust gases; otherwise they could be included in the film as impurities. To avoid this, it is essential to choose the right deposition precursors and conditions. This is particularly valid for the deposition of vanadium (IV) oxide, as vanadium has different oxidation states; the oxygen partial pressure, for instance, is critical in controlling the phase deposited.

There many different types of Chemical Vapour Deposition processes; they can be classified considering, for instance, the pressure at which they operate (i.e. atmospheric pressure, low pressure), the form of energy given to cause the reaction (i.e. heat, light or plasma), the reactor used (i.e. cold or hot wall, with horizontal or vertical substrate), etc.

The work reported here was performed using Atmospheric Pressure Chemical Vapour Deposition (APCVD), Aerosol Assisted Chemical Vapour Deposition (AACVD) and a combination of these two techniques. Therefore, more explanations will be given for these two methodologies. In both cases a cold-wall reactor, with a horizontal substrate, was used.

APCVD is probably the simplest CVD process, as the deposition chamber is operated at atmospheric pressure and the reaction is initiated by heat, from the high temperature of the substrate. The precursor(s) are generally placed in one or more bubblers; they are vaporised by applying an appropriate temperature to the bubbler(s) and, subsequently, carried into the reactor by a carrier. The main limitation of APCVD is that the precursors have to be volatile compounds, for their vaporisation to happen.

If compared with other CVD methodologies, APCVD is relatively cheap and easy to operate, as it does not require a high level of vacuum or high temperatures. This makes it ideal for industrial applications. However, this technique can present problems if doped or multi-component films have to be deposited; in these cases it is not always easy to

control the relative amounts of each component in the gas phase, and therefore, the final concentrations in the deposited films. This is especially true if the volatilities of the different precursors are significantly different.

In the AACVD process, the precursors are transported into the reactor into an aerosol mist. The precursors (either liquid or solid) are dissolved in an appropriate solvent; from this, the aerosol is generated, normally by ultrasonic atomisation. The main advantage of this methodology is that the precursors do not have to be volatile, but simply soluble in the solvent used to generate the aerosol. This allows the use of non-volatile precursors, which it would not be possible to use otherwise.

The choice of the solvent, however, is crucial to obtain the aerosol, and therefore, deposit a coating with good properties. To generate the aerosol by ultrasonic atomisation, high frequency sounds wave are applied. Depending on the characteristics of the solvent and the frequency applied, the diameter of the droplets will be different; the correlation is given by Lang's equation (Lang, 1962; Hou, 2006):

$$d = 0.34 \cdot \left(\frac{2\pi\sigma}{\rho f^2} \right)^{1/3}$$

In the equation, d is the diameter of the droplet, σ is the surface tension of the solvent, ρ is its density and f is the value of the frequency of the sound waves applied to generate the aerosol.

As with APCVD, the reaction in an AACVD deposition is initiated by the high temperature of the substrate. The conversion of the precursors into the products normally takes place in the aerosol droplets. Subsequently, due to the high temperature of the substrate, the solvent evaporates and the product(s) get adsorbed on the surface of the substrate, to form the film. The deposition process can be very complicated. Similarly to APCVD, in AACVD many different experimental parameters can affect the nature and characteristics of the deposited film. In particular, the nature of the solvent is an element specific to this methodology which can have a great influence on the features of the final product.

AACVD is a methodology which can be easily used at industrial level, due to its simplicity and the relatively low cost to run it. It is the ideal technique for the deposition of doped or multi-component films, as more than one precursor needs to be used; with

AACVD, in fact, generally there is a more direct correlation between the compositions of the precursors' solutions and that of the deposited films.

Figures 5 and 6 show the experimental apparatus used for APCVD and AACVD respectively.

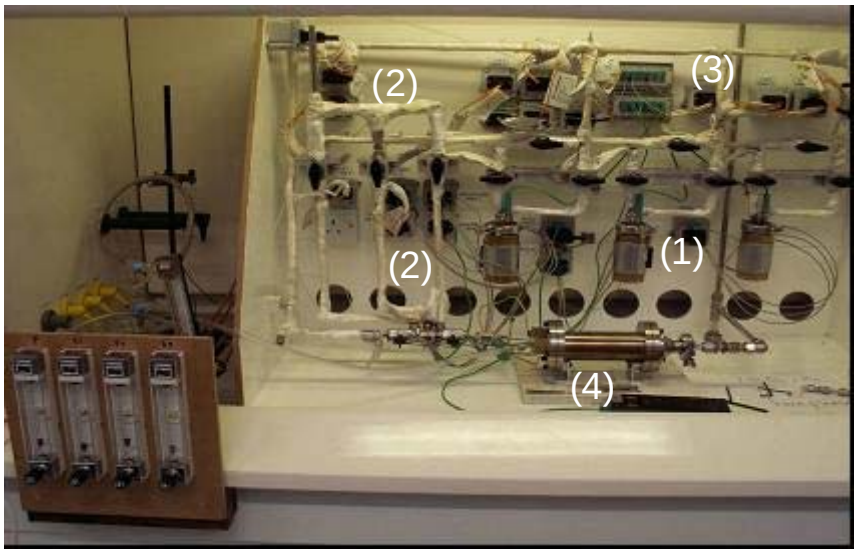

Figure 5. Experimental apparatus for the APCVD process. (1) Bubblers containing the precursors; (2) Gas lines; (3) Temperature controller; (4) Cold wall flat bed reactor.

Figure 6. Experimental apparatus used for the AACVD process. (1) Gas line; (2) Flask containing precursors; (3) Ultrasonic humidifier; (4) Heat controller; (5) Cold wall, flat bed reactor.

1.6 Previous work on vanadium (IV) oxide with CVD methodology

The first data reported for vanadium (IV) oxide films produced by CVD all referred to a two-step process: first, a deposition was performed, which led to the formation of the vanadium (V) oxide coating. Subsequently, a reduction to vanadium (IV) oxide was done,

using an appropriate reducing atmosphere. Depositions with this procedure were carried out with different precursors, such as vanadyl tri(iso-propoxide), vanadyl tri(iso-butoxide), VCl_4 or $VOCl_3$ (Greenberg, 1983; Takahashi, 1989; Field, 2000). For the last two precursors, oxygen sources such as water, ethanol or carbon dioxide were used.

In another two-step deposition, vanadyl acetylacetonate, $VO(acac)_2$, was used to deposit vanadium (IV) oxide in the metastable phase B; this was then converted into the tetragonal phase by annealing at 500^oC in argon (Sahana, 2002a and Shahana 2002b). Vanadium (III) acetonate was also employed for an APCVD deposition process; a slow post-deposition cooling was performed after the deposition (Maruyama, 1993).

More recent work reported the deposition of vanadium (IV) oxide thin films in a single step process, using APCVD. Some of this work was performed at the Chemistry Department of University College London, in the same research group where Clara Piccirillo worked.

Vanadium (IV) chloride (VCl_4) and $VOCl_3$ were both used as precursors, with water as an oxygen source for the deposition. In the first case (VCl_4), different vanadium oxides were deposited, depending on the deposition conditions. For instance, the ratio between VCl_4 and water, and substrate temperature, all had an effect on the phase formed; VO_2, V_2O_5, or V_6O_{13} were detected in the different experiments (Manning, 2002). Similar results, with different formed phases, were also reported in a more systematic study performed by Vernardou (Vernardou, 2006). An analogous pattern was observed when $VOCl_3$ was employed, as different experimental conditions lead to the formation of the different oxides (Manning, 2004b). Vanadium (IV) oxide was obtained, but the deposition was not uniform on the substrates; in fact vanadium (V) oxide (V_2O_5) or an oxide with mixed oxidation states (V_6O_{13}) were detected in some parts of the substrate (Manning, 2004a).

W-doped vanadium (IV) films were also deposited with APCVD. Vanadium (IV) chloride and tungsten (VI) ethoxide were used as precursors, with water as an oxygen source; the results showed a concentration of tungsten up to 1.2 % in the thin films. This led to a decrease in the Tc to a value of 42^oC (Manning, 2004c). Films with higher tungsten concentration were deposited using $VOCl_3$ and WCl_6 as precursors, with water as an oxygen source. In this case, the dopant content was as high as 3.1%; this corresponded

to a transition temperature of 5°C (Manning, 2004a). Films deposited in these conditions could, therefore, be employed as solar control coatings.

1.7 Gold nanoparticles

Metallic gold is an element which shows different properties and behaviour when it has a nanoparticular structure. Features such as chemical reactivity, optical properties and melting point change when the metal is in the form of nanoparticles; the shape and the dimensions of the particles themselves have an effect on these properties.

The synthesis, the properties and the application of gold nanoparticles constitute a very large and important area of research. These nanoparticles can be used in many different fields, such as medicine, industrial catalysis, etc. Gold nanoparticles can also be included in a host matrix, to form a two-phase composite material.

A complete discussion of this topic is beyond the scope of this work and, therefore, it will not be presented here; in literature, the review paper written by Daniel e al. gives a very comprehensive summary of the different aspects of gold nanoparticles (Daniel, 2004). The features reported in this section are only the ones relevant to the research performed on vanadium (IV) oxide thin films by Clara Piccirillo. Hence, the only topics described in details will be the optical properties of the nanoparticles and the synthesis of nanoparticle thin films using AACVD methodology.

Gold nanoparticles have a different structure depending on their size; Figure 7 shows the correlation between their dimensions the corresponding optical properties.

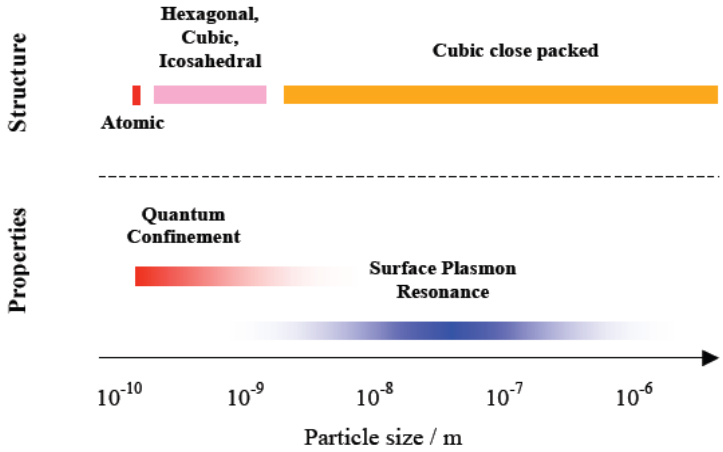

Figure 7. Correlation between size and properties for gold particles.

The diameter of a gold atom is approximately 2.7×10^{-10} m. When the particle size is about 10^{-9} m, the gold atoms are assembled in clusters with a countable number of

atoms. The most common shapes for these clusters are hexagonal, cubic and icosahedral; atoms are arranged in 12-coordinate concentric spherical shells. Nanoparticles with these dimensions show a quantisation of electronic energy levels (quantum confinement).

Particles with greater diameter (between 3 x 10^{-9} and 5 x 10^{-7} m), on the contrary, have a cubic closed packed structure, like in the bulk solid material. At this level, the number of gold atoms is higher and they are not countable anymore. The main feature of the nanoparticles of these sizes is Surface Plasmon Resonance (SPR). For particles with a diameter greater than 5 x 10^{-7} m, SPR is not observed anymore, and the same behaviour as bulk gold is observed.

A surface plasmon (SP) is defined as "a coherent and collective oscillation of free electrons at a boundary between a metal and an insulator" (Ritchie, 1957). Normally, all the free electrons are involved in the excitation at the metal surface (Barnes, 2003). In an ideal metal, completely defect-free, the frequency of the oscillation is only affected by the dielectric property of the material, as no boundary conditions are imposed. For real systems, however, there are boundary conditions; this means that parameters such as the size and the shape of the metal can affect the frequency of the SP oscillation.

A Surface Plasmon Resonance (SPR) is observed when an electromagnetic radiation couples to the SP; this happens when the frequency of the radiation coincides with that of the SP. As a consequence, light will be absorbed at that frequency.

As mentioned above, the resonating frequency of a SP can vary, depending on the characteristics of the nanoparticle; this means that the light absorption will also take place at a different frequency. Solutions of gold particles, for instance, generally show a purple-red colour (see Figure 8); the hue of the colour, however, can change depending on several factors, such as the refractive index of the solvent used, and the shape and dimensions of the particles.

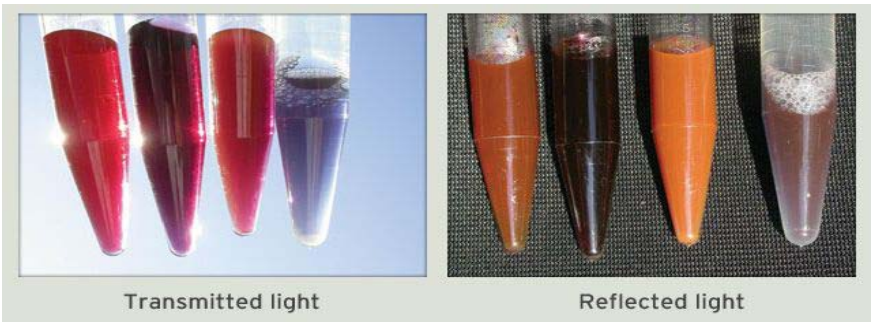

Figure 8. Solutions of gold nanoparticles of different dimensions.

For spherical particles, the maximum in the SPR absorption can change by as much as 200 nm, as a red shift is observed for particles with greater diameter (from about 525 to 750 nm, for particle diameters between 40 and 190 nm). For non-spherical particles, the influence of the size is even more enhanced; in fact, a value of $\lambda_{max} > 1000$ nm was observed for rod-shaped particles (Palgrave, 2007a). The SPR absorption, and therefore the solution colour, however, can also be affected by other parameters, such as the uniformity of the size of the particles.

If gold nanoparticles are deposited as thin films, the SPR is still present. This absorption band will be observed if gold is deposited as pure one-component film, but also if gold nanoparticles are deposited as dopant/minor component inside a host matrix, in a multicomponent material. SPR characteristics, however, will be influenced by several parameters; the most significant ones are the particles' size and shape, the uniformity in the shape of the particles, the dielectric properties of the host matrix, the film thickness and the surface roughness (Link, 2004; Irit, 2007; Luo, 2005).

The synthesis of gold nanoparticles, both in solution and as thin films, was performed using various methods (Daniel, 2004; Palgrave 2007 and reference therein). Here we report the results obtained with AACVD methodology.

Gold nanoparticle thin films were deposited using $HAuCl_4$ as precursor; the presence in solution of some surfactants such as tetraoctylammonium bromide (TOAB), cetyltrimethylammonium bromide (CTAB) or tetraethylammonium bromide (TEAB) resulted in a more uniform distribution of the dimensions of the particles (Palgrave, 2008).

Composite materials of gold nanoparticles with semiconductors were also deposited, using host matrixes such as TiO_2, WO_3 and MoO_3. In all thin films SPR was observed, whose characteristics depended on the refractive index of the host matrix (Palgrave, 2006; Palgrave, 2007b). The colour of the deposited films was influenced by the presence of the nanoparticles, for instance the $Au@TiO_2$ thin film was strongly coloured (blue in transmission and red in reflectance).

2. Improvement of vanadium (IV) oxide properties

As reported in sections 1.4 and 1.6, the synthesis and properties of vanadium (IV) oxide were widely investigated in recent years. Despite this, however, more work needs to be done to obtain thin films which can be used commercially as solar control coatings. For this to happen, a material with improved characteristics and performance has to be obtained. It is, therefore, essential to understand better the correlation between the microstructure of the films and their properties. Further research on the topic will give a deeper knowledge about vanadium (IV) oxide thin films, helping to develop a more functional material.

Here are some of the issues which have to be considered in the development of a VO_2-based solar control coating.

An important characteristic of this thermochromic material is the extent of the change of its optical properties in the infrared region, when undergoing the MST; this aspect was described in detail in section 1.1. For vanadium (IV) oxide, the results obtained until now are encouraging; however, they have to be improved to achieve a substantial energy saving and make vanadium (IV) oxide thin films worth being used. More investigation is therefore needed, to understand which are the parameters affecting the change of the optical properties.

The width of the hysteresis loop is also a property that can be crucial for the efficiency of solar control in energy saving. In fact, a material with a very wide loop will mean a very slow transition from one phase to the other; this will make the material less suitable for such use. As described in section 1.3, in some cases the presence of dopant had an effect on the width of the hysteresis loop. However, a more systematic investigation is needed, to understand the correlation between the experimental deposition conditions and the width of the loop.

Another aspect which needs to be considered for a window coating is its colour: as mentioned above, vanadium (IV) oxide is yellow-brown; the hue of its colour is not particularly pleasant to look at, and it is not considered acceptable for a coating on a window. In addition to their unpleasant appearance, if applied on a window these films may limit the light going inside a room; this can cause discomfort in the environment. Furthermore, their use may require additional lighting in the buildings were they are

employed; in this way, the energy saving associated with their use may be annulled or greatly reduced.

To use the material as a window coating, the process used for its synthesis has to be simple and effective, and it has to produce films that are stable and durable. Furthermore, considering its application on a bigger scale, it has to be easily scaled up from the laboratory to an industrial scale. As highlighted in section 1.5, Chemical Vapour Deposition is the ideal technique for this; the deposition conditions, however, have to be optimised. It would be also important to perform the deposition process using non-chlorinated, more environmentally friendly precursors.

3. Work presented by Clara Piccirillo

3.1. Research institution and topic

Clara Piccirillo's research into vanadium (IV) oxide and its application as a thermochromic material was performed in the Chemistry Department of University College London (UK). She worked there as experienced researcher between October 2005 and December 2008, under the supervision of Prof. Ivan P. Parkin.

The main theme of the work was the use of Chemical Vapour Deposition methodology to prepare undoped and doped vanadium (IV) oxide thin films. This technique was chosen considering its feasibility for scale-up to industrial production; furthermore, the group of professor Parkin had already the knowledge, the experience and the facilities to perform the experimental work (see section 1.6). The two main research lines were:

- The use of AACVD to synthesise vanadium (IV) oxide thin films, both undoped and doped. This technique had never been used before for this kind of material. The elements used as dopants were limited to W(VI) and Nb(V), considering the results reported in literature (see section 1.3).
- The optimisation of the deposition processes using the APCVD methodology: the results previously obtained by Professor Parkin's group were considered as a guideline to improve the characteristics and the properties of the films.

The work addressed some of the features highlighted above to improve the performance of vanadium (IV) oxide as solar control coating. In particular, the main targeted issues were:

- The use of chlorine-free precursors, for both APCVD and AACVD.
- The improvement of the change of the optical properties of the material with the MST.
- A significant change in the colour of the films, to make them usable as window coatings, with the inclusion of gold nanoparticles into the vanadium (IV) oxide lattice.

3.2 Contribution given by Clara Piccirillo

During her period at University College London, Clara Piccirillo worked together with several colleagues of the same department: Dr. Russell Binions and Dr. Christopher Blackman, both post-doc researchers, and Mr. Robert Palgrave, a PhD student until

September 2007. For this reason, they are co-authors in the papers and the conference presentation written and/or given during this period.

Considering the experimental work she performed, her main tasks were the use of AACVD methodology – she was the only one working with this technique to deposit vanadium (IV) oxide – and the characterisation of the deposited films. For characterisation, the methods she employed were x-ray diffraction, Raman spectroscopy, SEM/EDX, water contact angle measurements and UV-Vis-IR measurements of transmittance and reflectance. Regarding this last technique, a new spectrometer (Perkin Elmer lambda 950) was purchased by her group when she started her research. She became responsible for it, dealing with its maintenance, doing measurements for/with other people, and analysing and interpreting the data.

As she performed the deposition of all the thin films via AACVD, and most of the characterisation, she was the first author on the papers written on the AACVD technique.

As an experienced researcher, however, Clara Piccirillo was involved not only in this experimental part of the work, but also in many other aspects. She actively contributed to the development of other parts of the project, such as the deposition of vanadium (IV) oxide thin films with the APCVD technique. In fact, she was involved in the planning of the experiments to be performed, in the discussion and understanding of the results and in the decision on how to continue the work. This was done by holding regular meetings with her co-workers and her supervisor; the various aspects of the experimental work and the possible meanings of the results were discussed. Furthermore, she also performed many analyses of the samples prepared by APCVD; in particular, she dealt with Raman spectroscopy and UV-Vis-IR transmittance/reflectance measurements, both measuring the samples and interpreting the data. Although not having directly synthesised the APCVD samples, Clara Piccirillo had a major intellectual input into the papers in this area.

As she was fully engaged in every scientific aspect of the project, she had her name in all the articles published on the topic of APCVD. However, she was not the first author, because she did not do the actual deposition of the vanadium (IV) oxide coatings.

Much of the work of Clara Piccirillo was performed as a part of a European Network (Thermoglaze); because of this, she also took a major part in the management of the project. She prepared project reports, liaised with the other partners of the network, organised meetings with them and presented results at these project meetings.

3.2. Published papers

The work performed by Clara Piccirillo resulted in 7 publications in peer reviewed journals. In this section, a presentation of each article is reported: a short summary will be given, highlighting the most important findings and elements of novelty.

Based on the topics covered, they are divided into 4 subgroups: (a) papers reporting work with AACVD, (b) papers reporting work with APCVD, (c) papers reporting work with combined AACVD and APCVD, (d) other publications. Within each subgroup, the articles are reported considering the sequential order in which the research was performed, and not the by the publication date of the papers.

(a) Papers reporting work with AACVD

- C. Piccirillo, I.P. Parkin, R. Binions: "Synthesis and Functional Properties of Vanadium Oxides: V_2O_3, VO_2, and V_2O_5 Deposited on Glass by Aerosol-Assisted CVD." *Chem. Vap. Depos.*, **13**, 145-151, (2007).

  The results reported in the paper show how the experimental conditions of AACVD can influence the nature of the compound formed. This is a particularly critical issue for vanadium oxides, as vanadium has different oxidation states.

  The paper shows how the use of different solvents can lead to the formation of different oxides (V_2O_3 with methanol, VO_2 or V_2O_5 with ethanol). It was the first time that this kind of kind of investigation was performed; in fact, previously it was always assumed that the solvent was inert, acting only as a simple carrier of the species into the deposition chamber. This was demonstrated not to be the case.

  It also shows the effects of the flow conditions in the reactor, as using the same reaction precursor and solvent but a different nitrogen flow rate, the phase formed was different (VO_2 or V_2O_5 at 1.5 and 3 L/min respectively).

  These were the first published data about any vanadium oxides prepared by AACVD. Regarding VO_2 and its thermochromic properties, the value of the transition was lower than the one reported in literature (56^{o}C instead of 68^{o}C). This was in agreement with data for films prepared by APCVD (Binions, 2004).

- C. Piccirillo, I.P. Parkin, R. Binions: "Synthesis of W-doped VO_2 by Aerosol Assisted Chemical Vapour Deposition (AACVD)." *Thin Sol. Films*, **516**, 1992-1997, (2008).

This paper reports the preparation with AACVD of VO_2 doped with tungsten.

In this work, the findings described above were used, as a basis to select the optimum experimental conditions for VO_2 deposition with AACVD.

Results showed that tungsten was successfully included in the VO_2 lattice. A linear correlation was observed between the amount of tungsten in solution and that in the films; this confirmed the potential of AACVD for the accurate deposition of doped thin films.

A similar linear correlation was observed between the value of the transition temperature and the tungsten content, Tc reducing with increasing W content. The width of the hysteresis loop, however, was not affected by the amount of dopant included in the film. This work confirmed that tungsten is the most effective dopant for VO_2 for the reduction of the transition temperature, as a W/V atomic ratio of 2 % led to a Tc value of 28^{o}C, making the material suitable for a window coating operating in a continental climate.

All the precursors used were chlorine-free (vanadyl acetylacetonate and tungsten ethoxide); they are, therefore, more environmental friendly. This is an important issue if considering the application of this process at industrial level.

These results were the first to be published about W-doped VO_2 prepared with AACVD.

- C. Piccirillo, R. Binions, I.P. Parkin: "Nb-doped VO_2 thin films prepared by Aerosol Assisted Chemical Vapour Deposition." *Europ. J. Inorg. Chem.*, **25**, 4050-4055, (2007).

  The research reported here is about the synthesis of Nb-doped VO_2 thin films using AACVD. As with the doping with tungsten, the experimental conditions were selected considering the results previously published (see above).

  The dopant (niobium) was successfully included in the oxide lattice, with concentrations as high as 3.7 % (Nb/V atom ratio), and the transition temperature was lowered to 35^{o}C. The use of chlorine-free precursors (vanadyl acetyl acetonate and niobium ethoxide) also makes the process feasible at industrial level.

  The results published here were the first on Nb-doped VO_2 with AACVD. Furthermore, such a high concentration of niobium as a dopant was never reported before in VO_2 made by any method. Despite this, however, this study confirmed that

niobium is less effective as a dopant compared to tungsten. In fact, there is a limit for the amount of Nb dopant that can be included in the film, and the decrease in the transition temperature due to the dopant is smaller than that observed with tungsten.

(b) Papers reporting work with APCVD

- C.S. Blakcman, C. Piccirillo, R. Binions, I.P. Parkin: "Atmospheric Pressure Chemical Vapour Deposition of thermochromic tungsten-doped vanadium dioxide thin films for use in architectural glazing" *Thin Sol. Films*, **517**, 4565 (2009).

  In this paper, a systematic investigation of the performance of VO_2 (undoped and doped) thin films prepared by APCVD is reported. The work was performed to optimise the results previously obtained (Manning, 2004a, b & c), and to have a more complete knowledge on the system.

  Different deposition precursors (VCl_4, WCl_6) and experimental conditions (higher nitrogen flow rates) were used, to improve the reproducibility of the results.

  Undoped VO_2 thin films of different thicknesses were synthesised, to establish a correlation between the films' thickness and their optical properties. The results showed that 70 – 90 nm is the most suitable thickness range for VO_2 thin films. In fact, these coatings show significant transmittance in the visible (about 60 % at 570 nm) and noticeable changes in the optical properties in the infrared.

  W-doped VO_2 coatings were also deposited, with different amounts of dopant included in their structure, the highest concentration being 8.2 atomic %. This corresponded to a transition temperature of -28^{o}C. The film with 1.56 atomic % of tungsten would be the most appropriate as a solar control coating, as its Tc was 20^{o}C.

  W-doped VO_2 thin films showed a change in colour, from brown-yellow towards blue. This effect, however, was more obvious for the highly doped films (tungsten concentration higher than 3 atomic %).

  These results represented a substantial progress in the quality and the performance of the thin films.

- R. Binions, G. Hyett, C. Piccirillo, I.P. Parkin: "Doped and un-doped vanadium oxide thin films prepared by Atmospheric Pressure Chemical Vapour Deposition from vanadyl acetylacetonate and tungsten hexachloride; the effect of

crystallographic orientation of thermochromic properties." J. Mat. Chem., 17, 4652-4660, (2007).

In this work, the influence of the gas flow rate in the APCVD process on the thin film's morphology and properties was investigated.

A mixture of nitrogen and oxygen in the ratio 98:2 was used, and different flow rates (between 5 and 10 L/min) were employed. The results showed a change the transition temperature of undoped VO_2 up to 10^oC; the width of the hysteresis was also affected. The difference in these properties was explained considering the different crystallographic orientation that the different films had.

For W-doped VO_2 films, the flow rate conditions had less influence in the value of the transition temperature. The coatings deposited with these methods, however, showed a bigger change in the infrared transmittance when undergoing the MST transition.

These results were the first published covering the influence of the flow conditions on the film's properties. They confirm the correlation existing between microstructural properties and coating performances.

The use of a chlorine-free vanadium precursor (vanadyl acetylacetonate) made the process more environmentally viable. Also, the appearance of these films was better than the ones deposited before; this is a crucial point for an application as a window coating.

(c) Papers reporting work with combined AP and AACVD

- R. Binions, C. Piccirillo, R. Palgrave, I.P. Parkin: "Hybrid Aerosol Assisted and Atmospheric Pressure Chemical Vapour Deposition of Gold doped Vanadium Dioxide." *Chem. Vap. Depos.*, **14**, 33-39, (2008).

  This paper describes the combination of the two CVD methodologies, AACVD and APCVD, to deposit gold-doped VO_2. These were the first published results on the combined hybrid use of these two CVD techniques.

  VO_2 was deposited using APCVD with vanadyl acetylacetonate as a precursor; the deposition conditions were chosen considering the investigations previously performed and mentioned above. Gold was added into the films with an AACVD process, using $HAuCl_4$ as precursor.

  Gold was detected in the VO_2 structure, between the crystallites, in the form of nanoparticles, for concentrations as high as 1.00 (Au/V atom ratio). The main effect of

the gold doping in the VO_2 matrix was a significant change in colour: from brown-yellow to greenish -blueish, depending on the amount of gold present. This was due to the presence of the Surface Plasmon Resonance band, normally detected in gold nanoparticle thin films (see section 1.6). A reduction in the transition temperature value was also observed (Tc ≈ 52°C), probably due to the strain induced in the lattice.

This was a very important achievement for the use of these films as solar control coatings, as one of the main problems for the commercialisation of VO_2 has always been the unpleasant colour. It showed a very promising way to improve the characteristics of the films; more work on this topic was performed later (see section 5).

(d) Other publications

- R. Binions, C.S. Blackman, T.D. Manning, C. Piccirillo, I.P. Parkin: "Thermochromic coatings for Intelligent Architectural Glazing." *J. Nano Res.*, **2**, 1-20, (2008).

  This article was an invited review, which reports the most important aspects regarding the use of VO_2 thin films as solar control coating. The review covers the thermochromic behaviour of VO_2, the physical principles behind it and the changes associated with its doping. It also gives a summary about the different methods used to prepare VO2 thin films. The main focus is on the work performed at University College London with the CVD methodology, both AP and AA.

3.3 Conference presentations

The work performed by Clara Piccirillo was also presented at national and international conferences; here there is a list of all the conferences presentations, reported in chronological order. There were three oral presentations and a poster. The first three were all presented by Clara Piccirillo; only the last one was given by Dr. Binions, as Clara Piccirillo did not attend the conference.

- C. Piccirillo, R. Binions, I.P. Parkin: "Aerosol Assisted CVD of Vanadium Oxides Thin Films." ***UK CVD Network meeting, London, 5th July 2006, United Kingdom.***
- C. Piccirillo, R. Binions, I.P. Parkin: "Vanadium Oxides Thin Films deposited by Aerosol Assisted Chemical Vapour Deposition." ***International Conference on Metallurgical Coatings and Thin Films, San Diego, 23-27 April 2007, United States.***

- R. Binions, C. Piccirillo, I.P. Parkin: "Hybrid Aerosol Assisted and Atmospheric Pressure Chemical Vapour Deposition of Gold Doped Vanadium Dioxide Thin Films." ***UK CVD Network meeting, Salford, 20th July 2007, United Kingdom.***
- R. Binions, C. Piccirillo, I.P. Parkin: "Tungsten doped vanadium dioxide thin films prepared by atmospheric pressure chemical vapour deposition from vanadyl acetylacetonate and tungsten hexachloride." ***Sixteenth European Conference on Chemical Vapour Deposition, Den Haag, 16-21 September 2007, Netherlands.***

The content of these presentations overlaps with that published in the papers; for this reason, no more description will be given.

4. Summary of the results

The diagram below summarises the work performed by Clara Piccirillo, in relation to the previous work in this field and to the successive developments.

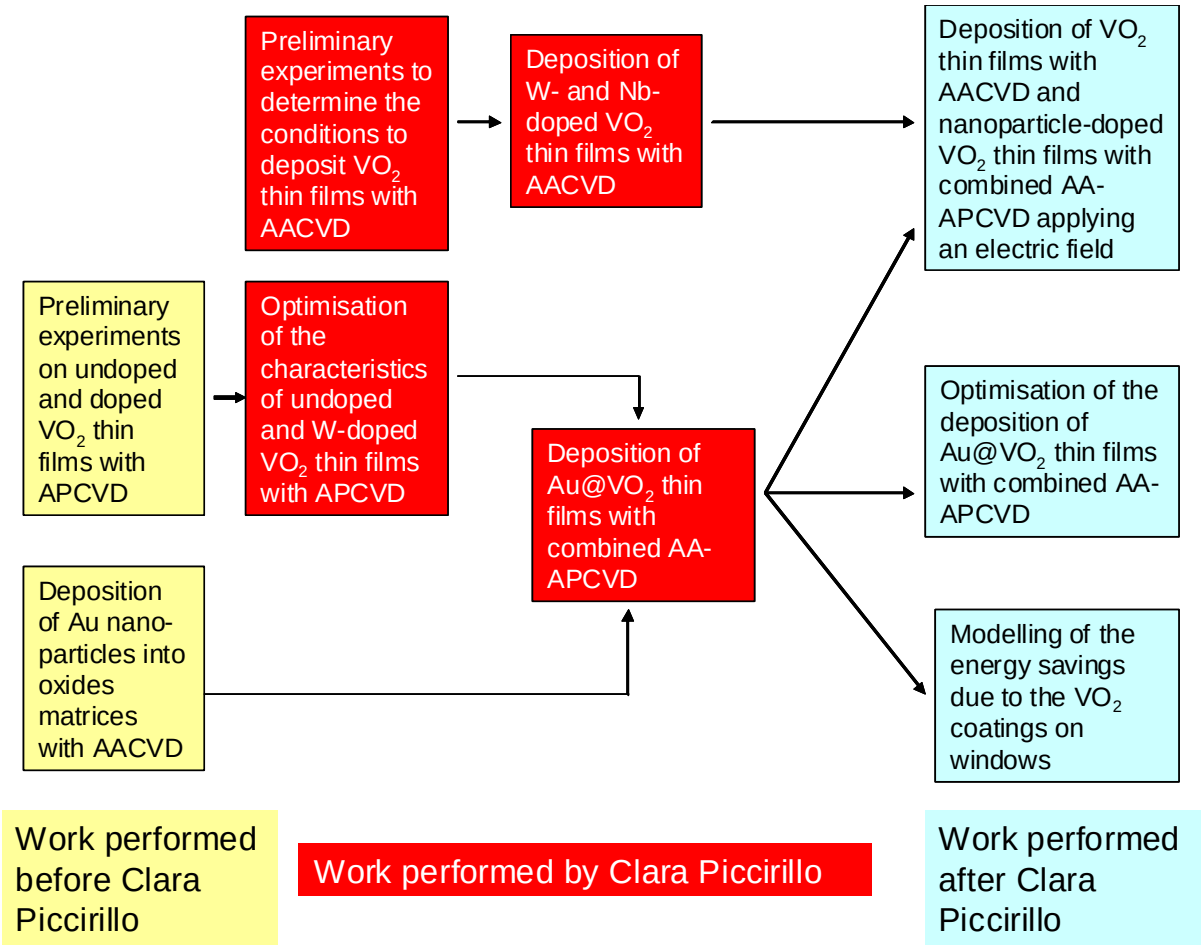

From the diagram it can be seen how the work was part of a structured research programme into the development of thermochromic films. It was carried out as a sequential series of experiments in two parallel lines of research. The work was so successful it was further developed by subsequent researchers for commercial applications.

The research carried out by Clara Piccirillo and the results associated with it were significant for the understanding of AACVD and APCVD synthesis of vanadium oxide films, and the study and development of vanadium (IV) oxide as a solar control coating.

In this section, a summary of the results of her work is presented, while in the next one a brief description of the continuation of her research is given.

4.1 Summary of the main outcomes

- AACVD methodology was employed to deposit vanadium oxides with different oxidation states. The conditions required to deposit single phase vanadium (III), vanadium (IV) and vanadium (V) oxides were discovered. This study showed that both the solvent employed for the aerosol, and the flow conditions, have an important effect on the phase formed, when atoms with several different possible oxidation states are deposited.
- AACVD deposition of doped vanadium (IV) oxide was achieved, using either tungsten or niobium. In both cases, a significant decrease in the value of the transition temperature was observed. Also, the width of the hysteresis loop of the doped samples was smaller, if compared with the undoped ones.

  Tungsten was shown to be more effective, with a reduction in the Tc value of about $20^{o}C$ for 1 atom % in the lattice. Samples with transition temperature of $28^{o}C$ were deposited; these films could function as solar control coatings.

  Niobium-doped samples showed a transition temperature as low as $35^{o}C$. Such a low value of T_c was never reported before with Nb.
- AACVD proved to be a suitable technique to deposit these kinds of thin film. The control of the deposition conditions and/or the concentration in solution allowed the synthesis of different materials, or the same material with a different dopant concentration. These results showed the great potential of this methodology; this is particularly important as it can be easily applied at industrial level.
- APCVD was employed to deposit vanadium (IV) oxide thin films, single phase and doped. Both the deposition precursors and conditions were different than those previously employed; in this way the reproducibility of the system was improved.
- It was shown that the thickness of the films prepared by APCVD may affect their optical properties. The effect on the transmittance in the visible, and on the change in the absorbance and reflectance in the infrared for the MST transition, was studied. Films with about 70 -90 nm thickness were shown to be the most suitable as window coatings.
- It was proved that the deposition conditions in the APCVD process (flow rate) can influence the crystallographic orientation in the vanadium (IV) oxide coatings. This can

have an effect on the optical properties of the material, such as the width of the hysteresis.

- W-doped vanadium (IV) oxide thin films deposited with APCVD showed a greater optical switching in the infrared region, when undergoing the MST transition.
- Chlorine-free precursors were used to deposit pure VO_2 thin films with both APCVD and AACVD. With AACVD, it was also possible to obtain W- and Nb-doped thin films using chlorine-free precursors. For APCVD, however, this was not possible; the most suitable tungsten precursor was WCl_6, due to its high vapour pressure. The use of chlorine–free precursors is an important consideration for any subsequent industrial scale-up of the process.
- APCVD and AACVD methodologies were used combined together, to deposit Au-doped VO_2 thin films. The presence of gold caused a noticeable change in the colour of these coatings, from brown to blue-green. A blue-green colour is considered much more acceptable in a commercial window glass.

The total number of citations for the papers presented here was 89 when this document was written.

5. Successive developments

The work performed by Clara Piccirillo was continued by a PhD student in the same Department (Mr. Manfredi Saeli), under the supervision of Professor Ivan P. Parkin. She was partially involved in his supervision. The research and the results achieved by Clara Piccirillo were essential for the work of Mr. Saeli, as he continued the work started by her and her colleagues.

The main focus of his research was the optimisation of the deposition of undoped and Au-doped vanadium (IV) oxide thin films, using the two combined CVD methodologies (APCVD and AACVD). To achieve this, a surfactant was used (tetraoctyl ammonium bromide – TOAB) to control the dimensions of the gold nanoparticles and/or the morphology of the vanadium (IV) oxide film itself. The optimisation was successful, as the deposited materials had a better appearance and showed improved optical properties.

In particular, the use of TOAB and Au together led to a more uniform distribution of the dimensions of the gold nanoparticles; this allowed a better control of both film morphology and colour. A further reduction in the transition temperature was also detected ($Tc \approx 45^{o}C$). When only the surfactant agent was employed, an effect on the film growth morphology was observed; in fact, the average grain size was smaller. This caused a reduction of the transition temperature to $34^{o}C$; it was the first time that the Tc value was lowered by over $30^{o}C$ without any dopant but only by changing the film morphology.

A study was also performed on the energy savings associated with the use of these coatings on the windows. Modelling software (Energy Plus) was used to simulate the energy consumption. Buildings with various window orientations were considered, and different European cities were chosen, to take into account the different climates. The results of the simulation showed that the use of these coatings resulted in an energy saving greater than that obtained with some commercial coatings. These materials were especially effective for southern European climates; in some cases the additional energy saving was about 10% higher in comparison with currently available solar thin films. This work was published in four papers in peer reviewed journals, as listed below, and Clara Piccirillo was a co-author of all four.

- M. Saeli, R. Binions, C. Piccirillo, I.P. Parkin: "Templated Growth of Smart Coatings: Hybrid Chemical Vapour Deposition of Vanadyl Acetylacetonate with Tetraoctyl Ammonium Bromide." ***Appl. Surf. Sci.,* 255**, 7291 (2009).

- M. Saeli, R. Binions, C. Piccirillo, G. Hyett, I.P. Parkin: "Templated Growth of Smart Nanocomposite Thin Films: Hybrid Aerosol Assisted and Atmospheric Pressure Chemical Vapour Deposition of Vanadyl Acetylacetonate, Auric Acid and Tetraoctyl Ammonium Bromide." ***Polyhedron***, **28**, 2233 (2009).
- R. Binions, M. Saeli, C. Piccirillo, I.P. Parkin, I. Ridley: "Nanocomposite Thermochromic Thin Films and Their Application in Energy Efficient Glazing." ***Sol. Energy Mat. Sol. Cells,* 94**, 141 (2010).
- M. Saeli, C. Piccirillo, I.P. Parkin, R. Binions, I. Ridley: "Optimisation of Thermochromic Thin Films on Glass; Design of Intelligent Window." ***Adv. Science Technol.,* 75**, 79 (2010).

These results achieved by Mr. Saeli show that the work performed by Clara Piccirillo had a long-term impact on the continuation of the research; with these findings, the development of a finite commercial product became more feasible.

Further developments of Clara Piccirillo's work were carried out by Dr. Binions, at University College London; in fact, he continued to perform deposition of vanadium (IV) oxide thin films with both AACVD and hybrid AP and AA CVD methodologies. He used the AACVD technique whilst applying an electric field to the deposition substrate - this led to films with different morphologies and surface properties. Using the hybrid technology, he deposited composite materials (nanoparticles@VO_2), with ceria and titania nanoparticles.

The results, published in several papers (Warwick, 2010; Warwick, 2011; Crane, 2010), demonstrate once again the validity and the long-term impact of the work of Clara Piccirillo.

6. References

D. Adler, J. Feinleib, H. Brooks, W. Paul, *Phys. Rev.*, 1967, **155**, 851.

R.A. Aiev, V.A. Klimov, *Phys. Sol. State*, 2004, **46(3)**, 532.

W. L. Barnes, A. Dereux, T. W. Ebbesen, *Nature*, 2003, **424**, 824.

F. Béteille; J.J. Livage, *Sol-Gel Sci. Technol.*, 1998, **13**, 915.

W. Burkhardt, T. Christmann, S. Franke, W. Kriegseis, D. Meister, B.K. Meyer, W. Niessner, D. Schalch, A. Scharmann, *Thin Solid Films*, 2002, **402**, 226.

W. Burkhardt, T. Christmann, B.K. Meyer, W. Niessner, D. Schalch, A. Scharmann, *Thin Solid Films*, 1999, **345**, 229.

F.C. Case, *J. Vac. Sci. Technol. A*, 1984, **2**, 1509.

E. Cavanna, J.P. Segaud, J.J. Livage, *J. Mater. Res. Bull.*, 1999, **34**, 167.

J. Crane, M.E.A. Warwick, R. Smith, N. Furlan, R. Binions, *J.Electrochem. Soc.*, 2011, **158(2)**, D62.

H. Cui, V. Teixeira, L. Meng, R. Wang, J. Gao, E. Fortunato, *Thin Solid Films*, 2008, **516**, 1484.

M. C. Daniel, D. Astruc, *Chem. Rev.s*, 2004, **104**, 293.

V. Eyert, *Ann. Physik*, 2002, **11**, 650.

M.N. Field, I.P. Parkin, *J. Mater. Chem.*, 2000, **10**, 1863.

J.B. Goodenough, *J. Solid State Chem.*, 1971, **3**, 490.

G.C. Granqvist, *Advanced Mater.*, 2003, **15**, 1789.

C.B. Greenberg, *Thin Solid Films*, 1983, **110**, 73.

T.J. Hanlon, J.A. Coath, M.A. Richardson, *Thin Solid Films*, 2003, **436**, 269.

T.J. Hanlon, R.E. Walker, J.A. Coath, M.A. Richardson, *Thin Solid Films*, 2002, 405, 234.

M.L. Hitchman, K.F. Jensen, in *Chemical Vapour Deposition Principles and Applications*; London Academic Press, 1993.

X. H. Hou, K. L. Choy, *Chem. Vap. Depos.*, 2006, **12**, 583.

N. Irit, T. A. Bendikov, I. Doron-Mor, Z. Barkay, A. Vaskevich, I. Rubinstein, *Journal of The American Chemical Society*, 2007, **129**, 84.

Y. Jiazhen, Z. Yue, H. Wanxia, *Thin Solid Films*, 2008, **516(23)**, 8554.

P. Jin, http://www.aist.go.jp/NIRIN/People/pjin/GIF/tc.gif. 2000.

P. Jin, S. Nakao, S. Tanemura, *Thin Solid Films*, 1998, **324**, 151.

R. J. Lang, *J. Acoust. Soc. Am.*, 1962, **34**, 6.

J.B.K. Kana, J.M. Ndjaka, P. Owono Ateba, N. Manyala, O. Nemraoui, A.C. Beye, M. Maaza, *Appl. Surf. Sci.*, 2008, **254(13)**, 3959.

J.B.K. Kana, J.M. Ndjaka, N. Manyala, O. Nemraoui, A.C. Beye, M. Maaza, *AIP Conference Proceedings*, 2008, **1047**, 119.

J. Lappalainen, S. Heinilehto, S. Saukko, V. Lantto, H. Jantunen, *Sens. Actuat. A, Phys.*, 2008, **142(1)**, 250.

S. Link, M. El-Sayed in *Semiconductor and Metal Nanocrystals*; (Ed.V. I. Klimnov) Marcel Dekker, New York, 2004, p. 45.

J. Livage, *Coord. Chem. Rev.*, 1999, **190-192**, 391.

S. Lu, L. Hou, F. Gan, *Thin Solid Films*, 1999, **353(1)**, 40.

Y. Luo, J. Ruff, R. Ray, Y. L. Gu, H. J. Ploehn and W. A. Scrivens, *Chem. Mater.*, 2005, **17**, 5014.

M. Maaza, O. Nemraoui, C. Sella, A.C. Beye, B. Baruch-Barak, *Opt. Commun.*, 2005, **254(1-3)**, 188.

J.B. MacChesney, J.F. Potter, H.J.J. Guggenheim, *Electrochem. Soc. Solid State Sci.*, 1968, **115**, 52.

T.D. Manning, I.P. Parkin, *J. Mat. Chem.*, 2004, **14**, 2554.

T.D. Manning, I.P. Parkin, *Polyhedron*, 2004, **23**, 3087.

T.D. Manning, I.P. Parkin, R.J.H. Clark, D. Sheel, M.E. Pemble, D. Vernardou, *J. Mater. Chem.*, 2002, **12(10)**, 2936.

T.D. Manning, I.P. Parkin, M.E. Pemble, D. Sheel, D. Vernardou, *Chem. Mater.*, 2004, **16**, 744.

T. Maruyama, Y. Ikuta, *J. Mater. Sci.*, 1993, **28**, 5073.

F.J. Morin, *Phys. Rev. Lett.*, 1959, **3**, 34-36.

M. Netsianda, P.E. Ngoepe, C.R.A. Catlow, S.M. Woodley, *Chem. Mat.*, 2008, **20(5)**, 1764.

Y. Nihei, Y. Sasakawa, K. Okimura, *Thin Solid Films*, 2008, **516(11),** 3572.

R.G. Palgrave, *PhD thesis*, University College London, 2007.

R.G. Palgrave, I.P. Parkin, *J. Amer. Chem Soc.*, 2006, **128(5)**, 1587.

R.G. Palgrave, I.P. Parkin, *Chem Mater.*, 2007, **19(19)**, 4639.

R.G. Palgrave, I.P. Parkin, *Gold Bull.*, 2008, **41(1)**, 66.

M. Pan, H. Zhong, S. Wang, J. Liu, Z. Li, X. Chen, W. Lu, *J. Cryst. Gr.*, 2004, **265(1-2)**, 121.

T.E. Phillips, R.A. Murray, T.O. Poehler, *Mater. Res. Bull.*, 1987, **22**, 1113.

J.C. Rakotoniaina, R. Mokrani-Tamellin, J.R. Gavarri, G. Vacquier, A. Casalot, G. Calvarin, *J. Solid State Chem.*, 1993, **103**, 81.

R. H. Ritchie, *Physical Review*, 1957, **1**, 874.

K.D. Roger, *Powder Diff.*, 1993, **8**, 240.

S. Saitzek, F. Guinneton, L. Sauques, K. Agiur, J.R. Gavarri, *Opt. Mater.*, 2007, **30(3)**, 407.

M.B. Sahana, M.S. Dharmaprakash, S.A. Shivashankar, *J. Mater. Chem.*, 2002, **12**, 333.

M.B. Sahana, G.N. Subbanna, S.A. Shivashankar, *J. Appl. Phys.*, 2002, **92**, 6495.

I. Takahashi, M. Hibino, T. Kudo, Jap. *J. Appl. Phys.*, 1996, **35**, L438.

I. Takahashi, M. Hibino, K. Tetsuichi, *Jap. J. Appl. Phys.*, 2001, **40**, 1391.

Y. Takahshi, M. Kanamori, H. Hashimoto, Y. Moritani, Y. Masuda, *J. Mater. Sci.*, 1989, **24**, 192.

C. Tang, P. Georgopoulos, M.E. Fine, J.B. Cohen, M. Nygren, G.S. Knapp, A. Aldred, *Phys. Rev. B*, 1985, **31**, 1000.

D. Vernardou, M.E. Pemble, D.W. Sheel, *Chem. Vap. Depos.*, 2006, **12**, 263.

M.E.A. Warwick, C.W. Dunnill, R. Binions, *Chem. Vap. Depos.*, 2010, **16**, 123.

M.E.A. Warwick, R. Binions, *J. Nanosci. Nanotech.* 2011, **11**, 8126.

G. Zhao, H. Kozuka, H. Lin, T. Yoko, *Thin Solid Films*, 1999, **339(1-2)**, 123.

Annex I: published papers

Chemical Vapor Deposition

DOI: 10.1002/cvde.200606540

Full Paper

Synthesis and Functional Properties of Vanadium Oxides: V_2O_3, VO_2, and V_2O_5 Deposited on Glass by Aerosol-Assisted CVD

By *Clara Piccirillo*, *Russell Binions*, and *Ivan P. Parkin**

Thin films of vanadium oxides were deposited on glass by aerosol-assisted (AA) CVD from vanadium(III) acetylacetonate and vanadyl(IV) acetylacetonate. The vanadium precursor, solvent, and carrier gas flow rate determined the phase of vanadium oxide formed (V_2O_3, VO_2, or V_2O_5). Films were characterized using various analytical techniques. VO_2 films were analyzed at various temperatures to study their thermochromic behavior. The V_2O_3 reflectance-transmission plots showed a cross-over (ideal behavior for a solar-control mirror).

Keywords: AACVD, Phase transition, Thin films, Vanadium oxides

1. Introduction

Thin films of vanadium oxide have been widely studied in recent years, due to their interesting technological applications. Vanadium(IV) oxide in the monoclinic form, VO_2(M), shows a thermally induced, reversible, metal-to-semiconductor transition to the rutile form VO_2 at 68 °C.[1] Both electrical and optical properties in the near infrared (IR) are remarkably affected by the transition; in fact VO_2(M) behaves as a semiconductor and does not reflect much solar energy; VO_2(R), on the other hand, behaves as a semimetal and reflects a much wider range of solar wavelength.[2] For this transition and for the associated property changes, VO_2 can be used as an intelligent window material. Recent results showed that a substantial reduction of the transition temperature can be obtained by doping VO_2 with W;[3] this considerably broadens the scope of applications and may allow the material to be tuned to window applications.

The vanadium(V) oxide V_2O_5 also shows a thermochromic phase transition at 257 °C.[4] Furthermore it is known to have electrochromic properties changing from blue to green and to yellow in a time of about two seconds.[5] It is also used as a catalyst in industrial processes, in the manufacture of solid-state lithium ion batteries, and as a gas-sensor.[6,7] Other vanadium oxides have been studied for their phase changes; an example being V_2O_3 for the Mott-Hubbard metal-insulator transition.[8]

Due to the multiplicity of vanadium stable oxidation states, it can be quite difficult to prepare a single-phase vanadium oxide thin film. To avoid the formation of a solid solution of different phases, it is necessary to select and control carefully the appropriate experimental deposition conditions. The use of different deposition precursors can lead to a more oxidizing environment, or the various fluid-dynamic conditions can stabilize one oxidation state more than another; hence oxidation, reduction, or dismutation reactions of the precursor can occur, leading to the formation of different phases.

Vanadium oxides have been prepared using various methodologies, such as sol-gel, sputtering, vacuum evaporation, and atmospheric pressure (AP) CVD.[9–14] We have shown previously that VO_2, VO_x, and V_2O_5 phases can be fabricated by using APCVD from reactions of VCl_4, $VOCl_3$, and water. The ratio of water to vanadium precursor and the substrate temperatures were the determining factors in which the oxide formed. In our work, in over five hundred deposition experiments, the V_2O_3 phase was never formed by using APCVD; this may have been because of the fact that the reaction conditions (i.e., the use of air and/or oxygen) favored the higher vanadium oxidation states (from IV upwards).

In this paper we describe the synthesis of different vanadium oxides phase using aerosol-assisted (AA) CVD. In this technique, the precursor is dissolved in a solvent and an aerosol of the solution is generated ultrasonically. The precursor is transported to the substrate through the aerosol droplets by a carrier gas. The advantage of AACVD over the standard APCVD is that the precursor does not need to be volatile, but just soluble in one of the solvents suitable for aerosol formation.[15] This allows the use of a

[*] Prof. I. P. Parkin, Dr. C. Piccirillo, Dr. R. Binions
Christopher Ingold Laboratories, Chemistry Department, University College London
20 Gordon Street, London, WC1H 0AJ (UK)
E-mail: i.p.parkin@ucl.ac.uk.

[**] This work was financially supported by the EU project Termoglaze. The authors would like to thank Pilkington Glass for providing the deposition substrates, Mr. Kevin Reeves for the help with scanning electron microscopy, Dr. Steve Firth for the help with Raman spectroscopy, and Dr. Geoff Hyett for the calculations of lattice indexes from XRD data. IPP thanks the Royal Society/Wolfson Trust for a merit award.

wider range of unconventional precursors.[16,17] Another advantage of AACVD is that it is simpler and more straightforward to use when more than one precursor has to be used, for instance to deposit doped thin films.

No systematic study has been conducted into the influence of the solvent on the phase of film formed; in this paper we report about AACVD experiments using various solvents, and we show how they play a key role in determining the reaction chemistry and the phase of vanadium oxide formed. Through manipulation of the conditions, the first thin film of V_2O_3 has been produced by using CVD. We also show that the vanadium oxide films have important, hitherto unreported, functional properties, including hydrophilicity (V_2O_5), hydrophobicity (V_2O_3), and solar control behavior (VO_2).

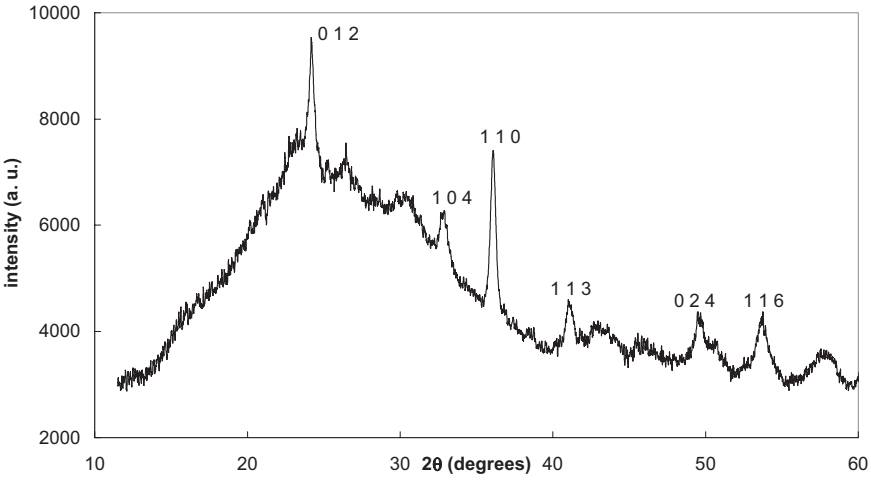

Fig. 1. XRD powder diffraction pattern for sample 3 - V_2O_3 thin film.

2. Results and Discussion

2.1. Synthesis and Characterization

AACVD of V_2O_3, VO_2, or V_2O_5 films was achieved on glass substrates at 500–600 °C (see Table 1). No film was obtained for temperatures below 500 °C; any change in temperature inside the above range did not affect the nature of the deposited phase. The concentration of the precursor was always between 0.01 and 0.1 mol dm^{-3}; the concentration affected the thickness of the deposit but not the nature of the phase. The growth rate depended on the concentration of the precursor in the solutions; for a solution concentration 0.05 mol dm^{-3} the average growth rate was 0.6 μm h^{-1}. All films passed the Scotch tape test but were scratched by a steel scalpel.

A X-ray diffraction (XRD) spectrum for sample 3 (V_2O_3 film) is shown in Figure 1. All of the vanadium oxide films showed the broad signal due to the amorphous glass substrate. In all cases, however, a clear diffraction pattern could be detected and assigned unambiguously. X-ray microfocus spot analysis (3 mm × 3mm squares; typically 5–10 points analyzed at random on the substrate) at various points of each film were analyzed. It was found that an individual film was of a uniform phase across the entire substrate. The XRD pattern shown in Figure 1 is in agreement with the data reported in the literature for V_2O_3 (karelianite), with no preferred orientation observed.[18] The film could be indexed with a rhombohedral cell, with $a = b = 5.020(5)$ Å and $c = 14.026(5)$ Å. These values match within error those from previous experiments ($a = b = 4.95(3)$ Å, $c = 14.00(3)$ Å).[14] The patterns for the VO_2 and V_2O_5 (not shown in the figure) were also in excellent agreement with data reported before and gave equivalent cell constants.[14] No preferred orientation is observed for VO_2 whilst a slight (110) preferred orientation was seen for V_2O_5.[19]

Raman spectroscopy for the V_2O_3 films showed no appreciable signal. This is probably due to the brown color of all the films and consequently low light scattering. No previous literature data were found reporting Raman spectrum for this vanadium oxide phase; we suspect V_2O_3 is not a good Raman scatterer. The Raman spectrum for sample 10 (VO_2 film) is shown in Figure 2a; all the peaks marked in the spectrum can be attributed to VO_2, in agreement with data previously reported.[14] It can be noticed that no other phase was detected and that there is no signal corresponding to graphitic carbon present, at 1355 cm^{-1}. As Raman spectroscopy is very sensitive to graphitic carbon, it is inferred that the films are free from carbon contamination. This latter point is an interesting result, considering that both the vanadium precursor

Table 1. AACVD conditions for deposition of vanadium oxides.

Sample number	Precursor	Solvent	N_2 flow rate [L min^{-1}]	Phase (from Raman and XRD spectroscopy)
1	$V(acac)_3$	Methanol/water 100:0	1.5	V_2O_3 karelianite
2	$V(acac)_3$	Methanol/water 60:40	1.5	V_2O_3 karelianite
3	$V(acac)_3$	Methanol/water 30:70	1.5	V_2O_3 karelianite
4	$V(acac)_3$	Methanol/water 0:100	1.5	V_2O_3 karelianite
5	$V(acac)_3$	Ethanol	1.5	VO_2 + other phases
6	$V(acac)_3$	Ethanol	> 3	V_xO_y mixed phases
7	$VO(acac)_2$	Methanol/water 100:0	1.5	V_2O_3 karelianite
8	$VO(acac)_2$	Methanol/water 60:40	1.5	V_2O_3 karelianite
9	$VO(acac)_2$	Methanol/water 40:60	1.5	V_2O_3 karelianite
10	$VO(acac)_2$	Ethanol	1.5	VO_2 (M)
11	$VO(acac)_2$	Ethanol	> 3	V_2O_5

Chemical Vapor Deposition

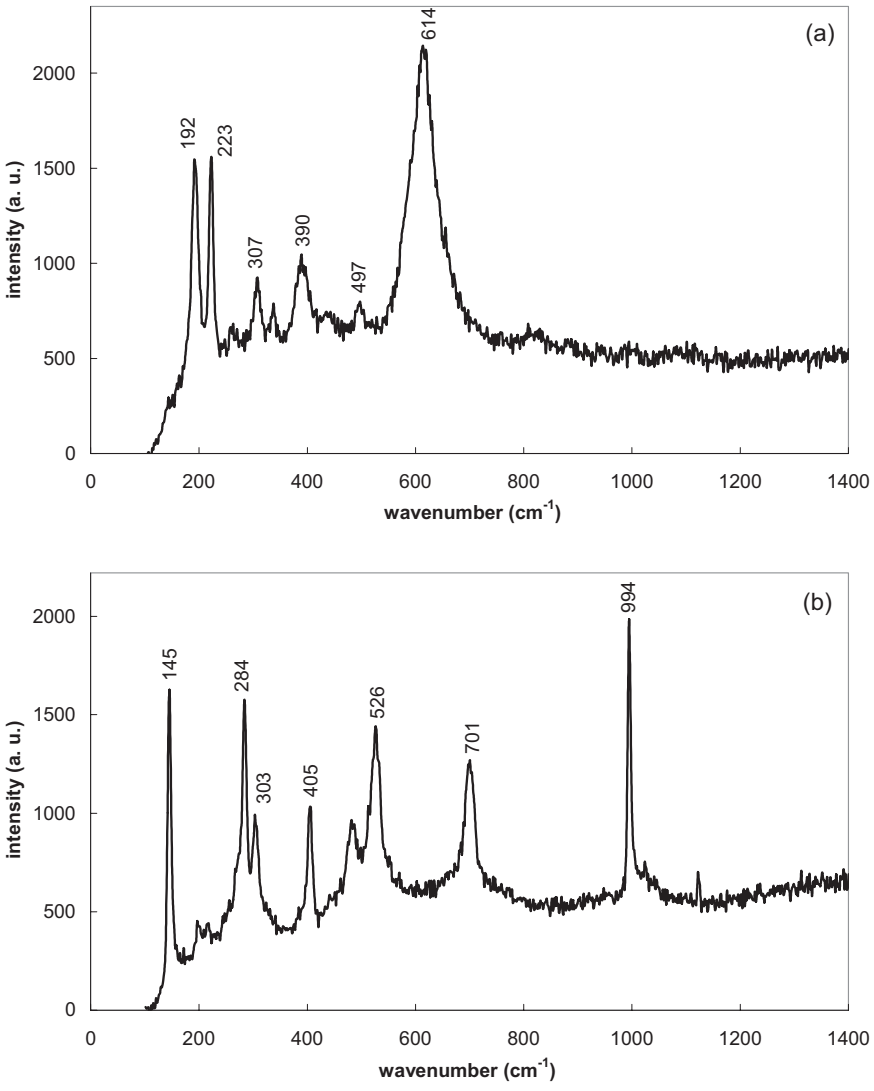

Fig. 2. Raman spectra for a) sample 10 (VO_2), and b) sample 11 (V_2O_5) thin films.

and the solvent contain carbon. This indicates that, with these deposition conditions, both the precursor and the solvent decompose into volatile fragments that do not get included in the films. Figure 2b shows the Raman spectrum for sample 11 (V_2O_5); similarly to VO_2, the peaks marked in the spectrum can be attributed to V_2O_5, there being a direct correlation with literature data in both intensity and peak position,[13,14] and no sign of graphitic carbon contamination.

Scanning electron microscopy (SEM) of the vanadium oxide films revealed different surface morphologies for samples 2, 10, and 11 (V_2O_3, VO_2, and V_2O_5 thin films – Fig. 3a, b, and c, respectively). Both the V_2O_3 and VO_2 films show surface nucleation and crystal growth. However, the dimensions of the microcrystallites are smaller for V_2O_3. For V_2O_5, island agglomeration is observed.

The optical properties of the films were also studied; representative transmittance and reflectance spectra are shown in Figure 4. The V_2O_3 thin film (sample 2, Fig. 4a) was relatively thick (500 nm) and shows low values of both transmittance and reflectance in the visible region. Surprisingly, the V_2O_3 film shows a large increase in reflectance at ca. 700 nm, and a crossover in the transmission and reflection curves. This behavior is quite rare, and indicative of films used in solar control applications, such as titanium nitride and silver metal. As such, the V_2O_3 films of appropriate thickness have potential application as solar control products. Sample 10 (VO_2 thin film, Fig. 4b), on the contrary, shows higher values of both reflectance and transmittance for a wider energy range. V_2O_5 deposits (sample 11, Fig. 4c) show a much higher transmittance, probably because of their brighter yellow color; the reflectance however is quite low. The qualitative behavior of other samples of each phase was similar to the one shown in the figure; small differences in intensity were sometimes observed, due to a variation in thickness of the samples.

2.2. Film Properties

Water contact angle measurements were carried out to determine the hydrophobic/hydrophilic nature of the oxides. The methodology used for the measurements only gives an approximate value of contact angle; however, this is sufficient to evidence different behaviors (if any) between the various vanadium oxides. Vanadium(V) oxide had marked hydrophilic behavior, with a contact angle in the range 3–5°, V_2O_3 was less hydrophilic with contact angle values between 16 and 25°, whilst VO_2 also showed marked hydrophobic properties (90–120°). The low angles for V_2O_5 are probably a results of the films being very porous. The VO_2 films were surprising hydrophilic.

Further analysis was carried out for VO_2 films, to investigate the transition from monoclinic to tetragonal structure. Raman spectroscopy was performed at various temperatures; the results are shown in Figure 5. It can be seen how the Raman pattern corresponding to the monoclinic form of VO_2 becomes less and less intense, as the temperature increases and gets close to the transition point (in the graphic, $T = 22$, 50 and 65 °C). At 75 °C (curve d), above the transition temperature, the Raman pattern completely dis-

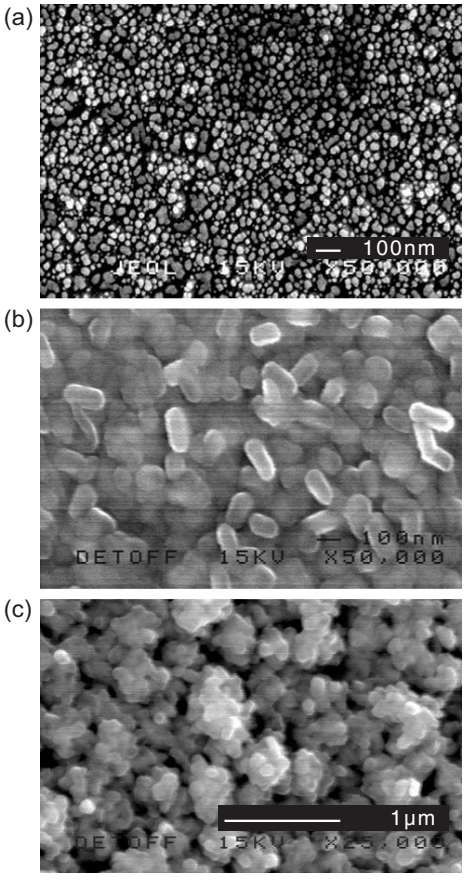

Fig. 3. SEM images of a) sample 2 (V_2O_3), b) sample 10 (VO_2), and c) sample 11 (V_2O_5) thin films.

appeared. Cooling down the sample to 50 °C, it can be seen how the Raman signal can be detected again, indicating the reversibility of the transition. This data is in agreement with previously published results.[14]

The transmittance of the film was also measured at various temperatures. Figure 6 shows the transmittance at 4000 cm^{-1} plotted against temperature. This value of energy was chosen because the change upon transition is quite large, and hence easier to monitor. Furthermore, this wavelength corresponds to thermal energy; therefore a change here gives an indication of the efficiency of VO_2 as an intelligent window material. It can be seen how the transmittance gradually decreases with increasing temperature, reaching the minimum between 70 and 80 °C. This is in agreement with the Raman data of Figure 5, which indicated the absence of VO_2 (M) at 75 °C. Cooling down the system, the transmittance increases again, hence the transition is reversible. Other VO_2 samples, not shown in the figure, showed similar qualitative behavior, with small differences in the width of the hysteresis loop. This is in agreement with previously published data,[20] according to which the width of the hysteresis loop can depend on factors such as film thickness and crystallite size.

2.3. Variation in Deposition Conditions

To investigate the role of solvent in AACVD, a wide range of different solvents were tried with both $[VO(acac)_2]$ and $[V(acac)_3]$. Methanol/water, ethanol/water, and ethanol met with the greatest success, and allowed a range of vanadium oxide films to be formed. All the $[VO(acac)_2]$ solutions were stable for a period of a week or more, while for $[V(acac)_3]$ a change in color was observed over after 24 h (from brown to turquoise), indicating a change in vanadium oxidation state. Fresh solutions were prepared before each deposition experiment.

The use of other solvents such as acetonitrile, acetone, or ethyl acetate as solvent all led to powdery black films. These films gave no discernable XRD pattern but did show significant carbon content by energy dispersive X-ray (EDX) analysis, and by Raman where a strong graphite signal was detected. This shows that in AACVD the role of the solvent is important in determining the course of the reaction, and may play a much more intimate role in the deposition than just acting as a transport agent. Use of acetonitrile, acetone, and ethyl acetate all led to the production of films with high graphite contamination.

From Table 1, it can be seen how the use of $[V(acac)_3]$ as the precursor led to the formation of V_2O_3 (karelianite) when methanol, water, or a mixture of the two solvents were used. This is probably because vanadium has an oxidation state (III) in the precursor, and it does not get oxidized during the deposition. This is the case even if a more oxidizing (or oxygen-rich) solvent like water is used. V_2O_3 thin films were previously prepared with various methodologies (i.e., epitaxially grown by evaporation physical vapor deposition (PVD)),[19,21] but never by CVD. The same phase was obtained using the same mixture of solvents but a different vanadium precursor ($[VO(acac)_2]$ in CH_3OH/H_2O). This clearly indicates how, in AACVD, the solvent can have a fundamental role in the preferential stabilization of a particular oxidation state. In this case, methanol, water, and the mixture of the two tend to stabilize V^{III}. This is reasonable, as there is no reported route to graphitization with methanol,[22] therefore the solvent may not act as an oxidant. It is likely that reduction from V^{IV} to V^{III} occurs at the substrate surface, as part of a decomposition reaction. This leads to the formation of V_2O_3.

The use of the same precursor but in a different solvent ($[VO(acac)_2]$ in ethanol) brought a change in the phase of the vanadium oxide deposited. As shown in Table 1, VO_2 and V_2O_5 were deposited at low and high nitrogen flow rate, respectively. All films were yellow in color; VO_2 deposits were darker, almost brown, whereas V_2O_5 ones were brighter yellow-green.

The vanadium oxidation state in the film depended to some extent on the carrier gas flow rate. This shows that the fluidodynamic conditions have an important effect in the AACVD process. At 1.5 L min^{-1}, the vanadium precursor forms the corresponding oxide without changes in the

Chemical Vapor Deposition

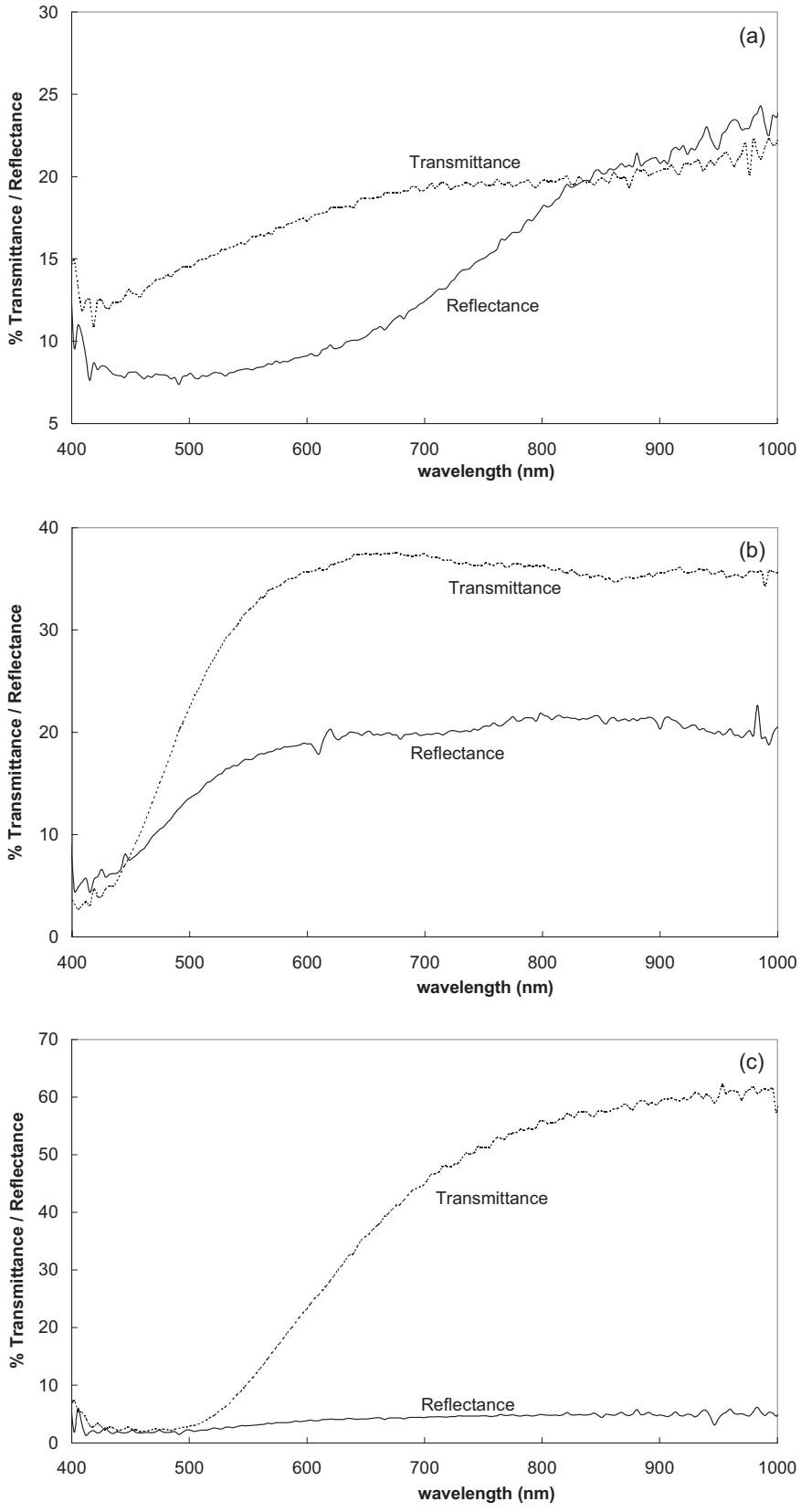

Fig. 4. Transmittance and reflectance spectra for a) sample 2 (V_2O_3), b) sample 10 (VO_2), and c) sample 11 (V_2O_5) thin films.

oxidation state; this indicates that ethanol just stabilizes the oxidation state (IV) without any oxidative reaction occurring. At flow rates in excess of 3 L min^{-1}, both the solvent and the precursor fluxes in the reaction chamber will be higher; however, assuming that the solvent decomposes more readily than the precursor, there will be a higher concentration of oxygen (in the form of solvent) for surface reaction. Indeed this is likely to be the case as only V_2O_5, and no other vanadium oxides, could be observed in the resultant films produced under these conditions.

The effect of ethanol and carrier gas flow rate on the vanadium oxidation state can be also observed when $[V(acac)_3]$ is used as the precursor. At a low nitrogen flow rate, VO_2 (M) is formed; this indicates that an oxidation from V^{III} to V^{IV} takes place, due to stabilization of the latter oxidation state by the ethanol. Other mixed phases (i.e., V_6O_{13}), however, were detected in the films, probably because a further oxidation reaction takes place. At a higher nitrogen flow rate, VO_2 (M) is not observed any longer but mixed phases are detected instead (i.e., VO_x, V_2O_5). It is likely that a further oxidation of vanadium takes place, resulting in the formation of mixed oxidation state vanadium oxide films.

These experiments show that a single phase vanadium oxide is obtained when $[V(acac)_3]$ in methanol/water or $[VO(acac)_2]$ in ethanol are employed; the use of $[V(acac)_3]$ in ethanol, on the contrary, does not seem suitable for this purpose.

These results can be compared with the ones obtained with APCVD: in previous work, different precursors were used, both C- and Cl-containing (i.e., $V(acac)_3$, vanadium alkoxides, VCl_4, and $VOCl_3$). Similar to our work, depending on the experimental conditions, various phases were deposited, such as VO_2, V_2O_5, VO_x, V_6O_{13}, and V_3O_7.[14,20,22] However, in much of the previous work, mixed phase vanadium oxides were often

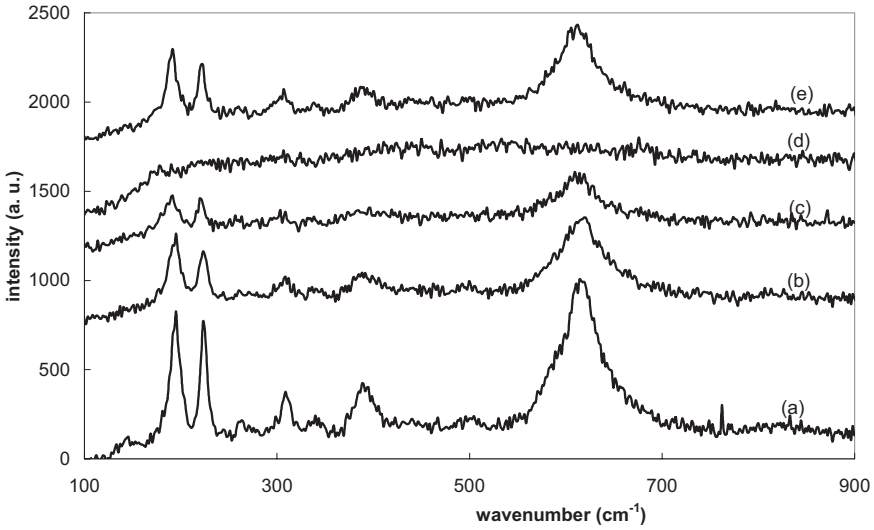

Fig. 5. Raman spectroscopy for sample 10 (VO_2 thin film) at various temperatures; a) 22 °C, b) 50 °C, c) 65 °C, d) 75 °C, and e) 50 °C cooling down.

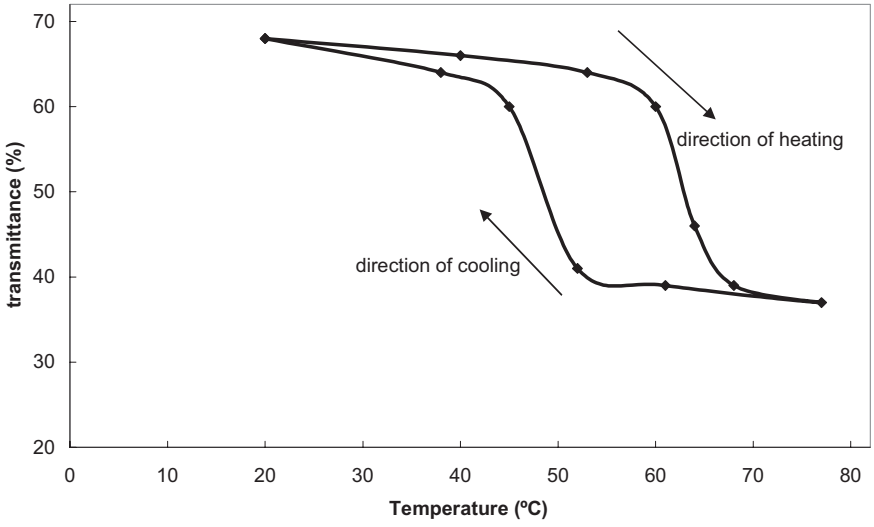

Fig. 6. Transmittance at 4000 cm^{-1} against temperature for sample 10 (VO_2 thin film).

produced, with VO_2 films often comprising of mixtures of VO_2, V_2O_5, and VO_x in different regions of the substrate. In this AACVD study, only a single phase was observed over the whole substrate. Furthermore the films showed a more uniform thickness profile. It can be seen why V_2O_3 was never obtained; the correct precursor set (using non-oxidizing co-reactants) was not employed. Hence it can be said that, in addition to the advantages mentioned above, AACVD methodology appears to be especially useful to deposit phases not obtainable by APCVD.

This work shows that the choice of solvent used in AACVD has a determining effect in deciding the phase of vanadium oxide formed. The effect of the solvent on the deposited phase was never studied properly before; in this work we have shown that it can have a critical role and, at least for this system, has a more significant effect than changing the substrate temperature. Polar solvents that contain a lot of carbon – such as acetone and ethyl acetate – were unsuitable for vanadium dioxide film formation by AACVD because of the formation of excessive carbon contamination. Mixed solvent systems with water worked best and a methanol/water system enabled a range of vanadium oxide phases to be obtained.

2.4. Film Functional Properties and their Applications

The vanadium oxide phases formed in this work showed a range of interesting functional properties. The VO_2 phase as expected showed a marked thermochromic transition; this was measured from the center of the hysteresis loop at 56 °C. This is some 12 °C lower than that expected for thick-film undoped VO_2. However, it does compare well with our previous findings for thin film VO_2 that shows a reduction in thermochromic transition for films less than 300 nm thick.[22] This reduction in switching temperature has been assigned to a stress induced reduction in T_c. Unexpectedly, the vanadium dioxide phase also proved to be very hydrophobic, with a water contact angle in excess of 100°. This hydrophobicity is not due to the surface roughness of the samples, as the SEM image reveals that the surfaces are smooth and lack the rugged projections needed for surface-induced hydrophobicity. It is likely that the surface chemistry is playing the greatest role in VO_2 and that the material forms a relatively low energy surface. The final functional property discovered in this study was the abrupt change in UV transmission reflection profile for the V_2O_3 films at ca 700 nm where the films became more reflective and less transmissive. This is exactly the behavior that is required for a solar control coating on a window. Such a film could provide a static solar control film if optimized, however the brown color of the film may limit application because of aesthetic reasons. Interestingly this V_2O_3 film acts as a static, nonintelligent version of the VO_2 films that show increase reflectivity above the critical temperature.

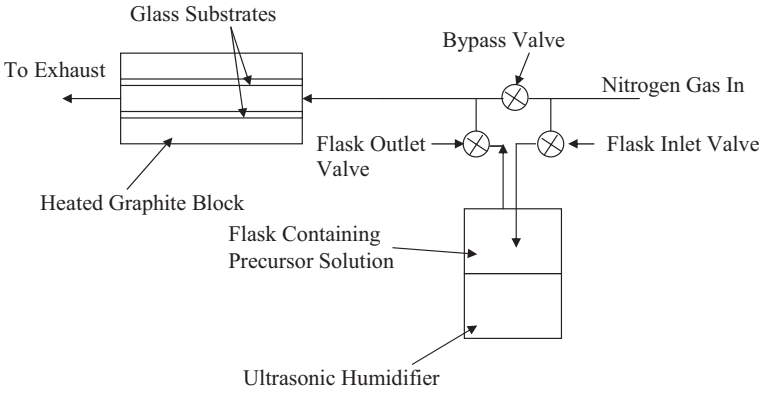

Fig. 7. Schematic representation of the AACVD deposition apparatus.

3. Conclusions

AACVD has been successfully employed to prepare a number of thin films of vanadium oxides. Notably, varying experimental conditions, particularly solvent and carrier gas flow, directly influenced the AACVD process and enabled several vanadium oxides to be formed. By tuning the conditions, single-phase V_2O_3, VO_2, and V_2O_5 could be formed across the whole substrate. This allowed V_2O_3 to be obtained for the first time by CVD. The films show a number of interesting functional properties; hydrophobicity (VO_2), heat mirror properties (V_2O_3), and hydrophilicity (V_2O_5).

4. Experimental

Film Deposition: Vanadium(III) acetylacetonate [$V(C_5H_8O_2)_3$, $V(acac)_3$] (Aldrich Chemical Company, 97 % purity) and vanadyl(IV) acetylacetonate [$VO(C_5H_8O_2)_2$, $VO(acac)_2$] were used as precursors for the deposition of vanadium oxide thin films. A precursor solution was made by dissolving [$V(acac)_3$] or [$VO(acac)_2$] in a series of solvents, as shown in Table 1. Depositions were carried out from solutions of various concentrations, in a range between 0.01 and 0.1 M.

An aerosol was generated on 50 mL of each solution using a Mountain Breeze humidifier; a nitrogen flow of 1.5–5 L min^{-1} (BOC, 99.9 %) was passed through the aerosol mist, directing the aerosol to a horizontal-bed, cold-wall CVD reactor.

Float glass (Pilkington Glass Plc) pre-coated with a silica barrier layer (50 nm thick, preventing diffusion of ions from the underlying glass) and sheets of dimensions 150 mm × 45 mm × 4 mm used as the substrates. Prior to deposition, the substrates were cleaned using water, acetone, and isopropyl alcohol, and dried in air. A Tempatron TC4800 thermostat was used to heat the substrates, with the temperature monitored by a Pt-Rh thermocouple. The substrates were heated to temperatures between 500 and 600 °C.

The aerosol passed between the heated substrate and a glass top plate, placed 8 mm above the substrate and parallel to it. The exhaust was vented into a fume cupboard. The gas flow was continued until all the precursor solution had passed through the reactor; it normally took between 40 and 70 min, depending on to the solvent. At the end of the deposition, the nitrogen flow through the aerosol was diverted and only nitrogen passed over the substrate. A schematic representation of the AACVD deposition apparatus is shown in Figure 7.

Film Characterization: XRD powder patterns were measured on a Bruker D8 diffractometer using filtered (Cu Kα1+α2) radiation in the reflection mode using glancing angle incidence (1.5°). SEM was carried out on a Hitachi filament scanning microscopy. EDX analysis was determined on a Phillips XL30 ESEM instrument, data were quantified using Oxford Inca Software. Raman measurements were carried out using a Renishaw system 1000 Raman spectrometer, with an Ar laser excitation source (514 nm). The Raman system was calibrated against the emission lines of argon. Reflectance and transmission spectra were recorded between 300 and 1100 nm on a Zeiss miniature spectrometer. Measurements were standardized relative to a rhodium mirror (reflectance) and air (transmission). Contact angles of deposited films were determined by measuring the spread of a 1 μL droplet of distilled water on the film surface. For measurements at different temperatures, an aluminum temperature cell, controlled by RS resistive heaters, Eurotherm temperature controllers, and k-type thermocouples was used to manipulate sample temperature. The sample temperature was measured using a k-type thermocouple taped directly onto the film surface.

Received: August 10, 2006
Revised: January 10, 2007

[1] T. D. Manning, I. P. Parkin, C. Blackman, U. Qureshi, *J. Mater. Chem.* **2005**, *42*, 4560.
[2] F. Morin, *J. Phys. Rev. Lett.* **1959**, *3*, 34.
[3] T. D. Manning, I. P. Parkin, M. E. Pemble, D. Sheel, D. Vernardou, *Chem. Mater.* **2004**, *16*, 744.
[4] G. S. Nadkarni, V. S. Shirodkar, *Thin Solid Films* **1983**, *105*, 115.
[5] J. Shimizu, K. Nagase, N. Mirura, N. Yamazoe, *Solid State Ionics* **1992**, *138*, L37.
[6] P. Poizot, S. Grugeon, L. Dupont, J. M. Tarascon, *Nature* **2000**, *407*, 496.
[7] G. Micocci, A. Serra, A. Tepore, S. Capone, R. Sella, P. Siciliano, *J. Vac. Sci. Technol. A* **1997**, *15*, 34.
[8] K. Held, G. Keller, V. Eyert, D. Vollhardt¸ V. I. Anisimov, *Phys. Rev. Lett.* **2001**, *86*, 5345.
[9] N. Ibris, A. M. Salvi, M. Liberatore, F. Decker, A. Surca, *Surf. Interface Anal.* **2005**, *37*, 1092.
[10] S. Deki, S. Aoi, Y. Kajinami, *J. Mater. Sci.* **1997**, *32*, 4269.
[11] C. Navone, J. P. Pereira-Ramos, R. Baddour-Hadjean, R. Salot, *J. Power Sources* **2005**, *146*, 327.
[12] Z. S. Guan, J. N. Yao, Y. A. Yang, B. H. Loo, *J. Electroanal. Chem.* **1998**, *443*, 175.
[13] M. N. Field, I. P. Parkin, *J. Mater. Chem.* **2000**, *10*, 1863.
[14] T. D. Manning, I. P. Parkin, R. J. H. Clark, D. Sheel, M. E. Pemble, D. Vernadou, *J. Mater. Chem.* **2002**, *12*, 2936.
[15] K. L. Choy, *Progr. Mater. Sci.* **2003**, *48*, 57.
[16] W. B. Cross, I. P. Parkin, *Chem. Commun.* **2003**, *14*, 1696.
[17] R. Binions, C. J. Carmalt, I. P. Parkin, *Thin Solid Films* **2004**, *9469-4700*, 416.
[18] R. E. Newnham, Y. M. de Haan, *J. Appl. Phys.* **1960**, *31*, 346.
[19] R. Enjalbert, J. Galy, *Acta Crystallogr., Sect. C* **1986**, *42*, 1497.
[20] P. Pfuner, J. Schoiswohl, M. Socks, S. Surney, M. G. Ramsey, P. F. Netzer, *J. Phys.*: *Condens. Matter* **2005**, *17*, 4035.
[21] O. Muller, J. P. Urbach, E. Goering, T. Weber, R. Barth, H. Schuler, M. Klemm, S. Horn, M. L. der Boer, *Phys. Rev. B: Condens. Matter Mater. Phys.* **1997**, *56*, 15056.
[22] R. Binions, C. J. Carmalt, I. P. Parkin, K. F. E. Pratt, G. A. Shaw, *Chem. Mater.* **2004**, *16*, 2489.
[23] T. Manning, *Ph.D. Thesis*, University College London **2004**.
[24] T. Maruyama, Y. Ikuta, *J. Mater. Sci.* **1993**, *28*, 5073.

Available online at www.sciencedirect.com
ScienceDirect
Thin Solid Films 516 (2008) 1992–1997
www.elsevier.com/locate/tsf

Synthesis and characterisation of W-doped VO_2 by Aerosol Assisted Chemical Vapour Deposition

Clara Piccirillo *, Russell Binions, Ivan P. Parkin

University College London, Chemistry Department, Christopher Ingold Laboratories, 20 Gordon Street, London, WC1H 0AJ, United Kingdom

Received 17 October 2006; received in revised form 25 May 2007; accepted 1 June 2007
Available online 13 June 2007

Abstract

W-doped vanadium dioxide thin films were deposited by Aerosol Assisted Chemical Vapour Deposition. Samples were characterised with several different techniques (i.e. X-ray Diffraction, Raman, Scanning Electron Microscopy–Energy Dispersive X-ray Analysis), to determine their composition and morphology. A study of their optical properties was also performed, to test the suitability of these materials as intelligent window coatings. Good changes in the transmittance and reflectance were observed above the transition temperature (decrease and increase respectively). A linear decrease in the transition temperature with increasing tungsten content was also seen, lowering it to room temperature.

Keywords: $V_xW_{1-x}O_2$; Tungsten dopant; Transition temperature; Intelligent material

1. Introduction

In recent years there has been great interest in vanadium (IV) oxide VO_2, due to its optical properties. At room temperature the most stable form of VO_2 is the monoclinic structure VO_2 (M); at higher temperatures, however, it spontaneously converts into the rutile structure VO_2 (R). This phase change corresponds to a semiconductor (low temperature) to metal to transition (high temperature); it takes place at 68 °C and it is completely reversible [1].

A significant change in the electrical and optical properties in the near IR region is observed when the phase transition takes place. In fact VO_2 (M) has the characteristics of a semiconductor and it does not reflect much solar energy; VO_2 (R), on the contrary, behaves as a semimetal and shows a much higher reflectance [2].

Vanadium dioxide represents a very promising material for intelligent window coating; in fact the increase in reflectance associated with a higher external temperature would mean a reduced solar gain on hot days. This would lower the air conditioning costs; the reduced electrical consumption would also contribute to a decrease in the CO_2 emissions [3].

For VO_2 to be functional and practical as an intelligent window material, the transition temperature has to be decreased from 68 °C to a value closer to room temperature. It has already been reported that a change in the transition temperature (either increase or decrease) can be achieved by inserting metal ion as dopants into the VO_2 lattice [4]. An example of metal raising the transition temperature for VO_2 thin films is titanium [5]; for lowering it, the most promising results have been achieved with tungsten [6]. W-doped VO_2 thin films have been prepared by several methods, including sol–gel [7], Radio Frequency (RF) sputtering [8], physical vapour deposition (PVD) [9] and atmospheric pressure chemical vapour deposition (APCVD) [6].

In this paper we report the synthesis of W-doped VO_2 thin films using Aerosol Assisted Chemical Vapour Deposition (AACVD). In AACVD the precursors are dissolved in a solvent and then an aerosol is generated ultrasonically. The precursor is transported to the substrate through the aerosol droplets by a carrier gas. The solvent needs to have the right physical and chemical properties for aerosol formation [10]; the precursors do not need to be volatile but just soluble in the solvent. This allows the use of a wider range of non-volatile precursors, that

* Corresponding author. Tel.: +44 20 7679 4658; fax: +44 20 7679 7463.
E-mail address: c.piccirillo@ucl.ac.uk (C. Piccirillo).

0040-6090/$ - see front matter © 2007 Elsevier B.V. All rights reserved.
doi:10.1016/j.tsf.2007.06.009

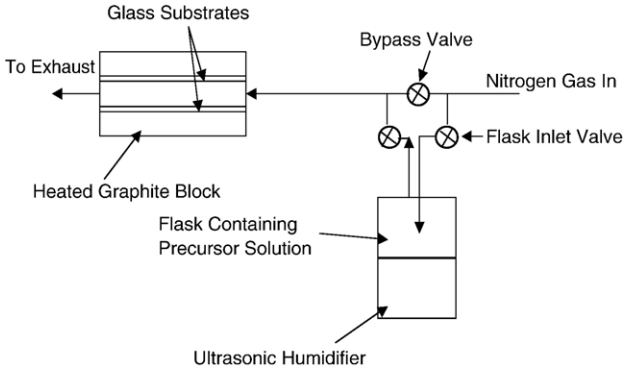

Fig. 1. Schematic representation of the AACVD deposition apparatus.

are not usable with APCVD [11,12]. Another advantage of the AACVD technique is that is simpler and more straightforward to use when more than one precursor is used, for instance to deposit doped thin films. In fact, compared with APCVD, it is far easier to control the precursors proportions in the solution rather than by mixing in the gas phase and hence have control on the metals proportions in the deposited film. Furthermore issues concerning gas phase nucleation blocking the carrier gas tubes are eliminated.

In previous work done by our group, the deposition process of undoped VO_2 with AACVD was studied [13]. It was shown that some experimental parameters, such as the nature of the precursor, the nature of the solvent and the speed of the carrier gas can affect the deposited vanadium oxide phases. The deposition conditions were optimised to obtain only VO_2 (M), with no other vanadium oxide phases or carbon contamination. Therefore, the same conditions were used here to deposit W-doped VO_2, with $[W(OC_2H_5)_5]$ as the tungsten precursor. The deposited films were characterised to determine their composition and structure; functional properties such as reflectance and transmittance in the UV and IR range were also studied. The use of a mixed precursor inside the aerosol gave good control in film stoichiometry and enabled the optical characteristics of VO_2 to be tuned.

2. Experimental details

2.1. Film deposition

VANADYL(IV) acetylacetonate $[VO(C_5H_8O_2)_2]$–$[VO(acac)_2]$ and tungsten (V) ethoxide $[W(OC_2H_5)_5]$ were purchased from Aldrich Chemical Co and used as supplied. The aerosol solution was made by dissolving both precursors into ethanol. For $[VO(acac)_2]$, a constant quantity was used, at 0.075 mol dm^{-3}; for tungsten, different molar amounts of $[W(OC_2H_5)_5]$ were used, in order to have a controlled W/V molar ratio (0.175–2.83%). An aerosol was generated on 50 ml of each solution using a Mountain Breeze humidifier; a nitrogen flow of 1.5 L min^{-1} (BOC, 99.9%) was passed through the aerosol mist, directing the aerosol to a horizontal bed cold wall CVD reactor.

Float glass (Pilkington Glass Plc.) was used as substrates; a SiO_2 layer, about 50 nm thin, used to suppress the diffusion of ions from the glass, coated the 150×45×4 mm sheets. Prior to the deposition, the substrates were cleaned using water, acetone and isopropanol and dried in air. A Tempatron TC4800 thermostat was used to heat the substrates, with the temperature monitored by a Pt–Rh thermocouple. The substrates were heated to a temperature of 550 °C.

The aerosol passed between the heated substrate and a glass top plate, placed 8 mm above the substrate and parallel to it. The exhaust was vented into a fume cupboard. The gas flow was continued until all the precursor solution had passed through the reactor; it normally took between 40 and 50 min. At the end of the deposition the nitrogen flow through the aerosol was diverted and only nitrogen passed over the substrate. A schematic representation of the AACVD deposition apparatus is shown in Fig. 1.

2.2. Film characterisation

X-ray Diffraction (XRD) patterns were measured on a Bruker D8 diffractometer using filtered ($CuK_{\alpha 1+\alpha 2}$) radiation in the reflection mode using glancing angle incidence (1.5°). Scanning Electron Microscopy (SEM) was carried out on a Hitachi filament scanning microscopy, the image was recorded at a voltage of 15 kV. Energy Dispersion X-ray analysis (EDX) was determined on a Phillips XL30 ESEM instrument operating at 7.5 kV. Data were quantified using Oxford Inca Software, with pure metallic vanadium and tungsten used as standards; for each element the collection time was 40 s. Four spots were measured for each sample, the average value from the four measurements was considered. Raman measurements were carried out using a Renishaw system 1000 Raman spectrometer, with an Ar laser excitation source (514 nm). The Raman system was calibrated against the emission lines of argon. Reflectance and transmission spectra were recorded between 300 and 2500 nm on a Perkin Elmer Lambda 950 UV–VIS spectrometer. Measurements were standardised relative to Spectralon® standard (reflectance) and air (transmission). For measurements

Table 1
Tungsten to vanadium molar ratio for the initial solution and the deposited samples

W/V % solution molar ratio	W/V% film molar ratio	Oxide stoichiometry	Transition temperature± hysteresis width (°C)
1.0	0.185	$V_{0.99815}W_{0.00185}O_2$	47±3
1.5	0.175	$V_{0.9825}W_{0.0\ 0175}O_2$	47±5
2.6	0.77	$V_{0.9923}W_{0.0077}O_2$	41±4
3.1	1.06	$V_{0.9894}W_{0.0106}O_2$	36±3
3.3	0.98	$V_{0.9902}W_{0.0098}O_2$	36±4
3.9	1.37	$V_{0.9863}W_{0.0137}O_2$	35±3
4.8	1.34	$V_{0.9866}W_{0.0134}O_2$	35±5
5.9	1.98	$V_{0.9802}W_{0.0198}O_2$	28±4
6.3	2.83	$V_{0.9717}W_{0.0283}O_2$	–

at different temperatures, an aluminium temperature cell, controlled by RS resistive heaters (cartridge heater, 50 W, 6.5×50 mm), Eurotherm temperature controllers and k-type thermocouples were used to manipulate sample temperature. Sample temperature was measured using a k-type thermocouple taped directly onto the film surface.

3. Results and discussion

3.1. Film deposition

Table 1 shows the W/V % molar ratio in the precursors solution; it can be seen that a large range of concentrations was used, to investigate the effect of different tungsten contents on the deposition process and on the film characteristics.

All films had the same appearance of undoped VO_2; they were yellow in colour with a hint of brown. All films passed the Scotch tape test but were scratched by a steel scalpel.

EDX measurements were performed to determine the amount of tungsten included in the vanadium oxide matrix. The instrument had to be used in wavelength dispersion mode (WDX), instead of the standard energy mode, to avoid the overlapping of the tungsten signal with the one from the silicon substrate. The results of the quantitative analysis are reported in Table 1 and shown graphically in Fig. 2. It can be seen that the amount of tungsten included in the film is about one third that expected from the stoichiometry of the solution; indicating that tungsten is slightly more reluctant to enter the film, possibly due to lower decomposition rates of the precursor. Despite this, however, there is good linear correlation between the tungsten content in the solutions and the in coatings. The fitting, performed with the least square method, has a correlation factor $r=0.96$. It can also be observed that films containing comparable tungsten content were deposited from solutions with similar precursor concentration. This shows the reproducibility of the deposition process; it also confirms how with AACVD methodology it is easier to control the ratio of different elements in a deposited film, compared for instance to APCVD.

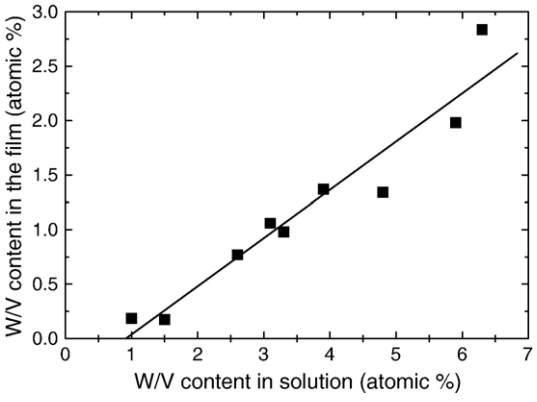

Fig. 2. W/V (atomic %) content in the film vs. the W/V (atomic %) content in the precursor solution. The metals concentration in the films was determined by EDX analysis.

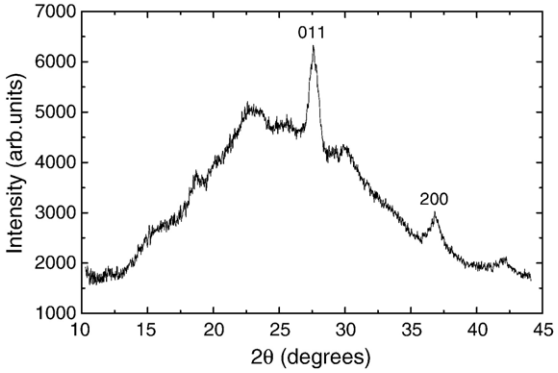

Fig. 3. XRD spectrum of $V_{0.9902}W_{0.0098}O_2$ thin film prepared by AACVD.

3.2. Film characterisation: phase deposited and morphology

All the thin films were characterised by X-ray diffraction to determine the nature of the deposited phases. Fig. 3 shows the XRD spectrum of sample $V_{0.9902}W_{0.0098}O_2$. Because the film was very thin, the broad signal from the glass substrate can still be observed. Despite this, however, a clear diffraction pattern can be identified, and it matches with the one of VO_2 (M) [6]. As previously reported for undoped VO_2 [13], no preferential orientation is observed. No other oxide phases, either of vanadium or of tungsten, are detected in the spectrum. Measurements taken on different parts of the same samples showed the same characteristics, indicating the homogeneity in their composition.

XRD spectra taken for other samples showed similar characteristics, with no change in the peak position with tungsten content. This indicates that the amount of tungsten in the solution does not affect the vanadium phase formed.

The only exception was the film with the highest tungsten concentration (i.e. 2.83%, $V_{0.9717}W_{0.0283}O_2$); in fact more peaks were detected in its spectrum. Literature data report the diffraction pattern of $V_{1-x}W_xO_2$ to be the same as the VO_2 one – with no other phases formed – for x as high as 0.026 [14]; considering the higher tungsten content of our film, it is reasonable to assume that the solubility limit of tungsten in vanadium was exceeded. For this reason, there is formation of W–O and/or W–V mixed phases. Due to the strong signal of the

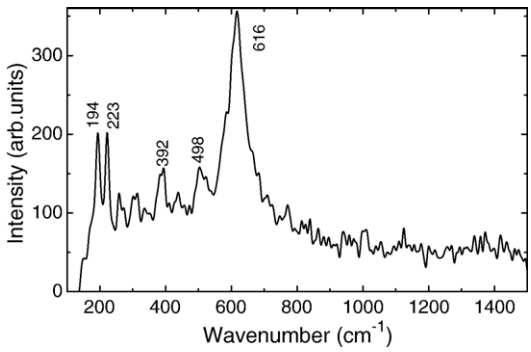

Fig. 4. Raman spectrum for $V_{0.9825}W_{0.00175}O_2$ thin film prepared by AACVD.

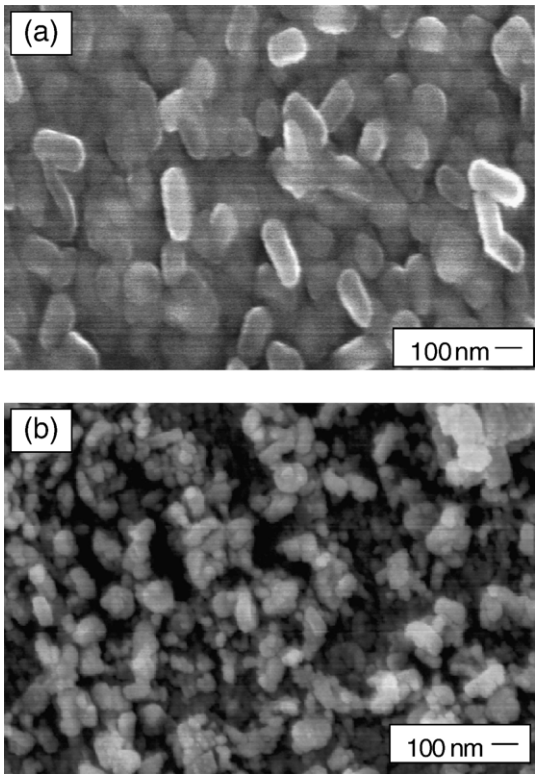

Fig. 5. SEM images for: (a) undoped VO_2, (b) W-doped VO_2 thin film prepared by AACVD.

glass substrate, it was not possible to identify clearly the nature of the mixed phases.

The samples were also analysed by Raman spectroscopy, Fig. 4 shows as an example the spectrum of film $V_{0.9825}W_{00175}O_2$. All the signals detected and marked in the spectrum can be assigned to VO_2 (M) [5], confirming that it is the only deposited phase. The spectrum also shows no sign of carbon contamination in the films (there is no signal corresponding to graphite, at 1355 cm^{-1}). Raman spectra of other samples all showed the same features; no other phase or carbon contamination was detected in any of them.

The absence of carbon contamination in the films was already observed by XPS analysis carried out for other VO_2 thin films deposited in similar conditions. These analyses showed a detectable carbon signals only on the surface of the films; a marked decrease in their intensity was observed moving from the surface to the bulk of the material. This indicated that the only carbon present was surface contamination. Therefore it is reasonable to think that the same thing happens for these W-doped VO_2 samples [15].

Scanning Electron Microscopy analysis was done to study the surface morphology of the deposited films. Fig. 5 shows the image of undoped VO_2 deposited by AACVD (Fig. 5a) compared with W-doped VO_2 (W/V=0.175% atom, Fig. 5b). It can be seen how the microscopic structure of the two films is quite different, indicating the influence of tungsten in the deposition mechanism. All other W-doped VO_2 samples – not shown in the figure – have similar surface morphology; this was observed also for the sample $V_{0.9717}W_{0.0283}O_2$, despite the higher tungsten concentration and the presence of unknown mixed phases in the XRD spectrum. This means that the amount of tungsten in the solution – and hence in the sample – does not change the deposition mechanism and consequently the surface structure.

3.3. Film characterisation: functional properties

The optical properties of the samples were also measured, to investigate the changes taking place for the monoclinic to rutile transitions. In particular, considering the applications of the films as intelligent window coating, the transmittance and the reflectance were measured above and below the transition temperature.

Fig. 6 shows these properties for W-doped VO_2 thin film ($V_{0.9902}W_{0.0098}O_2$). It can be seen how, comparing the behaviour above and below the transition temperature, there is almost no change in the visible range, while there are noticeable changes in the infrared. Fig. 6a shows a remarkable decrease for the transmittance above the transition temperature (up to about −30%), while an increase in the reflectance can be observed in Fig. 6b (about+9%). This is the behaviour expected from an intelligent window material.

Spectra for the other samples with different tungsten contents showed similar qualitative features; again the only exception was the $V_{0.9717}W_{0.0283}O_2$ film, which did not show any change in either reflectance or transmittance with temperature. Literature data report W-doped VO_2 films going through a phase transition (and hence changing the optical properties) for

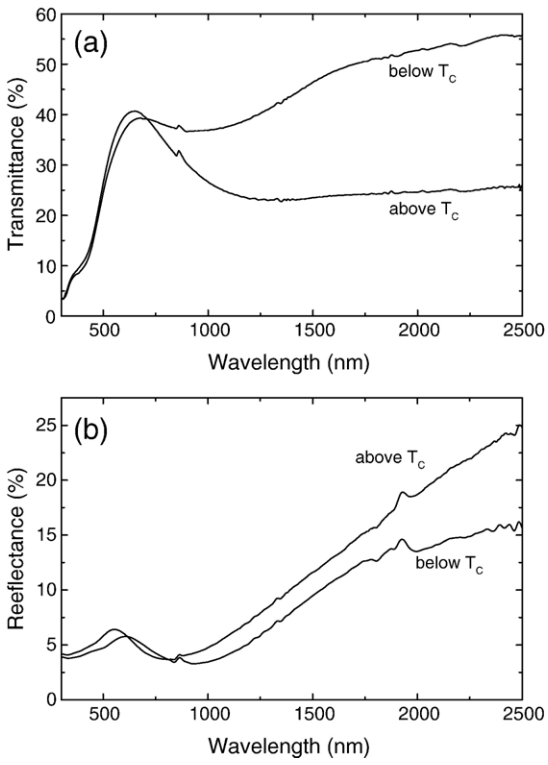

Fig. 6. Transmittance (a) and reflectance (b) IR spectra for $V_{0.9902}W_{0.0098}O_2$ thin film, above and below the transition temperature.

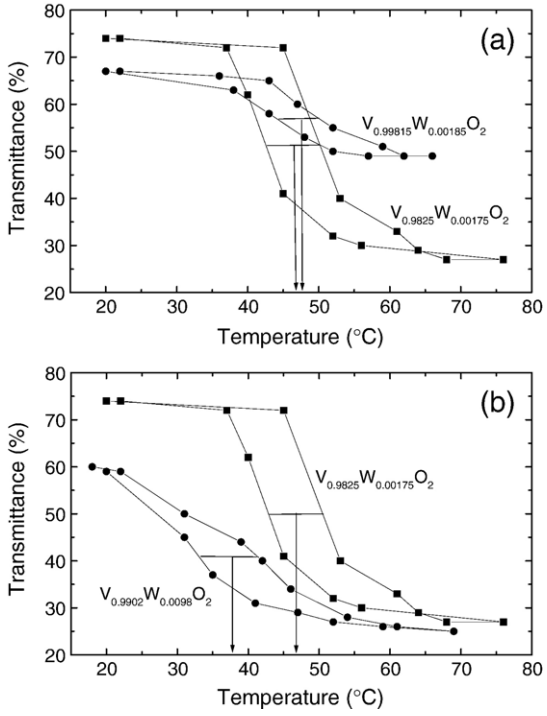

Fig. 7. Transmittance at 4000 cm^{-1} as a function of the temperature. (a) Samples $V_{0.99815}W_{0.00185}O_2$ and $V_{0.9825}W_{0.0\ 0175}O_2$; (b) Samples $V_{0.9825}W_{0.0\ 0175}O_2$ and $V_{0.9902}W_{0.0098}O_2$.

W/V ratio up to 2.6% atom [16].This in agreement with the XRD spectrum not showing any other phase apart from VO_2 [14]. In our case, the XRD of this sample showed the presence of other phases; this indicated that VO_2 is not the only phase, and hence it does not govern the optical behaviour to a measurable extent.

To determine the influence of the amount of dopant, the transition temperature was determined for every sample. This was done by measuring the transmittance at 2500 nm as a function of the temperature. This value of energy was chosen because the change upon transition is quite large (see Fig. 6), and hence easier to monitor. Fig. 7 shows as examples this kind of measurement for two samples similar tungsten content (0.185 and 0.175%, Fig. 7(a)) and for two samples with different tungsten content (0.175 and 0.98%, Fig. 7(b)).

It can be seen how all the samples show the same qualitative behaviour: in fact there is a gradual decrease in the transmittance with increasing temperature, reaching the minimum value between 70 and 80 °C. Cooling down the system, the transmittance increases again, showing the reversibility of the transition. The system, however, shows hysteresis. To determine the transition temperature, the mean value of transmittance is considered; the midpoint of the hysteresis loop for this value of transmittance is the transition temperature (see Fig. 7).

Comparing the samples with similar tungsten content (Fig. 7a), it can be seen how they show a difference both in the relative change of the transmittance and in the width of the hysteresis. These differences were previously observed [17], they can depend on factors such as film thickness and crystallite size; crystallite size can affect the transition temperature as well [6]. These two samples, however, have almost the same transition temperature, that is lower than for the undoped VO_2 [1]; this indicates the effect of tungsten as dopant. The fact that the temperatures are similar for the two samples is in agreement with their comparable tungsten content and it means that, in this case, the effect of the dopant is prevailing on the effect for the different structure.

Comparing the samples with different tungsten content (Fig. 7b), it can be observed how switching temperature decreases with tungsten content, indicating the effectiveness of the metal as dopant. Following this procedure, the transition temperature was estimated for all the samples (apart from sample 9), to establish a correlation with the tungsten content. The results are reported in Table 1 (T_c ± hysteresis width) and are shown in Fig. 8.

The undoped VO_2 sample deposited before with this methodology showed a transition temperature at about 58 °C, a value about 10° lower than the value normally observed for VO_2 (i.e. 68 °C) [13]. This decrease is caused by a strain in the film, an effect normally observed for films thinner than 300 nm [17]. Comparing this value (58 °C) with the data in Fig. 8, it can be stated that an amount of dopant of about 1% reduces the transition temperature of about 22 °C. This is in agreement with data published before for W-doped VO_2 thin films prepared by other techniques; in fact samples prepared with APCVD, PVD and RF sputtering, and containing about 1% tungsten, show a decrease of 20–25 °C [6,8,9].

However, the actual values of the transition temperatures for these AACVD-deposited samples are lower than the APCVD-deposited corresponding ones [6]. This is because, as mentioned above, the T_c value of the undoped AACVD-deposited VO_2 is lower [13].

From Fig. 8 it can be seen that there is a good linear relationship between the tungsten amount included in the films and the transition temperatures. Considering this, it can be said that the decrease in T_c value is caused mainly by the tungsten in the films and not by any strain effect. Increasing the dopant content, T_c can reach values close to room temperature; this makes the material suitable for intelligent window application.

Comparing the hysteresis width with the tungsten content (see Table 1), it does not seem to be any correlation between these two quantities; also, all the values are quite small (between 3 and 5 °C). A possible explanation for this behaviour is that, as mentioned above, the hysteresis width is affected by the

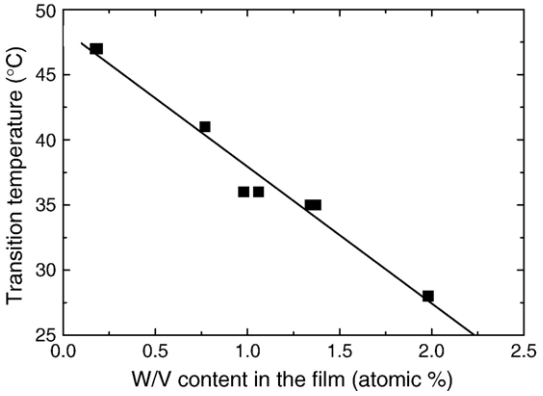

Fig. 8. Transition temperature vs. W/V content for $V_{1-x}W_xO_2$ thin films.

crystallite size; all the W-doped VO_2 samples showed a similar morphological structure, with comparable crystallite sizes (see Fig. 5). Therefore the width of the hysteresis loop will be comparable.

Considering the width for the undoped VO_2 thin films prepared by AACVD, it was observed that the value is bigger than the ones for W-doped VO_2 samples (±8 °C) [13]. This difference can be explained in terms of the surface morphologies shown in Fig. 5: in fact undoped and W-doped VO_2 sample have different structure, indicating different crystallites size and hence different hysteresis width.

The data reported here for AACVD-deposited W-doped thin films are different from what observed for APCVD-deposited samples; in fact the values for hysteresis width of these samples were much bigger; furthermore, an increase in the width with tungsten content was observed [6].

From these results, we can say that AACVD is an appropriate method to deposit W-doped VO_2 films, for some aspects even more suitable than APCVD. In fact, it is a technique simpler to use than APCVD, especially regarding the control of the amount of dopant in the film. Furthermore, no sample showed carbon contamination, even if all the precursors were C-containing one; this is an advantage over the samples deposited with APCVD [18]. Comparing films deposited with the two techniques and containing comparable amounts of tungsten (i.e. 1%), the ones prepared with AACVD showed a lower transition temperature. This can make the films easier to use as intelligent window material. The functional properties of the films were also good; in particular the width of hysteresis loop was smaller than the one observed for APCVD-deposited films and independent of the tungsten content. This would make the films more efficient as intelligent window coatings.

4. Conclusions

AACVD methodology was effectively employed to deposit W-doped VO_2 thin films. The characterisation of the deposits showed that, with tungsten content up to about 2% atom, the only present phase is $V_xW_{1-x}O_2$ (M), without the formation of any mixed W–O or W–V phases. A linear correlation between the amount of tungsten in the solution and the amount included in the films was observed. This shows the potentialities of AACVD methodology to deposit doped thin films; in fact, comparing with APCVD, is it easier to control the proportion of different elements in the deposition process.

A linear decrease in the deposition temperature with the tungsten content was observed, in agreement with data previously published. The transition temperatures of the doped samples were lower than the ones of samples with similar tungsten content, deposited with APCVD methodology. The films showed good functional properties, with reflectance increasing and transmittance decreasing above the transition temperature.

Acknowledgments

This was financially supported by EU project Termoglaze COOP-CT-2005-017761. Authors would like to thank Pilkington Glass for providing the deposition substrates, Mr. Kevin Reeves for the help with Scanning Electron Microscopy, Dr. Steve Firth for the help with Raman spectroscopy. I. P. Parkin thanks the Royal Society/Wolfson Trust for a merit award.

References

[1] T.D. Manning, I.P. Parkin, C. Blackman, U. Qureshi, J. Mater. Chem. 42 (2005) 4560.
[2] F. Morin, J. Phys Rev. Lett. 3 (1959) 34.
[3] EEA — European Environmental Agency, Energy and Environment in The European Union, 2006.
[4] T.E. Phillips, R.A. Murray, T.O. Poelher, Mater. Res. Bull. 22 (1987) 1113.
[5] F. Beteille, R. Morineau, J. Livage, M. Nagano, Mater. Res. Bull. 32 (1997) 1109.
[6] T.D. Manning, I.P. Parkin, M.E. Pemble, D. Sheel, D. Vernardou, Chem. Mater. 16 (2004) 744.
[7] I. Takahashi, M. Hibino, T. Kudo, Jpn. J. Appl. Phys. 40 (2001) 1391.
[8] W. Burkhardt, T. Christmann, B.K. Meyer, W. Niessner, D. Schalch, A. Scharmann, Thin Solid Films 345 (1999) 229.
[9] P. Jin, S. Nakao, S. Tanemura, Thin Solid Films 324 (1998) 151.
[10] K.L. Choy, Prog. Mater. Sci. 48 (2003) 57.
[11] W.B. Cross, I.P. Parkin, Chem. Commun. 14 (2003) 1696.
[12] R. Binions, C.J. Carmalt, I.P. Parkin, Thin Solid Films 469–470 (2004) 416.
[13] C. Piccirillo, R. Binions, I.P. Parkin, Chem. Vap. Depos. 13 (2007) 145.
[14] P. Jin, S. Tanemura, Jpn. J. Appl. Phys. 34 (1995) 2459.
[15] C. Piccirillo, R. Binions, I.P. Parkin, Eur. J. Inorg. Chem. to be published.
[16] W. Burkhardt, T. Christmann, B.K. Meyer, W. Niessner, D. Scalch, A. Scharmann, Thin Solid Films 345 (1999) 229.
[17] T. Maruyama, Y. Ikuta, J. Mater. Sci. 28 (1993) 5073.
[18] M.N. Field, I.P. Parkin, J. Mater. Chem. 10 (2000) 1863.

DOI: 10.1002/ejic.200700284

Nb-Doped VO_2 Thin Films Prepared by Aerosol-Assisted Chemical Vapour Deposition

Clara Piccirillo,[a] Russell Binions,[a] and Ivan P. Parkin*[a]

Keywords: Intelligent materials / Vanadium dioxide (M) / Transition temperature / Niobium doping

Niobium-doped vanadium dioxide ($V_xNb_{1-x}O_2$, x = 0–0.037) thin films were prepared by aerosol-assisted chemical vapour deposition (AACVD) of vanadyl(IV) acetonate and niobium(V) ethoxide in ethanol. Samples were analysed by EDX, XRD, Raman, XPS and SEM. The analyses confirmed the deposition of niobium, even if no separated phase was formed; the morphological structure of the films was affected by the dopant presence. The thin films showed thermochromic behaviour, with a marked change in optical properties above and below the switching temperature.

Introduction

Vanadium(IV) oxide (VO_2) is a material with many interesting characteristics, including a thermochromic phase transition. At room temperature, the most stable phase is the monoclinic VO_2 (M); at higher temperature the rutile phase VO_2 (R) is stabilised. Above a certain temperature, there is a spontaneous transition from the monoclinic to the rutile form, a metal-to-semiconductor transition (MST), that is completely reversible and takes place at 68 °C.[1] A remarkable change in the physical properties is detected on passing through the MST transition; VO_2 (M) behaves as a semiconductor and does not reflect much solar energy, whereas VO_2 (R) is a semimetal and shows markedly higher electrical conductivity and a much higher reflectance, particularly in the infrared range.[2]

Vanadium dioxide represents an ideal material for use as an intelligent window coating, that is a coating that modifies its behaviour in response to an external stimulus, i.e. heat. The low reflectance of the monoclinic phase assures that a coated window allows maximum solar gain on cooler days (T below T_c). The transition to the rutile phase, on the other hand, can help to reduce the heat gain in hot days. The effect would be to have a comfortable environment with reduced air-conditioning costs, which has economical and environmental benefits.[2]

For practical application an intelligent window coating should have its phase-transition temperature closer to a comfortable room temperature value. It has been reported previously that a change in the transition temperature can be obtained by doping metal ions into the VO_2 lattice; doping with titanium, for instance, raises the value of T_c[3] while tungsten, molybdenum and niobium lower it.[4,5]

Up to now, the best reduction in the transition temperature has been obtained by the use of tungsten; in fact W-doped VO_2 thin films have been prepared with different methodologies such as sputtering,[6,7] sol-gel,[8] atmospheric-pressure and aerosol-assisted chemical vapour deposition (APCVD and AACVD).[2,9] These films show a decrease in the transition temperature that is proportional to the amount of tungsten incorporated; samples containing about 1% tungsten, show a decrease of 20–25 °C.[2,6,7] Considering in particular the AACVD methodology, films with values of T_c close to room temperature were deposited.[9]

Niobium-doped VO_2 thin films have been prepared by sol-gel[10] and APCVD methodologies.[5] The results seemed particularly encouraging for APCVD samples; in fact, above the transition temperature, they showed a remarkable decrease in the transmittance in the infrared region, fulfilling the requirement for intelligent window coatings. The problem, however, was the difficulty to incorporate large enough amounts of niobium into the VO_2 films, in fact the highest niobium concentration achieved was 0.4%, corresponding to a T_c value of 55 °C.[11]

In this paper we report the first synthesis of Nb-doped VO_2 thin films with AACVD. With this methodology the precursor is dissolved in a solvent and an aerosol generated ultrasonically. An inert carrier gas transports the precursor (within the aerosol droplets) to the deposition reactor where the reaction takes place. The main advantage of AACVD deposition is that, unlike for APCVD, the precursor does not need to be volatile but just soluble in a solvent appropriate for the aerosol formation.[12] In this way it is possible to use different precursors, not normally used in APCVD.[13,14] Previous work indicates a strong correlation between metal ratios in the precursor solution and those found in the resultant film.[9] AACVD provides an easy method to prepare multi-component and/or doped films.

[a] University College London, Chemistry Department, Christopher Ingold Laboratories,
20 Gordon Street, London, WC1H 0AJ, UK
E-mail: i.p.parkin@ucl.ac.uk

Previous experiments were carried out by our group to deposit VO_2 (M) using AACVD methodology (Figure 1). The effect of different experimental parameters such as solvent, deposition temperature and gas-flow rate was studied and the deposition conditions were optimised to deposit VO_2(M) as the only phase and with no contamination.[15] The same experimental conditions were used to deposit Nb-doped VO_2, with $[Nb(OC_2H_5)_5]$ added as a niobium precursor. Depositions with different Nb/V ratios were performed; the deposited films were analysed to determine their composition, their structure and their behaviour as an intelligent window material.

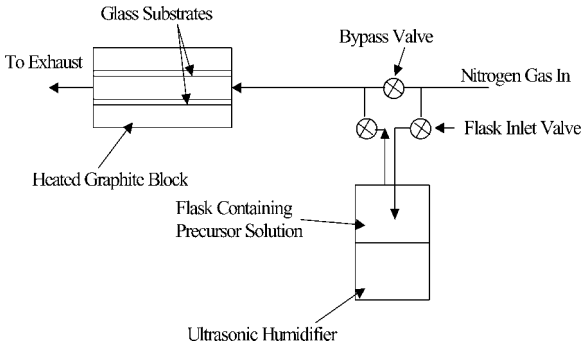

Figure 1. Schematic representation of AACVD experimental apparatus.

Results and Discussion

Film Deposition and Characterisation (Deposited Phases and Morphology)

Vanadium dioxide thin films with different amounts of niobium were deposited, by AACVD of a solution containing $[VO(acac)_2]$ and $[Nb(OEt)_5]$. Table 1 reports the Nb/V precursors ratio employed for the depositions. All deposited films were yellow in colour with some trace of brown, identical to undoped VO_2 films.[15] They all showed good adherence; they passed the Scotch tape test, but they could be scratched by a scalpel and were stable in air.

Table 1. Niobium/vanadium molar ratio for the initial solution and the deposited samples.

Sample	Nb/V solution molar ratio (%)	Nb/V film molar ratio (%)	$T_c \pm$ hysteresis width (°C)
1	1.3	0	58 ± 3
2	5.2	0	58 ± 3
3	7.5	2.6	42 ± 3.5
4	10.3	2.4	44 ± 3
5	12.4	2.2	35 ± 3
6	13.8	3.7	37 ± 3
7	14	3.0	35 ± 4
8	17	2.7	37 ± 3.5
9	18.9	2.8	41 ± 3

To determine the films' composition, i.e. the amount of niobium deposited in each film, EDX analyses were taken. The results are listed in Table 1. It can be seen that for precursor ratios in solution up to 5.2%, there is no niobium detected in the films. The reason for this behaviour is not clear, it is likely that the niobium precursor has to reach a critical concentration before it interacts with the vanadium; this would explain the sudden increase in the Nb/V film ratio from 0 to 2.6%.

For higher concentrations in solution, there is an increase of the niobium concentration in the deposits; however, the value reaches a plateau and it remains stable (within experimental error), despite the increase in concentration of niobium in solution. An explanation for these results can be that the value of the solubility limit on niobium in vanadium is reached; however, no data are available in literature to confirm this.

From this data it can be seen that niobium behaves very differently from tungsten in VO_2 films deposited by AACVD; in fact a linear correlation was observed for tungsten between the amounts of precursor in solution and the metal in the film.[9] Furthermore, a much greater proportion of the tungsten precursor was included in the VO_2 film as metal dopant (e.g. a W/V atom ratio of about 6% in solution corresponded to about 2% in the film).

The different behaviour of niobium confirms the difficulties previously reported with this metal already observed in APCVD.[11] In comparison a much greater amount of metal was deposited in the AACVD samples; this indicates the suitability of the technique for the deposition of multicomponent/doped films.

The XRD patterns of all samples were recorded to determine the nature of the phases present; Figure 2 shows the XRD spectrum of sample **5**. It can be seen, despite the glass background signal, that the deposited film is unambiguously VO_2(M).[2] Similarly to undoped VO_2 and W-doped VO_2 deposited by AACVD, no preferential orientation is observed.[9] No other phase was detected, neither for niobium nor for other vanadium oxides. Other areas of the same film showed the same pattern, indicating good homogeneity of the film. All the thin films investigated, with different niobium concentration, had the same characteristics; this indicates that the amount of dopant does not affect the nature of the phase deposited and that, under these conditions, it does not favour the formation of mixed phases.

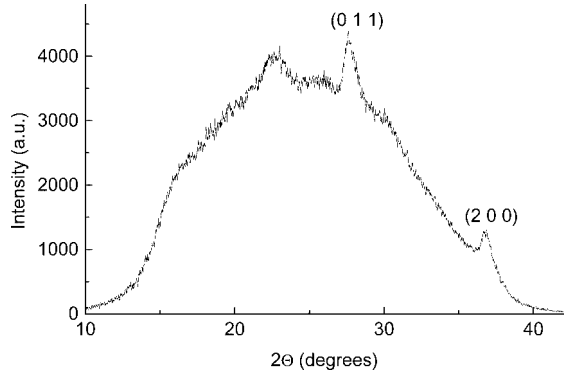

Figure 2. XRD spectrum of sample **5**.

The Raman spectrum of sample **5** is shown in Figure 3. It can be seen that it shows the characteristics VO_2 pattern. In fact all the detected signals can be assigned to VO_2 (M); furthermore, there is no signal corresponding to graphitic carbon (i.e. at 1355 cm^{-1}), indicating no carbon contamination of the film.

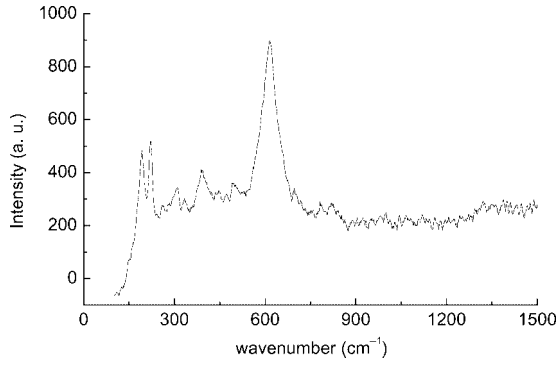

Figure 3. Raman spectrum for sample **5**.

XPS spectra of Nb-doped VO_2 samples were acquired to detect the possible other elements deposited in the film as impurities and to determine the oxidation states of the main film components. From the analysis of the survey spectrum (registered on the surface of the film), it was seen that the only additional element detected in the film is carbon. However, the intensity of the carbon signals decreased remarkably moving from the surface into the bulk of the film; this indicates the carbon is present only on the surface as contaminant from the external environment, but it is not present in the bulk of the film. This is in agreement with what was observed by Raman spectroscopy; in fact the signals in the Raman spectra are related to the bulk of a material and not just to its surface.

Figure 4(a) and (b) show the sections of the spectrum corresponding to the niobium and vanadium, respectively, for sample **5**; as mentioned above, the spectrum was registered on the surface of the film. The niobium peaks were detected for $Nb3d_{5/2}$ and $Nb3d_{3/2}$ at the binding energies of 207.0 and 209.2 eV. These values correspond to the binding energies of Nb_2O_5, therefore it follows that the niobium oxidation state is +5.[16] This is in agreement with previously published data,[11] hence it confirms that niobium does not change its oxidation state during the deposition. Spectra acquired in the bulk of the film show that niobium has the same oxidation state throughout the film.

The analysis of the part of the spectrum corresponding to vanadium shows that the main signal consists of two overlapping peaks at 516.2 and 517.4 eV (the deconvolution is shown in Figure 4). These two binding energies correspond to $V2p_{3/2}$ (+4) and $V2p_{3/2}$ (+5).[16] This indicates that, on the surface of the film, VO_2 is partly oxidised to V_2O_5.

Moving to the bulk of the film, however, only the peak corresponding to V^{IV} is detected (spectrum is not shown). These results are in agreement with the XRD and Raman results; in fact no V_2O_5 signal was observed by either technique (see Figures 2 and 3), because they analyse the bulk of the film and not just the surface.

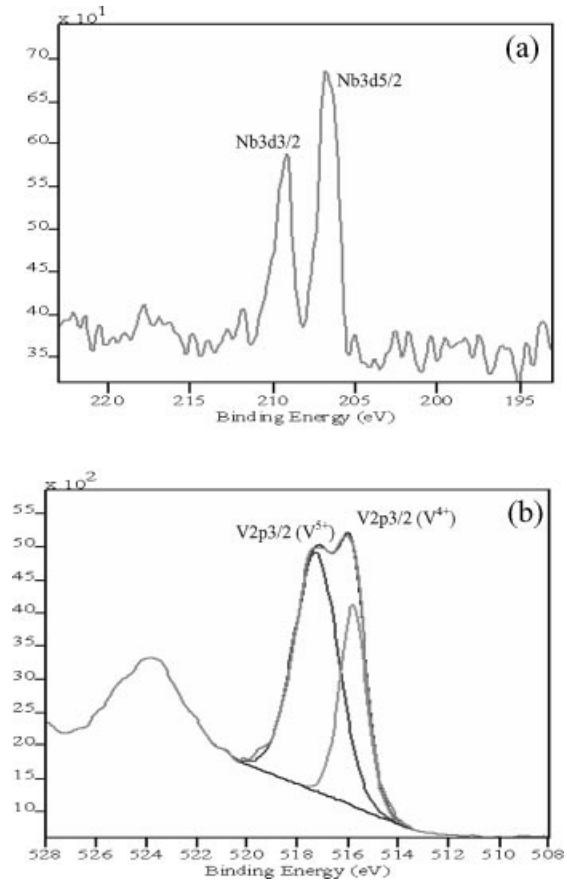

Figure 4. XPS spectrum for sample **5**: (a) niobium section; (b) vanadium section.

The morphology of the Nb-doped VO_2 thin films was studied by scanning electron microscopy (SEM). Figure 5 compares the surface structure of undoped VO_2 [Figure 5(a)] with the one of Nb-doped VO_2 [sample **7**, Fig-

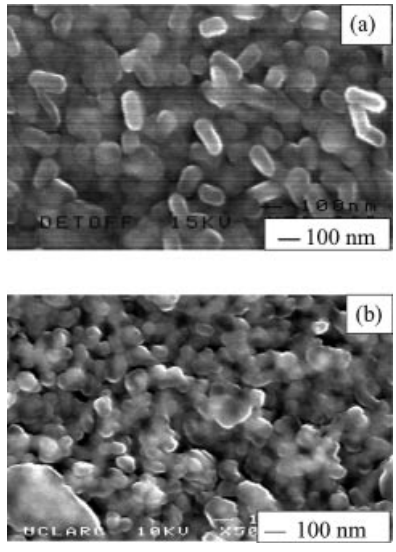

Figure 5. SEM images for (a) undoped VO_2; (b) sample **7**.

ure 5(b)], both deposited using AACVD. It can be observed that they look quite different, indicating the effect of niobium on the film structure. Other films with different niobium concentrations have a similar morphology, indicating that the amount of niobium does not have any influence on the morphology.

Film Characterisation: Functional Properties

The optical properties of the samples were investigated and their thermochromic change through the monoclinic-rutile phase transition studied. The change in transmittance and reflectance above and below the transition temperature was measured to assess the efficiency and the suitability of this material as an intelligent window coating.

Figure 6 shows the transmittance and reflectance spectra above and below the transition temperature for sample **9**. Considering the transmittance [Figure 6(a)], there is a significant decrease above the transition temperature (up to 30%) in the infrared range. The spectra of all the other samples showed the same features, with some changes in the extent of the decrease in the transmittance, which was dependant on the thickness of the films. This behaviour is analogous to the one shown by both undoped and W-doped VO_2.[9,15]

The change in the reflectance, however, has different characteristics depending on the niobium content of the film; Figure 6(b) and (c) show the reflectance spectra of samples **5** and **9**, respectively. For sample **5**, an increase above T_c can be observed for the full infrared range; for sample **9**, on the contrary, such increase can be seen only for wavelengths larger than 1650 nm. At about 1650 nm the two lines cross over, therefore the curve corresponding to the reflectance above T_c is slightly less intense than the one representing the reflectance below T_c. Similar to the Raman spectra, this different behaviour was observed for samples **6**, **7**, **8** and **9**, when the niobium concentration in the films is about 3%; the two curves cross over in a range of energy between 1550 and 1650 nm. The comparison of these results suggests that probably the presence of another phase affects the change in the reflectance, limiting it to a smaller energy range.

The value of the transition temperature was also determined for each sample. This was done by measuring the transmittance at 4000 cm^{-1} as a function of the temperature. Figure 7 shows as an example the measurements for samples **4** and **7** (Nb/V = 2.4 and 3.0%, respectively). As shown in Figure 7, the transition temperature was determined considering the average value of the transmittance; the midpoint of the hysteresis loop for this value of transmittance is the transition temperature. It can be seen that the larger the Nb/V ratio, the lower is the value of the temperature. This shows the effectiveness of niobium to decrease T_c. Table 1 reports the value of T_c for every sample ± the width of the hysteresis loop. Similarly to what is observed for W-doped VO_2 deposited with AACVD, the width of the hysteresis loop does not change with the decrease of the transition temperature which is constant between 3 and 4 °C.

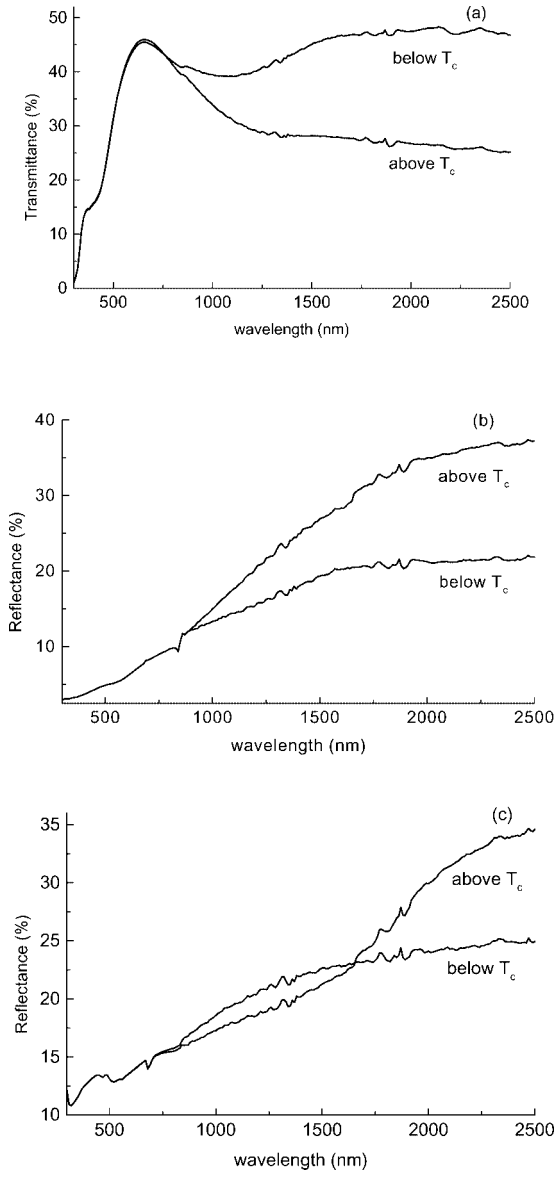

Figure 6. Optical properties above and below T_c. (a) Transmittance for sample **9**; (b) reflectance for sample **5**; (c) reflectance for sample **9**.

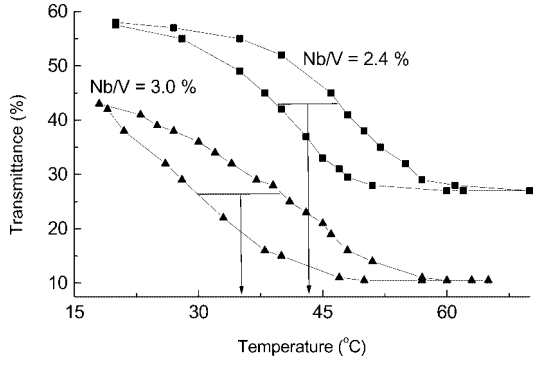

Figure 7. Transmittance at 4000 cm^{-1} as a function of the temperature for samples **4** and **7** (Nb/V atom ratio 2.4 and 3%, respectively).

Figure 8 shows the value of T_c as a function of the niobium content in the film and that a good linear correlation is established. From this data it can be seen that an amount of niobium in the film of 2% lowers the transition temperature by 15 °C. It follows that niobium is less effective than tungsten to decrease the value of T_c (for tungsten, 1% of dopant decreases T_c by about 22 °C);[9] it is, however, still possible to achieve values of transition temperatures close to room temperature.

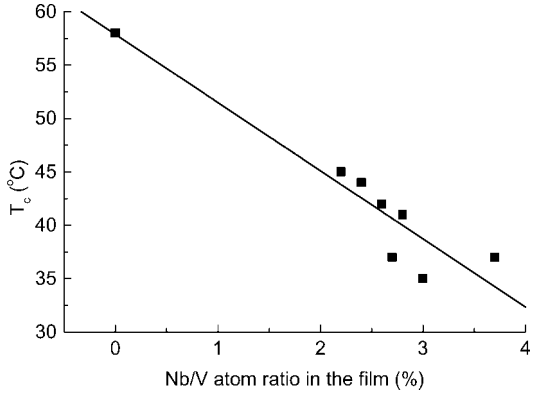

Figure 8. Transition temperature vs. the Nb/V atom ratio in the films.

Conclusions

Nb-doped VO_2 thin films were successfully deposited by *A*erosol-*A*ssisted *C*hemical *V*apour *D*eposition (AACVD). EDX analysis showed that an increase in the niobium concentration in solution correlates to an increase in niobium in the film as well, until a plateau is reached. Samples with a niobium content up to 3.7% (atom ratio) were prepared, VO_2 films with such high niobium concentrations were never deposited before. This indicates the suitability of the AACVD methodology to deposit doped thin films.

Films were characterised by several analytical techniques (XRD, Raman, SEM, XPS) to determine the nature of the deposited phase and to detect possible impurities. The functional properties of the films (reflectance/transmittance, transition temperature) were studied as well, to test their application as an intelligent material for window coating. Significant changes in the transmittance and reflectance properties were observed on passing the transition temperature; furthermore, a decrease in the transition temperature was observed, with a linear correlation, between the films' niobium content and the value of the temperature. These features indicate Nb-doped VO_2 as a suitable material for application in smart windows.

Experimental Section

Film Deposition: Vanadyl(IV) acetylacetonate $[VO(C_5H_8O_2)_2]$ = $[VO(acac)_2]$ and Nb^V ethoxide $[Nb(OC_2H_5)_5]$ were purchased from Aldrich Chemical Co and used as supplied. The aerosol solution was prepared by dissolving both precursors in ethanol. For $[VO(acac)_2]$, a constant concentration of 0.05 mol dm^{-3} was used. Different molar amounts of $[Nb(OC_2H_5)_5]$ were used, in order to have a varying Nb/V molar ratio (5.2–17 mol-%). An aerosol was generated from 50 mL of precursor solution using a Mountain Breeze humidifier; a nitrogen flow of 1.5 L min^{-1} (BOC, 99.9%) was passed through the aerosol mist, directing the aerosol to a horizontal bed cold wall CVD reactor. Sheets of float glass ($150 \times 45 \times 4$, Pilkington Glass Plc.) were used as deposition substrates; an SiO_2 layer, about 50 nm thick, was used to suppress the diffusion of ions from the bulk glass. Prior to the deposition, the substrates were cleaned using water, acetone and 2-propanol and then dried in air. A Tempatron TC4800 thermostat was used to heat the substrates, with the temperature monitored by a Pt-Rh thermocouple. The substrates were heated to a temperature of 500 °C. The aerosol passed between the heated substrate and a glass top plate, placed 8 mm above the substrate and parallel to it. The exhaust was vented into a fume cupboard. The gas flow was continued until all the precursor solution had passed through the reactor; it normally took between 40 and 50 min. At the end of the deposition, the nitrogen flow through the aerosol was diverted and only nitrogen passed over the substrate. A schematic representation of the AACVD deposition apparatus is shown in Figure 1.

Film Characterisation: X-ray powder diffraction patterns were measured with a Bruker D8 diffractometer using filtered (Cu-$K_{\alpha 1+\alpha 2}$) radiation in the reflection mode using glancing angle incidence (1.5°). SEM was carried out with a Hitachi filament scanning microscop. EDAX was determined with a Philips XL30 ESEM instrument, data was quantified using Oxford Inca Software. Raman measurements were carried out with a Renishaw system 1000 Raman spectrometer, with an Ar laser excitation source (514 nm). The Raman system was calibrated against the emission lines of argon. X-ray photoelectron spectroscopy (XPS) measurements were carried out with a VG ESCALAB 220i XL instrument using monochromatic Al-K_α radiation. Binding energies were referenced to surface elemental carbon at 284.6 eV. Depth profiling was carried out using a 3-kV argon ion gun operating at 0.5 μA to sputter the surface of the film. Reflectance and transmission spectra were recorded between 300 and 2500 nm with a Perkin–Elmer Lambda 950 UV/Vis spectrometer. Measurements were standardised relative to a Spectralon® standard (reflectance) and air (transmission). For measurements at different temperatures, an aluminium temperature cell, controlled by RS resistive heaters, Eurotherm temperature controllers and k-type thermocouples were used to manipulate the sample temperature. The sample temperature was measured using a k-type thermocouple taped directly onto the film surface.

Acknowledgments

This research was financially supported by the EU project Termoglaze COOP-CT-2005-017761. The authors would like to thank Pilkington Glass for providing the deposition substrates, Mr. Kevin Reeves for the help with scanning electron microscopy, Dr. Steve Firth for the help with Raman spectroscopy. I. P. P. thanks the Royal Society/Wolfson Trust for a merit award.

[1] F. J. Morin, *Phys. Rev. Lett.* **1959**, *3*, 34–36.
[2] T. D. Manning, I. P. Parkin, R. J. H. Clark, D. Sheel, M. E. Pemble, D. Vernadou, *J. Mater. Chem.* **2002**, *12*, 2936–2939.
[3] F. Beteille, R. Morineau, J. Livage, M. Nagano, *Mater. Res. Bull.* **1997**, *32*, 1109–1117.
[4] T. D. Manning, I. P. Parkin, M. E. Pemble, D. Sheel, D. Vernardou, *Chem. Mater.* **2004**, *16*, 744–749.

[5] T. D. Manning, I. P. Parkin, C. Blackman, U. Qureshi, *J. Mater. Chem.* **2005**, *15*, 4560–4566.
[6] W. Burkhardt, T. Christmann, B. K. Meyer, W. Niessner, D. Schalch, A. Scharmann, *Thin Solid Films* **1999**, *345*, 229–235.
[7] P. Jin, S. Nakao, S. Tanemura, *Thin Solid Films* **1998**, *324*, 151–158.
[8] I. Takahashi, M. Hibino, T. Kudo, *Jpn. J. Appl. Phys.* **2001**, *40*, 1391–1395.
[9] C. Piccirillo, R. Binions, I. P. Parkin, *Thin Sol. Films*, submitted for publication.
[10] C. B. Greenberg, *Thin Solid Films* **1983**, *110*, 73–82.
[11] T. D. Manning, Ph. D. Thesis, London, **2004**.
[12] K. L. Choy, *Prog. Mater. Sci.* **2003**, *48*, 57–170.
[13] W. B. Cross, I. P. Parkin, *Chem. Commun.* **2003**, *14*, 1696–1697.
[14] R. Binions, C. J. Carmalt, I. P. Parkin, *Thin Solid Films* **2004**, *469–470*, 416–419.
[15] C. Piccirillo, I. P. Parkin, R. Binions, *Chem. Vap. Depos.*, in press.
[16] C. D. Wagner, A. V. Naumkin, A. Kraut-Vass, J. W. Allison, C. J. Powell, J. R. Rumble, *NIST X-ray Photoelectron Spectroscopy Database*, version 3.4 (web version), NIST, **2003**, http://srdata.nist.gov/xps/.

Received: March 12, 2007
Published Online: July 11, 2007

Thin Solid Films 517 (2009) 4565–4570

Contents lists available at ScienceDirect

Thin Solid Films

journal homepage: www.elsevier.com/locate/tsf

Atmospheric pressure chemical vapour deposition of thermochromic tungsten doped vanadium dioxide thin films for use in architectural glazing

Christopher S. Blackman *, C. Piccirillo, R. Binions, Ivan P. Parkin

Department of Chemistry, University College London, 20 Gordon Street, London, WC1H 0AJ, United Kingdom

ARTICLE INFO

Article history:
Received 8 August 2008
Received in revised form 12 December 2008
Accepted 23 December 2008
Available online 10 January 2009

Keywords:
Vanadium oxide
Thermochromic
Tungsten doping
Chemical vapor deposition (CVD)

ABSTRACT

Atmospheric pressure chemical vapour deposition of VCl_4, WCl_6 and water at 550 °C lead to the production of high quality tungsten doped vanadium dioxide thin films. Careful control of the gas phase precursors allowed for tungsten doping up to 8 at.%. The transition temperature of the thermochromic switch was tunable in the range 55 °C to −23 °C. The films were analysed using X-ray diffraction, scanning electron microscopy, Raman spectroscopy and X-ray photoelectron spectroscopy. Their optical properties were examined using variable-temperature transmission and reflectance spectroscopy. It was found that incorporation of tungsten into the films led to an improvement in the colour from yellow/brown to green/blue depending on the level of tungsten incorporation. The films were optimized for optical transmission, thermochromic switching temperature, magnitude of the switching behaviour and colour to produce films that are suitable for use as an energy saving environmental glass product.

1. Introduction

Reducing the energy demands of residential and office buildings by controlling the amount of solar energy entering a building is one step that can be taken in the fight against global warming. One possible way to achieve this is by using a thin film of a thermochromic material on an exterior window [1].

During hot weather a 'smart' window would pass all or part of the visible radiation incident on the window and reflect the majority the Sun's near-infrared radiation; thus the need for the use of air conditioning is diminished. During cooler weather the same level of visible radiation would pass through the window whilst allowing some of the Sun's near-infrared radiation, limiting the need for internal heating. Such intelligent coatings could be used in a myriad of applications including windscreens of automobiles, sunscreens and greenhouses. The development of such coatings could lead to large savings in energy costs (e.g. power to air conditioning units), improved building environments, and environmental benefits (e.g. reduced CO_2 emissions).

Vanadium dioxide is a thermochromic material that is known to exist in four polymorphic forms; monoclinic VO_2(M) and rutile VO_2 (R) and two metastable forms VO_2(A) and VO_2(B) [2]. The monoclinic VO_2(M) converts to rutile VO_2(R) at 68 °C [3]. This is a fully reversible metal to semiconductor phase transition (MST) and is associated with large changes in electrical conductivity and optical properties in the near-IR region [4]. Above 68 °C, VO_2 behaves as a semi-metal and is reflecting to a wide range of solar wavelengths whilst below the MST it behaves as a semiconductor, and reflects significantly less in the near infrared.

Thermochromic properties and thermochromic materials for window glazing applications have been investigated previously [5,6]. By the late 1980's thin-film thermochromic properties had been demonstrated by a number of groups employing physical vapour deposition (PVD) [7] or sol–gel based deposition techniques [1,8–11]. These technology advances were not transferable into commercially relevant products because of inappropriate transition temperatures, low visible light transmission, unattractive visible colours and limited film durability.

Chemical vapour deposition (CVD) is an excellent method for applying thin films to glass substrates during commercial glass manufacture. Atmospheric Pressure CVD (APCVD) has been previously used to deposit VO_2 thin films on glass substrates. The process has the advantage of being easily integrated into float-glass production lines and has fast deposition rates. Vanadium alkoxides [12], [$V(acac)_3$] [13], $VO(acac)_2$ [14,15] and various oxovanadium reagents [16] have been used as deposition precursors. Vanadium(IV) chloride and an oxygen source such as methanol or ethanol has been used to prepare V_2O_5 which was subsequently post-reduced to VO_2 by heating in a reducing atmosphere [17], however the films were significantly contaminated with carbon[17]. Aerosol Assisted Chemical Vapour Deposition has also been used to deposit a range of vanadium oxides from V_2O_3 to V_2O_5 [18].

For thin-films of VO_2 to find practical use as smart window coatings, the MST needs to be reduced from 68 °C to a more ambient temperature that will depend on the climate the window is to be used in. Doping metal ions into the VO_2 lattice has been shown to increase or decrease the MST temperature (T_c) depending on factors such as size [19] and charge [20] of the dopant ion and subsequent changes in

* Corresponding author.
E-mail address: c.blackman@ucl.ac.uk (C.S. Blackman).

0040-6090/$ – see front matter © 2009 Elsevier B.V. All rights reserved.
doi:10.1016/j.tsf.2008.12.050

electron carrier density [21]. For films produced using PVD, thickness less than 30 nm has also been shown to influence the thermochromic transition temperature of VO_2, this has been explained in terms of a strain effect [16].

Tungsten has been shown to be the most effective dopant ion in reducing the MST of VO_2, it can optimally lower the T_c to about 25 °C at 2 atom% loading. Tungsten-doped VO_2 films have been previously prepared by sol–gel [1,22], physical vapour deposition methods [7,23] and CVD; both atmospheric pressure [14,24–27] and aerosol-assisted [28].

This paper reports a systematic investigation about the deposition of W-doped VO_2 with Atmospheric Pressure CVD; the effect of tungsten on the value of T_c was studied over a range of concentrations wider than ever previously reported. The effect of high tungsten content on the optical properties of the films was also considered, particularly regarding the optical transmission in the visible, the colour and the smart material functional properties (i.e. change in reflection and transmittance with temperature).

2. Experimental details

2.1. Film preparation

Nitrogen (99.999%, BOC, UK) was used as the system gas in all CVD reactions. The substrates were float glass with a 50 nm-thick SiO_2 barrier layer to stop diffusion of ions from the glass into the film (Pilkington Glass, UK). The glass substrates had dimensions 15 cm × 4.5 cm × 0.3 cm and were cleaned prior to use by wiping with a water-soaked tissue, then a propan-2-ol soaked tissue and finally rinsed with propan-2-ol. The substrates were allowed to dry in air prior to mounting in the CVD chamber.

All CVD studies were performed on custom built apparatus using a previously described procedure [24,25]. VCl_4 (99%, Aldrich, UK) and WCl_6 (99.9%, Strem, UK) were placed into separate bubblers. Distilled water was injected into the plain line gas-flow using a variable rate syringe driver and either a 1000 µL 'tuberculin' syringe or a Hamilton 250 µL gas tight syringe—all of the water was effectively flash evaporated as the plain line was heated to 150 °C. The VCl_4 bubbler was set to 50 °C using a flow rate of 0.4 L/min N_2, the N_2 plain flow was 10 L/min, the mixing chamber temperature 150 °C and the reactor temperature of 550 °C. To alter the VCl_4:H_2O ratio the speed of the syringe driver injecting the H_2O from a 250 µL syringe was varied. The temperature of the tungsten bubbler was varied to change the amount of tungsten in the resultant film. The time of each deposition experiment was varied in order to change the thickness of the resultant film. All films were produced at least in triplicate to check and ensure high levels of reproducibility.

2.2. Film analysis and characterization

Analysis of the deposited films consisted of UV/vis absorption, adhesion tests (scratch and abrasion resistance, Scotch tape test), vis/IR reflectance–transmittance, micro-Raman spectroscopy, scanning electron microscopy and wavelength dispersive analysis of X-rays (SEM/WDX), X-ray diffraction (XRD) and X-ray photoelectron spectroscopy (XPS). The samples were not cleaned prior to analysis. UV/vis absorption measurements were obtained on a Thermospectronic Helios spectrometer between 300–1100 nm. Reflectance–transmittance measurements were performed on a Perkin Elmer Lambda 950 spectrophotometer between 300–2500 nm; transmission measurements were calibrated in air, whilst reflectance measurements were calibrated to a Spectralon standard. The size of the MST and T_c were measured using a Perkin–Elmer 457 grating spectrometer set to 4000 cm^{-1} and calibrated against the spectrometer transmission in air at 4000 cm^{-1}. An aluminium temperature cell controlled by RS cartridge heaters, Eurotherm temperature controllers and type-K thermocouples was used to control the sample temperature. Measurements below room temperature were made by cooling the thin films sample using solid CO_2 prior to mounting in the temperature cell. Raman spectroscopy was performed on a Renishaw inVia spectrometer using a 514.5 nm 6 mW laser at 50× magnification; sample temperature was controlled by a Linkam THMS600 variable temperature cell with a liquid nitrogen pump. SEM images were obtained on a Jeol JSM-6301F scanning electron microscope at 15 kV accelerating voltage. Samples were prepared by deeply scoring the film side of the substrate to cause shelling of the film and hence a distinct edge between the film and substrate. Wavelength dispersive analysis of X-rays was performed on a Philips XL30 ESEM instrument using Inca analytical software (Oxford Instruments) with an accelerating voltage of 5 kV. X-ray analysis of the films was determined on a Bruker D8 GADDS diffractometer using Cu K_α radiation at 1.54 Å collimated with either a 15 cm long 0.05 mm collimator (1–2 mm^2 illumination area) or 7 cm long 0.1 mm collimator (3–5 mm^2 illumination area) with a 5° incident angle. Diffraction patterns at different temperatures were obtained by acquiring discrete data at various temperatures. The temperature was controlled using the aluminium sample holder described above. X-ray photoelectron spectrometry was performed on a VG ESCALAB 2201 XL instrument

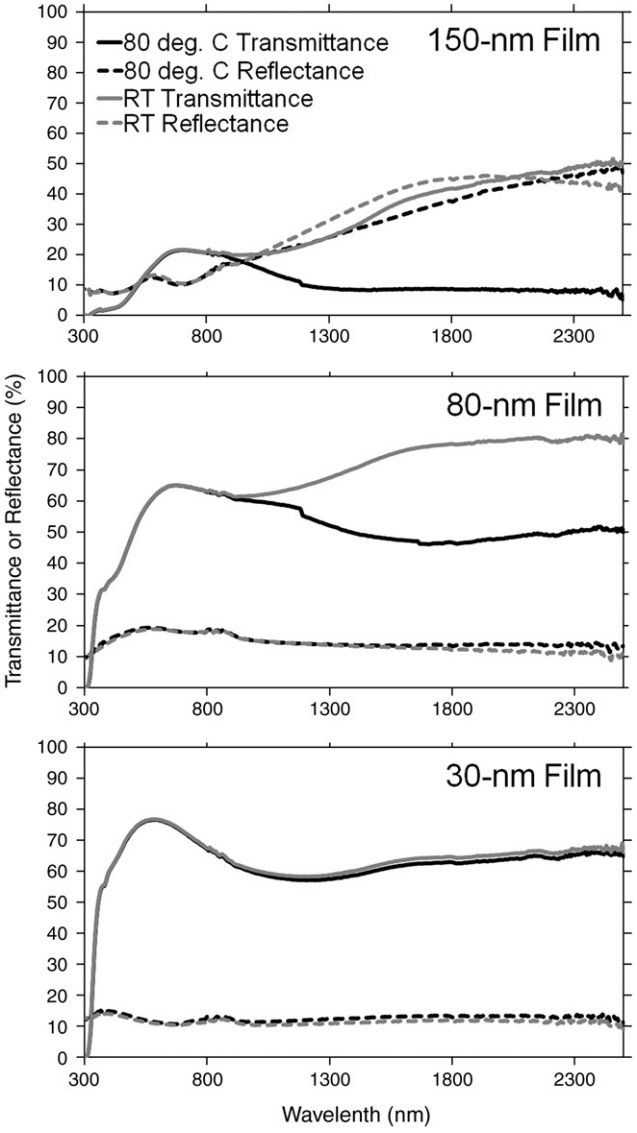

Fig. 1. Transmission and reflection spectra at room temperature and 80 °C for 30 nm, 80 nm and 150 nm thick VO_2 films prepared by APCVD of VCl_4 and water at a 1:3 ratio corresponding to deposition time of 30, 60 and 240 s respectively.

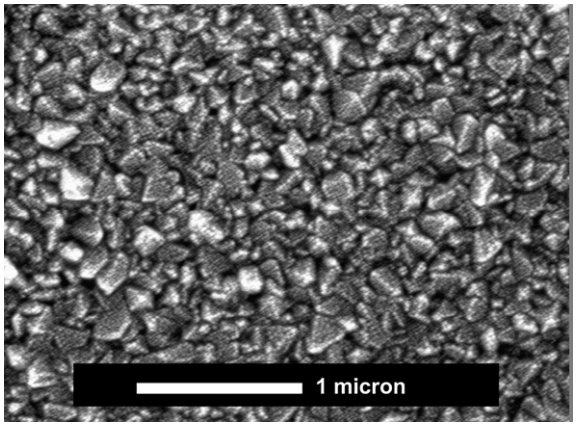

Fig. 2. SEM image of W-doped doped 80 nm thick VO_2 film prepared by APCVD of VCl_4, WCl_6 and water with a VCl_4:H_2O ratio of 1:3; temperature of the WCl_6 bubbler of 130 °C.

using monochromatic Al K_α X-rays with pass energy of 50 eV. Samples were not cleaned prior to use and a flood gun was used to control charging and the binding energies were referenced to an adventitious C 1 s peak at 284.8 eV. Depth profile measurements were obtained using argon beam sputtering (etch voltage 5 kV). XPS data was analysed using CasaXPS software version 2.0.11. Samples were subjected to scratch and abrasion tests with a piece of tissue, a brass stylus and a steel stylus. Samples were considered to pass the test if they remained unmarked to the naked eye. Additionally the Scotch tape test was performed; in this test a piece of Scotch tape is placed on the film and removed. The sample fails the test if any of it delaminates and remains on the Scotch tape.

3. Results

The APCVD reaction of vanadium (IV) chloride, tungsten(VI) chloride and water afforded thin films of un-doped or tungsten doped vanadium dioxide on glass substrates depending on the exact conditions used. The films were a transparent yellow/brown colour in appearance, unless they had more than 2.5 at.% tungsten doping in which case they appeared bluer (but just as transparent) in colour. The films were adherent to the glass substrate and could not be removed by abrasion with a paper towel or the application of Scotch tape. They could however be marked with a brass or steel stylus.

Experimental conditions that reliably produced glassy and adherent films of VO_2 were determined. Un-doped VO_2 thin films were deposited using a plain flow of 10 L/min N_2, with the VCl_4 bubbler temperature set to 50 °C and a bubbler flow rate of 0.4 L/min, with a VCl_4:H_2O ratio of 1:3. The change in optical and functional properties with film thickness were examined to identify the range of film thickness appropriate to give optical transparencies in an acceptable range. Once deposited, the films were analyzed for optical and functional properties by measuring the room-temperature and high-

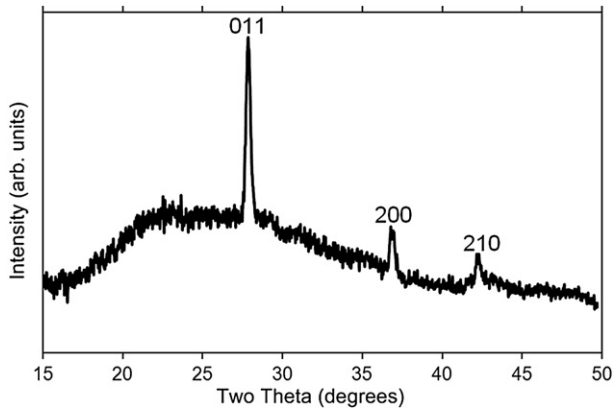

Fig. 3. X-ray diffraction pattern (below T_c) of a 1.5 at.% W-doped 80 nm thick VO_2 thin film.

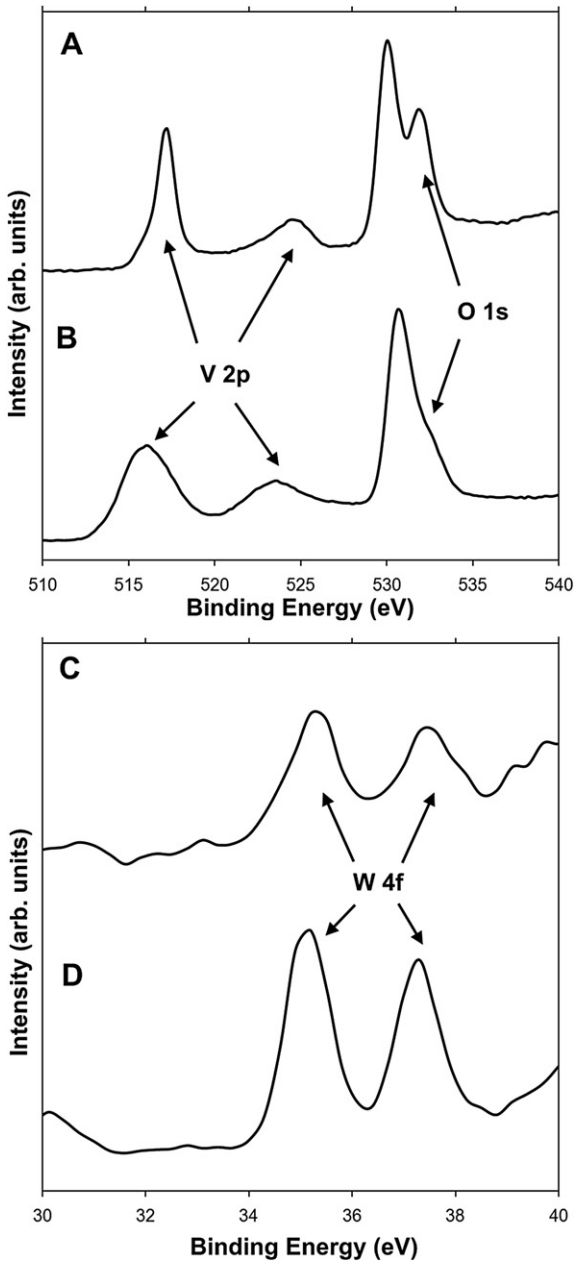

Fig. 4. XPS V 2p and O 1 s spectra of the (A) as-deposited and (B) etched surface of 1.5 at.% W-doped VO_2 films and W 4f spectra of (C) 1.5 at.% and (D) 8 at.% W-doped VO_2 films.

Table 1
Summary of WCl_6 bubbler temperature and resultant at.% W-dopant concentration and T_c.

WCl_6 bubbler temperature (°C)	W-dopant concentration (at.%) in film[value (standard deviation)] as measured by WDAX.	T_c (°C) [value (error)] as determined by Raman spectroscopy and Infra red hysteresis measurements.
100	0.12 (0.10)	55 (±5)
110	0.28 (0.11)	50 (±5)
120	0.64 (0.06)	45 (±5)
130	1.56 (0.36)	20 (±2.5)
152	1.75 (0.29)	5.5 (±2.5)
165	3.00 (1.89)	−15.5 (±2.5)
177	3.56 (0.71)	−19.0 (±2.5)
195	8.20 (0.93)	−28 (±2.5)

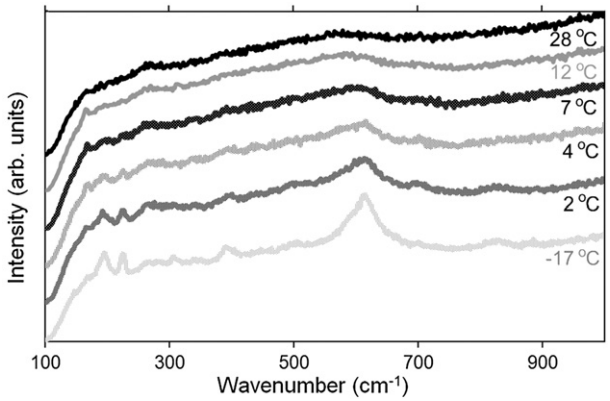

Fig. 5. Variable temperature Raman spectra of 1.75 at.% W-doped VO_2 film deposited with a tungsten precursor bubbler temperature of 152 °C.

temperature transmission and reflectance spectra between 300 and 2500 nm. A variety of film thickness (film thickness was determined by cross sectional SEM) were examined to elucidate the most suitable thickness for use in architectural glazing. Fig. 1 shows spectra for un-doped films with varying thickness.

The 30 nm-thick films had a peak transmission of 77% at 570 nm (Fig. 1), as compared to 86% (570 nm) for plain glass, the 80 nm-thick films had a transmission of 60% (570 nm) (Fig. 1) and the 150 nm-thick films 15% at 570 nm (Fig. 1). As seen previously [14] transmission in the visible decreases with increasing film thickness. The functional properties are also related to thickness. The thinnest film investigated, 30 nm (Fig. 1A), had virtually no change in properties when going through the MST. Increasing the film thickness to 80 nm (Fig. 1) lead to a 35% change in transmission at 2500 nm. Increasing the film thickness further to 150 nm (Fig. 1) saw a similar change of 35% at 2500 nm.

The next stage was to investigate tungsten doped films. W-doped VO_2 thin films with a thickness of 80 nm were deposited using a plain flow of 10 L/min N_2, with the VCl_4 bubbler temperature set to 50 °C and a bubbler flow rate of 0.4 L/min, with a VCl_4:H_2O ratio of 1:3 with a run time of 60 s. The N_2 flow rate through the WCl_6 bubbler was set to 2 L/min and the temperature of the bubbler varied between 100 °C and 195 °C to change the amount of tungsten in the gas phase.

Scanning electron microscopy (Fig. 2) revealed that the films were composed of an agglomeration of irregular particles. XRD (Fig. 3) revealed that the only crystalline phase present was that of monoclinic vanadium dioxide. This was the case for all samples irrespective of the level of tungsten doping. XPS of the samples revealed that a variety of vanadium oxidation states were present on the surface of the films (Fig. 4A) [29]. The species responsible for this are considered to be VO_2 and V_2O_5. Surface oxidation is common with vanadium oxides and has been seen previously [24–27,30]. Upon etching (Fig. 4B) the higher oxidation state material (V_2O_5) diminishes and VO_2 is the dominant phase, however quantification of the environments is unreliable after etching. Surface tungsten species were also examined for samples where tungsten was doped at a variety of levels (Fig. 4C and D) and showed the expected decrease in tungsten content for the films deposited with lower tungsten ratios.

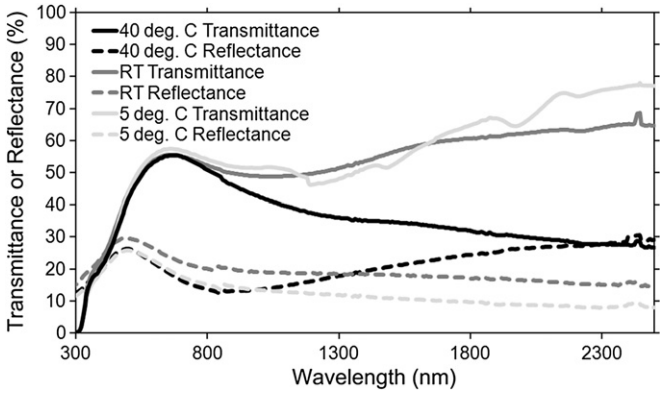

Fig. 6. Transmission and reflection data for a 1.75 at.% W-doped 80 nm thick VO_2 film at 40 °C, room temperature and 5 °C.

Table 2
Transmission and reflection colour co-ordinate data for un-doped and W-doped VO_2 films.

Tungsten doping (at.%)	Transmission				Reflectance			
	Dominant wavelength (nm)	L^*	a^*	b^*	Dominant wavelength (nm)	L^*	a^*	b^*
0	572	80.20	0.78	17.51	567	50.11	−0.85	4.15
3.5	472	42.33	−0.71	−6.53	571	56.69	−0.34	35.79

The amount of tungsten in the resultant films was characterized using WDX over a minimum of 10 spots on the film surface (Table 1). The MST was determined by measuring the T_c temperature using transmission data at 4000 cm^{-1} for those films with T_c above room temperature or with variable temperature Raman spectroscopy to determine those at or below room temperature (Fig. 5).

The MST is easy to characterize using Raman spectroscopy. The low temperature phase has a number of clear bands in its Raman spectrum. The high temperature phase has no discernible bands (has become metallic in nature). In the example shown in Fig. 5 the T_c occurs between 4 and 7 °C, i.e. it is 5.5 ± 1.5 °C.

Transition temperature values are presented in Table 1 along with atomic percentages of tungsten doping. The table shows that up to 8.2 at.% tungsten doping could be achieved and that any transition temperature between 55 and −28 °C could be produced. This data indicates a pseudo linear decrease in transition temperature of 22 °C/at.% tungsten doping up until 3.5 at.%; above this doping level, each additional tungsten atom% causes a reduction in transition temperature of 2 °C.

As an example, for a typical film doped with ~1.75% W the optical transmission changed by ~40% at 2500 nm between the hot (40 °C) and cold (5 °C) measurements (Fig. 6). In this instance the full thermochromic transition is not observed until below room temperature (19 °C). The films also had a transmission of >60% at 570 nm and as such would be suitable for use in architectural glass.

Another effect of the addition of tungsten to the films was a change in the visible colour of transmission, this can be seen in Table 2, where the LAB colour coordinates for undoped and W-doped thin films are reported. A change of about 100 nm for the dominant wavelength in transmission was observed for W-doped VO_2 samples; this corresponds to a change in colour from yellow/brown to a more aesthetically pleasing silver/blue. The value of the blue/yellow parameter b^* also changed remarkably: the undoped VO_2 sample showed a positive value, indicating a stronger yellow colour, while the W-doped one showed a negative value, characteristic of a blue colour.

4. Discussion

Previous work published on tungsten-doped VO_2 thin films utilising a system of $VOCl_3$, WCl_6 and water gave films with a transmission of ~11% at 570 nm [26]. In the previous work performed using VCl_4 as the vanadium source [27] with tungsten(VI) ethoxide and water coreactants, unpredictable results were obtained with films containing variable mixtures of VO_2 and V_2O_5 as observed by XRD, and the maximum visible transmission reported was approximately 40% at 570 nm. Control of film thickness was lacking, which is critical for optimising optical transmission whilst maintaining optimum functional properties, and therefore despite having the characteristic functional switch

required the films were inherently unsuitable for application in architectural glazing due to the low optical transmission caused by excessive thickness. In this work, however, a previously unreported system of $VCl_4/WCl_6/H_2O$ was used with a diluent nitrogen flow five times greater than those previously employed [26,27]. This improved the reproducibility of the results; furthermore the use of higher flow rates led to films where VO_2 is the only observable phase (XRD), and V_2O_5 is only detectable in significant quantities at the film surface (XPS). There were also notable improvements in the visual appearance of the film, and coverage of and adhesion to the substrate was greatly improved over that was seen in previous work [26,27]. Films grown at higher nitrogen diluent flow rates were more transparent (570 nm) and adhesive than those deposited at lower rates. Most likely this was due to the elimination of gas phase nucleation which has been reported as the cause of many blockages and powdery deposits in previous work [26,27]. The use of higher flow rates was also significant in allowing WCl_6 to be successfully employed as a tungsten precursor. Previously this precursor has been used at high bubbler temperatures (240 °C +) [26], and with the deposition equipment used it is virtually impossible to keep all of the material in the gas phase, i.e. preventing blockages, without losing control of film thickness, as witnessed by the deposition of relatively thick films and consequent lower visual transmission. By using higher flow rates the bubbler temperatures can be lowered, whilst maintaining control of film thickness and eliminating blockages.

A linear relationship between the level of tungsten doping and the T_c has been reported previously with an approximate 20 °C change/1% tungsten doping [31]. However, this was measured only up to 3 at.% tungsten-doping, whereas in the current work the change in T_c was found not to extrapolate in the same linear fashion above 3.5 at.% tungsten doping. Table 2 indicates that the relationship between tungsten doping and T_c appears to be linear up to 3.5 at.% tungsten-doping, with an approximate 22 °C change/at.% tungsten, similar to that seen in previous research. Above this level of doping each atom% of tungsten leads to a change in T_c of 2 °C. There are two possibilities as to why this is occurring. The first is that the tungsten is approaching its solubility limit in the vanadium dioxide. If this were the case we would expect to see evidence of some tungsten metal or tungsten oxide in our characterisation results. However, there is no evidence of any secondary phase in our XRD (Fig. 3.) or XPS (Fig. 4D.) analysis. Nor is there any evidence of a tungsten oxide phase from Raman spectroscopy (Fig. 5.). The second possibility relates to the crystal structure distortion associated with tungsten doping that disrupts vanadium pairs and lowers T_c [19–21]. We suggest that the tungsten doping reaches a critical level that causes the optimum distortion to the crystal structure, and that above this level additional doping has a much less significant effect; because the crystal structure has become so distorted that there is space for additional tungsten atoms to be incorporated without causing as significant a distortion. The switching temperatures at high tungsten loading reported here are the lowest that have been reported for a doped VO_2 film.

Films suitable for use in architectural glazing would maximise the functional properties of the coating whilst having a high transmission at 570 nm, preferably in excess of 60% [23]. The thermochromic properties of VO_2 thin films are dependent on thickness, the largest changes in optical properties are seen above a critical thickness of 70 nm [14]. The ideal film would have the maximum acceptable thickness which corresponds to the minimum acceptable optical transmission. In our case this is in the range 70–90 nm thick. Also the film must be adherent and visually appealing.

Films deposited with a VCl_4:H_2O ratio of 1:3 produced glassy, adherent films with the added benefit of having a more appealing green tint in transmission. At this reactant ratio there was no appreciable reduction of the functional properties of the film. For the film to be useful, the thermochromic transition needs to be reduced to around room temperature. From the precursor set used in this work a tungsten doping level in the range of 1.6–1.7 at.% would achieve this. Optical properties typical of an optimised film of 80 nm thickness with tungsten doping of 1.66% are presented in Fig. 6. Three temperature regimes were employed; hot (35 °C), room temperature (24 °C) and cold (15 °C). The optical data at 15 °C were partially affected by the condensation of moisture on the film surface during analysis. It is apparent from the data that there is a continued switch in film properties below room temperature, indicating the film is still responding to temperature changes below 24 °C. A large change (50%) in transmission at 2500 nm and a significant change in reflection (20%) is observed between the 'cold' and 'hot' values. Another significant factor is the colour of the films; previous work has shown that tungsten doped vanadium dioxide films retain the yellow/brown colour of un-doped vanadium dioxide films [14,24–27]. In this work tungsten doping above 2.5 at.% causes the colour to change to a more attractive silver/blue colour. Films with tungsten doping less than 2.5 at.% were greener in colour than had been previously observed; we attribute this to the formation of V_2O_5 at the surface of the films as seen from XPS (Fig. 4A). The formation of V_2O_5 at the surface is not a new phenomena but in previous studies the films were much thicker (~300 nm) and powdery than those here, which were always glassy, hard and adherent under these conditions, and as such this effect was not observed. We therefore conclude that this system has the best combination of functional and optical properties, combined with appropriate switching temperature, as required for architectural glazing of any CVD deposited VO_2 thin films.

5. Conclusion

Thin films of VO_2, suitable for use in architectural glazing, have been deposited onto glass substrates using a reliable and reproducible APCVD method. Changing the ratio of vanadium precursor to water alters the appearance of the films from powdery brown to adherent and transparent, with an improvement to a greener colour. This change is also accompanied by a change in the transmission of the films in the near infrared and the size of the MST is dependent on the thickness of the film being above a certain level. Controllable doping of the films with tungsten is demonstrated. This allows the temperature at which the thermochromic switch occurs to be controlled. A benefit of tungsten doping is the films obtain an attractive blue colour in transmission further improving the aesthetic properties.

Acknowledgements

The EPSRC is thanked for providing the grant for this work. The contributions of Mr. Steven Schooling are acknowledged and Mr. Simon Hurst and Dr Troy Manning of Pilkington Glass are thanked for their input and useful discussions. Mr. Kevin Reeves of UCL Archaeology is thanked for assistance with SEM and associated techniques and Mr. Rob Palgrave is thanked for XPS. I.P.P. thanks the Royal Society/Wolfson Trust for a merit award. RB thanks the Royal Society for a Dorothy Hodgkin Fellowship.

References

[1] C.B. Greenberg, Thin Solid Films 110 (1983) 73.
[2] C.h. Leroux, G. Nihoul, G. Van Tendeloo, Phys. Rev. B 57 (1998) 5111.
[3] D.K. Rogers, Powder Diffr. 8 (1993) 240.
[4] F.J. Morin, Phys. Rev. Lett., 3 (1959) 34.
[5] J.B. MacChesney, J.F. Potter, H.J. Guggenheim, J. Electrochem. Soc. 115 (1968) 52.
[6] L.A. Rayabova, I.A. Serbinov, A.S. Daresky, J. Electrochem. Soc. 119 (1972) 427.
[7] M.H. Lee, M.G. Kim, H.K. Song, Thin Solid Films 291 (1996) 30.
[8] M. Nygren, M. Israelsson, Mater. Res. Bull. 4 (1969) 881.
[9] W. Burkhardt, T. Christmann, B.K. Meyer, W. Niessner, D. Schalch, A. Scharmann, Thin Solid Films 345 (1999) 229.
[10] S. Tanemura, Jpn. J. App. Phys. 34 (1995) 2459.
[11] I. Takahashi, M. Hibino, T. Kudo, Jpn J. App. Phys. 35 (1996) L438.
[12] J. Livage, Coord. Chem. Rev. 192 (1999) 391.
[13] T. Maruyama, Y. Ikuta, J. Mater. Sci. 28 (1993) 5073.
[14] R. Binions, G. Heytt, C. Piccirillo, I.P. Parkin, J. Mater. Chem. 17 (2007) 4652.

[15] R. Binions, C.S. Blackman, T.D. Manning, C. Piccirillo, I.P. Parkin, J. Nano Res. 2 (2008) 1.
[16] D. Barreca, L.E. Depero, E. Franzato, G.A. Rizzi, L. Sangaletti, E. Tondello, U. Vettori, J. Electrochem. Soc. 146 (1999) 551.
[17] M.N. Field, I.P. Parkin, J. Mater. Chem. 10 (2000) 1863.
[18] C. Piccirillo, I.P. Parkin, R. Binions, Chem. Vap. Depos. 13 (2007) 145.
[19] J.B. MacChesney, H.J. Guggenheim, J. Phys. Chem. Solids 30 (1969) 225.
[20] T.E. Phillips, R.A. Murray, T.O. Poehler, Mater. Res. Bull. 22 (1987) 1113.
[21] J.W. Pierce, J.B. Goodenough, Phys. Rev. B 5 (1972) 4104.
[22] F. Béteille, J. Livage, J. Sol–Gel Sci. Technol. 13 (1998) 915.
[23] M.A. Sobhan, R.T. Kivaisi, B. Stjerna, C.G. Granqvist, Sol. Energy Mater. Sol. Cells 44 (1996) 451.
[24] T.D. Manning, I.P. Parkin, R.J.H. Clark, D. Sheel, M.E. Pemble, D. Vernardou, J. Mater. Chem. 12 (2002) 2936.
[25] U. Quershi, T.D. Manning, I.P. Parkin, J. Mater. Chem., 14 (2004) 1190.
[26] T.D. Manning, I.P. Parkin, J. Mater. Chem. 14 (2004) 2554.
[27] T.D. Manning, I.P. Parkin, M.E. Pemble, D. Sheel, D. Vernardou, Chem. Mater. 16 (2004) 744.
[28] C. Piccirillo, I.P. Parkin, R. Binions, Thin Sol. Films 516 (2008) 1992.
[29] D. Briggs, M.P. Seah (Eds.), Practical Surface Analysis, 2nd Edition, Volume Auger and X-ray Photoelectron Spectroscopy, Wiley, 1990.
[30] C. Piccirillo, R. Binions, I.P. Parkin, Eur. J. Inorg. Chem. 25 (2007) 4050.
[31] G.V. Jorgensen, J.C. Lee, Solar Energy Mater. 14 (1986) 205.

Doped and un-doped vanadium dioxide thin films prepared by atmospheric pressure chemical vapour deposition from vanadyl acetylacetonate and tungsten hexachloride: the effects of thickness and crystallographic orientation on thermochromic properties

Russell Binions, Geoffrey Hyett, Clara Piccirillo and Ivan Paul Parkin*

Received 12th June 2007, Accepted 28th August 2007
First published as an Advance Article on the web 13th September 2007
DOI: 10.1039/b708856f

The atmospheric pressure chemical vapour deposition reaction of vanadyl acetylacetonate and tungsten hexachloride with oxygen led to the production of thin films of tungsten doped monoclinic vanadium dioxide on glass substrates. Scanning electron microscopy and X-ray diffraction indicated that the films had different morphologies and crystallinities depending on the deposition conditions used. Transmission and reflectance measurements showed a significant change in properties in the near infra-red either side of the metal to semiconductor transition. Variable temperature transmission studies show that the metal to semiconductor transition was lowered by tungsten doping. The effect of film thickness was studied with un-doped and doped films. It was found that film thickness limited the intensity of light passing through the film and the extent of the thermochromic transition but was found not to influence the hysteresis width or temperature of transition. Different film growth conditions led to a range of film morphologies which profoundly affected the resulting optical properties of the films. It was found that film morphology and preferred crystallographic orientation had a marked influence on the width and switching temperature of the thermochromic transition.

Introduction

Thin films of vanadium(IV) oxide have been the subject of intensive research efforts in recent years due to their potential applications as an intelligent window coating[1,2] and other advanced applications such as data storage[3,4] and infrared modulators.[5] These technologies are based on the thermochromic metal to semiconductor transition which occurs in the pure un-doped bulk material at 68 °C, associated with the structural adjustment from the low temperature monoclinic phase (VO_2(M)) to the higher temperature rutile phase (VO_2(R)).[6] This structural transformation causes significant changes in electrical conductivity and optical properties. The rutile material is metallic and reflects a wide range of solar radiation, whereas the monoclinic phase is a semiconductor.

For VO_2 to be effective as an intelligent window coating it is desirable to lower the transition temperature from 68 °C to nearer room temperature. Doping studies have shown that the transition temperature can be altered by the incorporation of metal ions into the VO_2 lattice.[7,8] It was found the most effective metal ion dopant was tungsten.[9]

Tungsten doped VO_2 films have been prepared by a variety of methods including sol–gel,[10] sputtering,[11] and CVD methodologies.[6,12–23] CVD routes to the production of doped VO_2 films are generally considered more attractive because of the compatibility of CVD processes with high volume glass manufacture and the physical properties of CVD produced films which are usually adherent and long lasting. Various studies have been conducted on the growth of tungsten doped thin films using vanadium tetrachloride or vanadium oxychloride as a vanadium precursor and tungsten hexachloride or tungsten ethoxide as a precursor to tungsten doping. In all cases water was used as an oxygen precursor.[9,24] In the current study vanadyl acetylacetonate was utilised as the vanadium precursor and tungsten hexachloride as the tungsten precursor. Vanadyl acetylacetonate was preferred to vanadium chloride or vanadium oxychloride as this precursor does not suffer from gas phase nucleation as has been observed previously.[9,24] Tungsten hexachloride was preferred to tungsten ethoxide because previous studies have highlighted the poorer mass transport properties of tungsten ethoxide.[22] Vanadyl acetylacetonate has received some attention in the production of VO_2 films by CVD and atomic layer deposition[19,20,25] but little attention in doping studies. Although some work has been done to suggest that film thickness has an influence on the metal–semiconductor transition temperature using CVD methods, no systematic study has been conducted. A study of vanadium dioxide films produced by PVD methods (RF sputtering) found that decreasing film thickness led to a significant reduction of the metal–semiconductor transition temperature between 3–150 nm.[26] Here we report the first systematic study into the effect of film thickness on the metal–semiconductor transition for both doped and un-doped monoclinic vanadium dioxide thin films. Furthermore we show how, for the first time, film morphology, microstructure, and most particularly preferred crystallographic

Materials Chemistry Research Centre, Department of Chemistry, 20 Gordon Street, London, UK WC1H 0AJ.
E-mail: i.p.parkin@ucl.ac.uk; Tel: +44 (0) 20 7679 4669

orientation influence the functional properties of thermochromic thin films.

Experimental

A 98% nitrogen, 2% oxygen mixture was obtained from the British Oxygen Company (BOC) and used as supplied in the plain line. Nitrogen (99.99%) was obtained from BOC and used as supplied in the bubbler lines. Coatings were obtained on SiO_2 coated float glass. APCVD experiments were conducted on 150 mm × 45 mm × 3 mm pieces of glass using a flat-bed cold-walled APCVD reactor. The glass was cleaned prior to use by washing with petroleum ether (60–80 °C) and isopropanol and then dried in air. A graphite block containing a Whatman cartridge heater was used to heat the glass substrate. The temperature of the substrate was monitored by a Pt–Rh thermocouple. Independent thermocouple measurements indicated that temperature gradients of up to 50 °C cm^{-1} were observable at 600 °C across the surface of the glass. The rig was designed so that four independent gas lines could be used. All gas handling lines, regulators and flow valves were made of stainless steel and were of 6.5 mm internal diameter except for the inlet to the mixing chamber and the exhaust line from the apparatus that were 13 mm in diameter. In these experiments three gas lines were used. Gases came directly from a cylinder and were preheated by passing along 2 m lengths of stainless steel tubing, which were curled and inserted inside a tube furnace. The temperatures of all the gas inlet lines were monitored by Pt–Rh thermocouples and Eurotherm heat controllers.

Vanadyl acetylacetonate (99.99%) was obtained from Aldrich and used without further purification and was placed into a stainless steel bubbler. The bubbler was heated to 175 °C by a heating jacket and vanadyl acetylacetonate introduced into the gas streams by passing hot nitrogen gas through the bubbler. Tungsten hexachloride (99.9%) was obtained from Aldrich and used without further purification and placed into a stainless steel bubbler, the temperature of this bubbler was controlled as a method of introducing different amounts of tungsten into the growing film. The two components of the system were mixed by the use of two concentric pipes of 6.5 mm and 13 mm internal diameter respectively, the inner pipe being 3 cm shorter than the outer pipe. The concentric pipes were attached directly to the mixing chamber of the coater. Gas flows were adjusted using suitable regulators and flow controllers. The exhaust from the reactor was vented directly into the extraction system of a fume cupboard. All of the apparatus was baked out with nitrogen at 150 °C for 30 minutes before use. Deposition experiments were conducted by heating the horizontal-bed reactor and the bubblers to the desired temperatures before diverting the nitrogen line through the bubbler and hence to the reactor. Deposition experiments were timed by use of a stopwatch and were conducted between 30 s and 30 min in order to vary the thickness of the samples. The maximum possible deposition temperature with this equipment was 600 °C. At the end of the deposition only nitrogen was allowed to flow over the glass substrate until the substrate was sufficiently cool to handle (~60 °C). Samples were handled and stored in air. The substrate temperature for deposition was kept constant at 525 °C as this has been found to be the optimal temperature to grow monoclinic vanadium dioxide thin films. Nitrogen flow rates were varied between 0.5 and 10.0 L min^{-1}.

Table 1 Experimental gas flow conditions utilised in this study

	Fast	Intermediate	Slow
$[VO(acac)_2]$ bubbler flow	10 L min^{-1}	8 L min^{-1}	5 L min^{-1}
N_2 (2% O_2) plain flow rate	1 L min^{-1}	2 L min^{-1}	5 L min^{-1}
Deposition time	30 s to 3 min	5 to 15 min	20 to 40 min

Films were grown using a variety of conditions which have been divided into three classes: fast, intermediate and slow—indicating the time for deposition. Typically fast depositions took place with high flow rates and for less than three minutes, intermediate depositions were typically run for 15 min with lower flow rates, slow depositions were run for 30 min with low flow rates. The experimental conditions are summarised in Table 1.

Electron microprobe analysis was performed on a JEOL EMA and referenced against vanadium and oxygen standards. EDAX and WDAX were conducted using a Philips XL30 ESEM instrument. SEM images were acquired on a Jeol 6301F field emission instrument. X-Ray diffraction patterns were measured on a Bruker D8 diffractometer using monochromated ($CuK_{\alpha 1+2}$) radiation in the reflection mode using a glancing incident angle of 1.5°. Rietveld analysis was conducted on these patterns using the March–Dollase model to determine preferred orientation relative to the [001] crystal direction. In this model the extent of preferred orientation relative to the chosen plane is given by the *r* factor. An *r* factor of 1 indicates no preferred orientation along the chosen direction. A value below 1 indicates a tendency for the chosen crystal direction to lie perpendicular to the substrate, while a value above 1 indicates a preference parallel to the substrate. Reflectance and transmission spectra were recorded between 300 and 2500 nm on a Perkin Elmer Lambda 950 UV-VIS spectrometer. UV-Vis spectra were obtained using a Helios double beam instrument. Raman spectra were acquired on a Renishaw Raman system 1000 using a helium–neon laser of wavelength 632.8 nm. The Raman system was calibrated against the emission lines of neon. Transmittance–temperature studies were performed on a Perkin-Elmer 457 grating spectrometer set to 4000 cm^{-1}. An aluminium temperature cell controlled by RS resistive heaters, Eurotherm temperature controllers and k-type thermocouples was used to manipulate sample temperature. Sample temperature was measured using a k-type thermocouple taped directly onto the film surface. Film thickness was measured directly by scanning electron microscopy then correlated with EDAX and optical transmission data.

Results

Atmospheric pressure chemical vapour deposition reactions of vanadyl acetylacetonate ($[VO(acac_2]$) and 2% oxygen led to the production of vanadium(IV) oxide films on glass substrates. In some cases the films were doped with tungsten by the addition of tungsten hexachloride into the reaction gas stream.

A spread of film thicknesses ranging from 30 nm to 2000 nm was produced using a variety of different gas flow conditions (Table 1). The films were transparent yellow/brown in transmission, the colour darkening with film thickness. The thickest films (2000 nm) were entirely opaque and appeared a reflective dark blue in colour. All of the films (doped and un-doped) passed the Scotch tape test and could not be marked by a brass scalpel, they could, however, be marked by a steel scalpel. EDAX and WDAX indicated atomic ratios consistent with the production of vanadium dioxide and the absence of contaminants such as chlorine.

Un-doped films

X-Ray powder diffraction confirmed the production of monoclinic vanadium dioxide (Fig. 1) from the reaction of $[VO(acac)_2]$ at 525 °C. The thicker films tended to be more crystalline. The recorded X-ray diffraction patterns all had very large backgrounds, caused by scattering from the amorphous glass substrate. The lattice parameters and cell volumes determined from indexing of the Bragg peaks in the $P2_1/c$ space group were similar in all cases for un-doped films, with: a = 5.70(2) Å, b = 4.50(2) Å, c = 5.31 (2) Å, β = 122.2(1)° and a unit cell volume of 115(1) Å^3. These are comparable to previous literature values[27] of a = 5.7529(3) Å, b = 4.5263(3) Å, c = 5.3825(3) Å, β = 122.602(4)°, unit cell volume = 118.07 ± 1.0 Å^3. Interestingly different deposition conditions produced films with different preferred orientation relative to the 001 direction. An r factor of 1 indicates no preferred orientation along the chosen direction. A value below 1 indicates a tendency for the chosen crystal direction to lie perpendicular to the substrate, while a value above 1 indicates a preference parallel to the substrate. The undoped VO_2 films produced using slow growth conditions had r factors greater than 1, with an average of 2.0, in contrast to the films produced under fast and medium growth conditions which had r factors of less than 1 (with average values of 0.72 and 0.68 respectively) indicating a strikingly different orientation of the crystallites.

Films produced under similar conditions had related morphologies (Fig. 2). Films grown under the slow growth

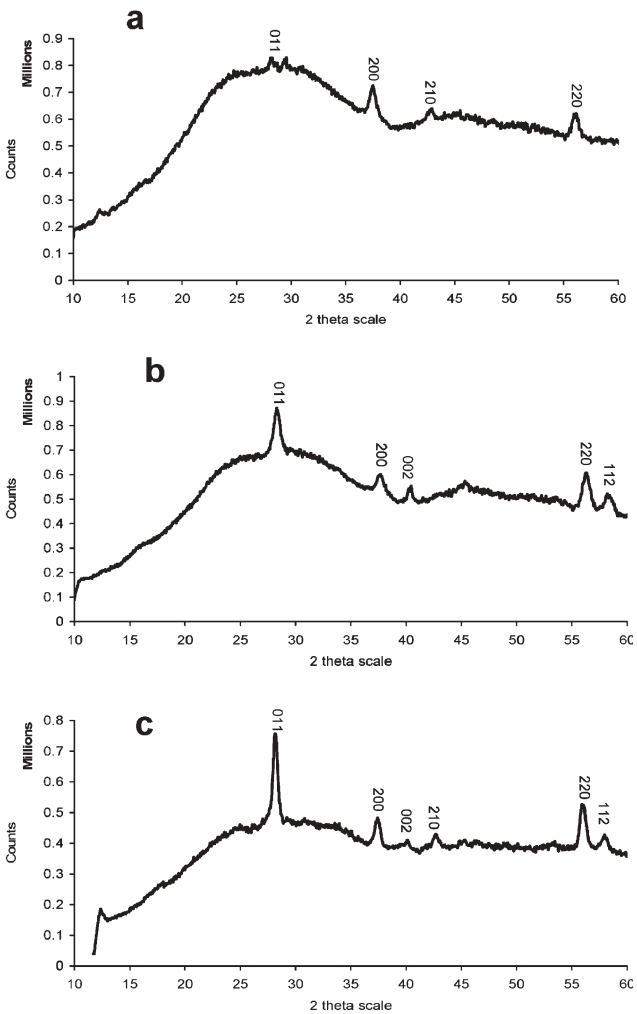

Fig. 1 X-Ray diffraction patterns from VO_2 films produced using different deposition conditions. Slow conditions (a) used a $[VO(acac)_2]$ bubbler flow rate of 5 L min^{-1} for a deposition time of 30 min, intermediate (b) 8 L min^{-1} for a deposition time of 10 min, and fast (c) 10 L min^{-1} for a deposition time of 2 min. In all cases the bubbler temperature was kept constant at 175 °C and the substrate temperature constant at 525 °C.

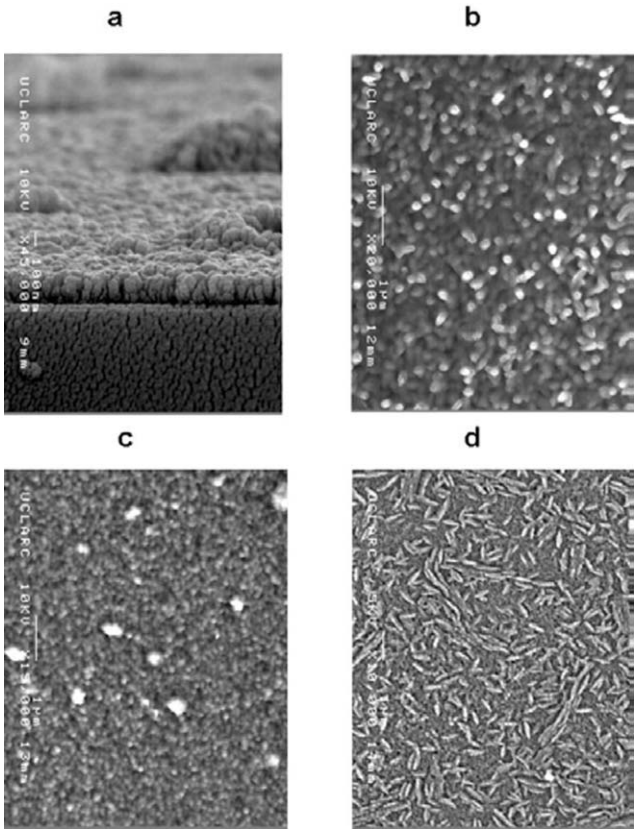

Fig. 2 Representative scanning electron micrographs (a: side on, b–d: plan view) of VO_2(M) films made by using different conditions: a, b) slow, c) intermediate and d) fast. For a the scale bar represents 100 nm, in all other cases the scale bars represent 1 micron. Slow conditions used a $[VO(acac)_2]$ bubbler flow rate of 5 L min^{-1} for a deposition time of 30 min, intermediate 8 L min^{-1} for a deposition time of 10 min, and fast 10 L min^{-1} for a deposition time of 2 min. In all cases the bubbler temperature was kept constant at 175 °C and the substrate temperature constant at 525 °C.

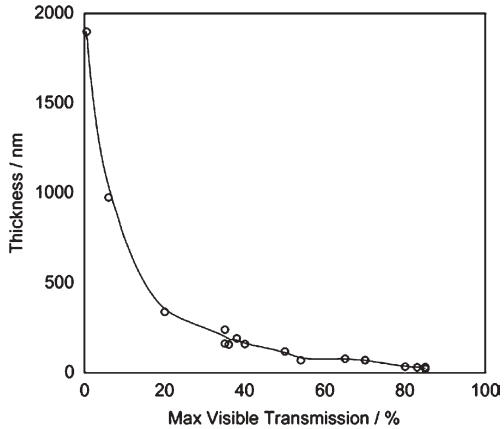

Fig. 3 Correlation between maximum visible transmission and film thickness.

conditions, typically a deposition timed for half an hour, had morphologies which were consistent with columnar island growth (Fig. 2a), the islands were relatively symmetrical. Typically each island was around 100 nm across, larger sizes were not observed. Films produced with intermediate conditions (10 min deposition) had distorted island morphology where the islands were no longer symmetrical but of a similar size. The films produced with fast conditions (1 min deposition) were different: the morphology consisted of particles that looked similar to 'French runner beans', it would appear that this is because several nucleation sites have grown along a particular axis and fused together. Again these particles are typically around 100 nm across.

Fig. 3 indicates the correlation between film thickness and maximum visible transmission. Overall these data best fit a power series, but for films of 200 nm thickness and less there is a pseudo-linear relationship. This effect is independent of the growth conditions used in producing the film indicating that each methodology produced films with similar densities.

Fig. 4 and 5 contain typical optical data collected from samples produced using the three condition sets. In all cases the metal–insulator transition is observed. It is found that the extent of the transition is dependent on film thickness. Typically no or a minimal (1–2% change) transition could be observed for films with a thickness of 50 nm or less and no change for films below 40 nm thickness. Films with a thickness of 50 to 80 nm typically had a change in transmission at 2500 nm of up to ~25%, films that were thicker than this displayed changes that varied between 25 and 55% at 2500 nm, though this effect was limited for very thick films; in some cases the un-switched transmission at 2500 nm was very low and on switching is reduced to zero which may only be a change of 10%.

Similar effects were seen with the reflectance properties of the films. Little or no effect was observed from films that were 50 nm thick or thinner. Films between 50 and 80 nm had a reflectance change at 2500 nm of up to 15%, above 80 nm thickness the change in reflectance could be up to 40% but did not directly correlate with film thickness. There is a jump in the reflectivity at 850 nm–1000 nm. This is ideal behaviour for smart glazing as the greatest portion of IR radiation is between 800 nm and 1400 nm.

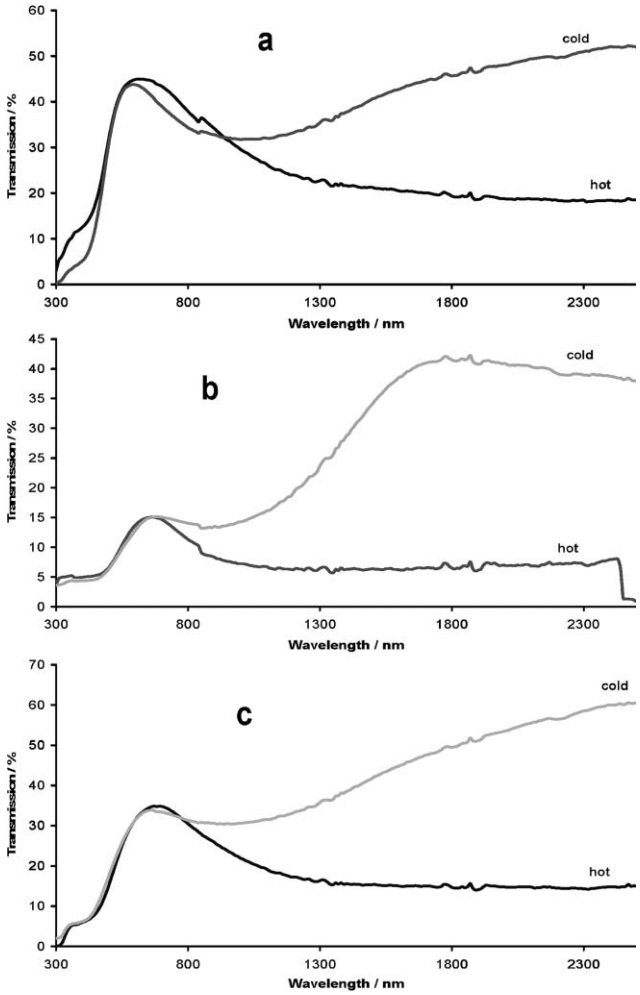

Fig. 4 Optical transmission properties of a film produced using a) slow conditions, b) intermediate conditions and c) fast conditions. Slow conditions used a $[VO(acac)_2]$ bubbler flow rate of 5 L min^{-1} for a deposition time of 30 min, intermediate 8 L min^{-1} for a deposition time of 10 min, and fast 10 L min^{-1} for a deposition time of 2 min. In all cases the bubbler temperature was kept constant at 175 °C and the substrate temperature constant at 525 °C.

Hysteresis loops are shown in Fig. 6 for films produced from the three condition sets. Films grown at faster growth rates have thinner hysteresis widths and a lower transition temperature. The results are summarised in Table 2. A variety of films of different thickness were investigated: it was found that the films had similar hysteresis properties to others made under the same set of conditions, and that this was independent of thickness. There appears to be no relationship between film thickness and hysteresis properties.

Doping studies

Doping the VO_2 films with small amounts of tungsten leads to several changes compared to the un-doped films. The X-ray diffraction patterns of the doped films produced using fast and slow conditions are similar (Fig. 7) to each other with the Rietveld refinement finding that both have an *r* factor of less than 1 (0.6 and 0.8 respectively), indicating that the crystallites are aligned with the [001] direction parallel to the substrate.

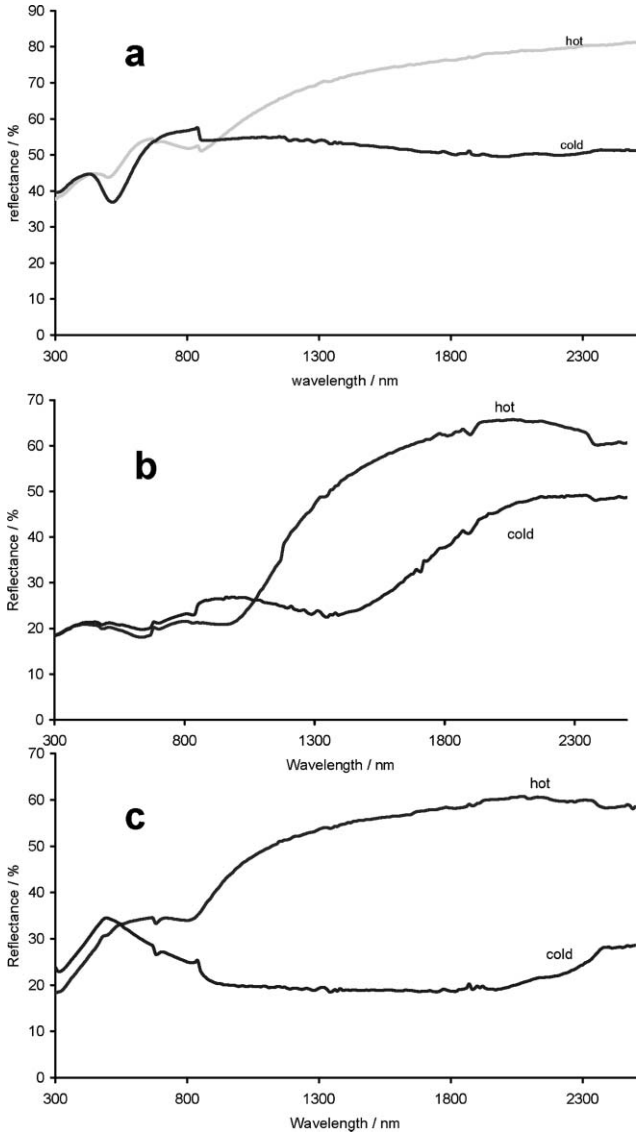

Fig. 5 Optical reflectance properties of a film produced using a) slow conditions, b) intermediate conditions and c) fast conditions. Slow conditions used a $[VO(acac)_2]$ bubbler flow rate of 5 L min^{-1} for a deposition time of 30 min, intermediate 8 L min^{-1} for a deposition time of 10 min, and fast 10 L min^{-1} for a deposition time of 2 min. In all cases the bubbler temperature was kept constant at 175 °C and the substrate temperature constant at 525 °C.

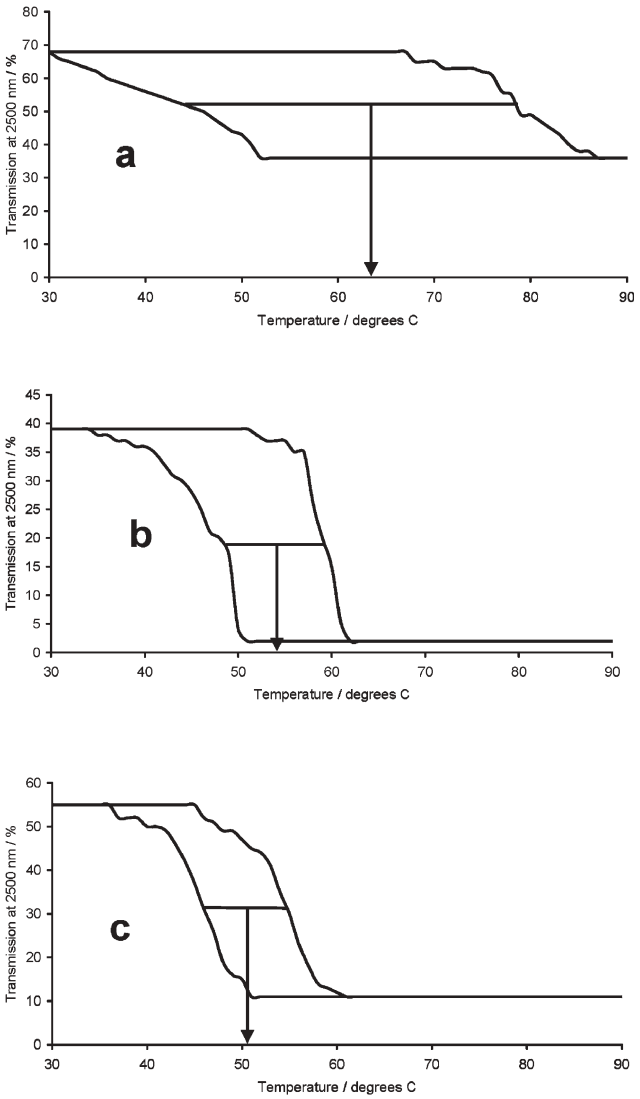

Fig. 6 Change in hysteresis width with differing film growth conditions. Slow conditions (a) used a $[VO(acac)_2]$ bubbler flow rate of 5 L min^{-1} for a deposition time of 30 min, intermediate (b) 8 L min^{-1} for a deposition time of 10 min, and fast (c) 10 L min^{-1} for a deposition time of 2 min. In all cases the bubbler temperature was kept constant at 175 °C and the substrate temperature constant at 525 °C.

This was also observed in the X-ray diffraction patterns of un-doped films produced using fast conditions but in contrast to the un-doped films formed under the slow conditions, where the [001] direction was found to be preferentially aligned perpendicular to the substrate. As is expected from doped films, there is an increase in cell volume compared to the un-doped films to 117 $\pm$ 1.0 $Å^3$. All doped monoclinic vanadium dioxide thin films in this study had similar cell dimensions with average values of a = 5.73(2) Å, b = 4.53(4) Å, c = 5.33 (3) Å, β = 122.0(3)°.

EDAX and WDAX were used to determine vanadium and tungsten content. EDAX mapping (500 spots) with a tungsten variation of 0.1 atom% indicated that tungsten was homogeneously dispersed throughout the film suggesting the formation of a solid solution rather than a separate phase, indeed no evidence for a secondary phase is observed in the X-ray diffraction patterns of these samples (Fig. 7).

Table 2 Change in transition temperature and hysteresis width with experimental conditions. Slow conditions used a $[VO(acac)_2]$ bubbler flow rate of 5 L min^{-1} for a deposition time of 30 min, intermediate 8 L min^{-1} for a deposition time of 10 min, and fast 10 L min^{-1} for a deposition time of 2 min. In all cases the bubbler temperature was kept constant at 175 °C and the substrate temperature constant at 525 °C

Condition set	Transition temperature/°C	Hysteresis width/°C
Slow	63	33
Intermediate	54	13
Fast	52	10

Similar film morphologies are observed for doped films as were seen for un-doped films (Fig. 8). Both doped and

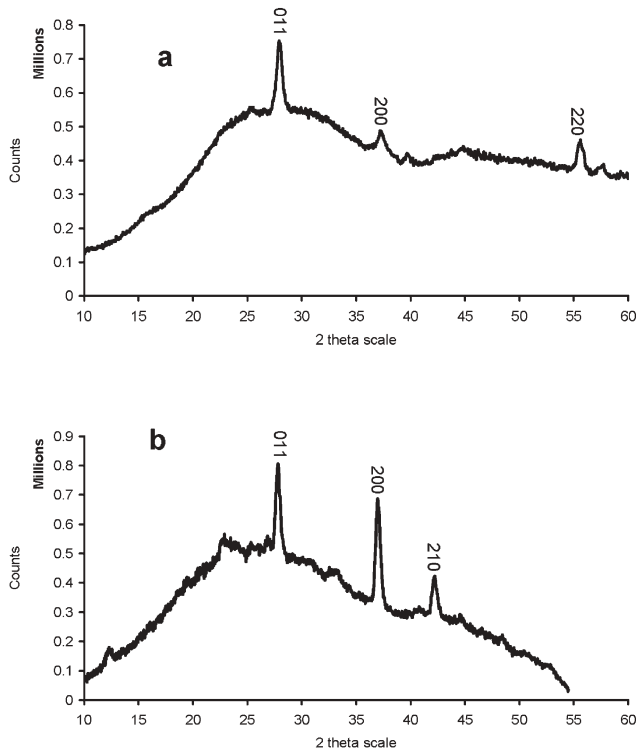

Fig. 7 X-Ray diffraction patterns of doped VO_2 films produced using different deposition conditions. Slow conditions (a) used a $[VO(acac)_2]$ bubbler flow rate of 5 L min^{-1} for a deposition time of 30 min, and fast (b) 10 L min^{-1} for a deposition time of 2 min. In all cases the bubbler temperature was kept constant at 175 °C and the substrate temperature constant at 525 °C. The $[WCl_6]$ bubbler flow rate was kept constant at 1 L min^{-1}, the bubbler temperature was varied to adjust the amount of tungsten doping. Both of the samples shown here contain 0.5 ± 0.1 atom% tungsten as determined by EDAX and WDAX.

un-doped films produced using the slow conditions were similar; this is, perhaps, unexpected because of the change in orientation observed in the X-ray diffraction patterns of these films. The morphologies of the films produced using the fast conditions were similar to the un-doped films seen previously.

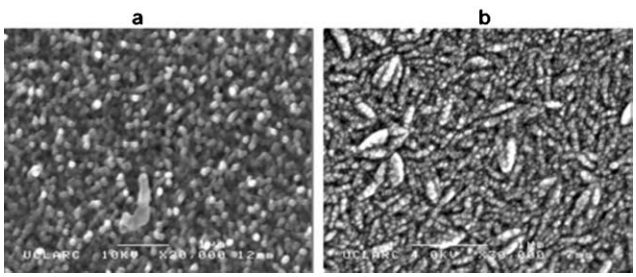

Fig. 8 SEM micrographs of doped samples: a) slow conditions b) fast conditions. Slow conditions used a $[VO(acac)_2]$ bubbler flow rate of 5 L min^{-1} for a deposition time of 30 min, and fast 10 L min^{-1} for a deposition time of 2 min. In all cases the bubbler temperature was kept constant at 175 °C and the substrate temperature constant at 525 °C. The $[WCl_6]$ bubbler flow rate was kept constant at 1 L min^{-1}, the bubbler temperature was varied to adjust the amount of tungsten doping. Both of the samples shown here contain 0.5 ± 0.1 atom% tungsten.

Fig. 9 and 10 contain optical data for doped films grown using fast and slow conditions. These are not appreciably different in form from the un-doped examples and the same thickness related trends are observed, similarly there is a jump in reflectivity around 900 nm.

The extent of the transition is dependent on film thickness. Typically no or a minimal (1–2% change) transition could be observed for films with a thickness of 50 nm or less and no change for films below 40 nm thickness. Films with a thickness of 50 to 80 nm typically had a change in transmission at 2500 nm of up to ~25%, films that were thicker than this displayed changes that varied between 25 and 55% at 2500 nm, though this effect was limited for very thick films; in some cases the un-switched transmission at 2500 nm was very low and on switching is reduced to zero which may only be a change of 10%.

Similar effects were seen with the reflectance properties of the films. Little or no effect was observed from films that were 50 nm thick or thinner. Films between 50 and 80 nm had a reflectance change at 2500 nm of up to 15%, above 80 nm thickness the change in reflectance could be up to 40% but did not directly correlate with film thickness.

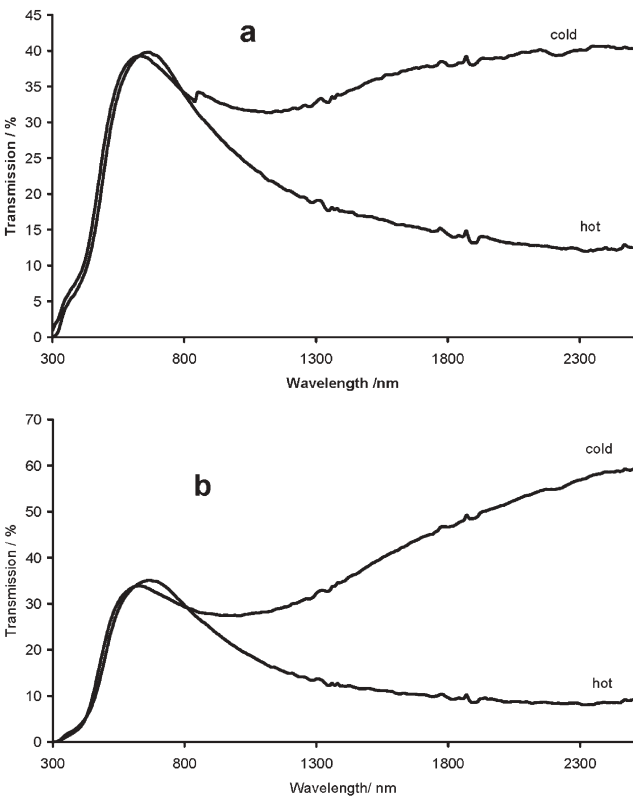

Fig. 9 The optical transmission properties of a doped sample produced using a) the slow condition set and b) the fast condition set. Slow conditions used a $[VO(acac)_2]$ bubbler flow rate of 5 L min^{-1} for a deposition time of 30 min, and fast 10 L min^{-1} for a deposition time of 2 min. In all cases the bubbler temperature was kept constant at 175 °C and the substrate temperature constant at 525 °C. The $[WCl_6]$ bubbler flow rate was kept constant at 1 L min^{-1}, the bubbler temperature was varied to adjust the amount of tungsten doping. Both of the samples shown here contain 0.5 ± 0.1 atom% tungsten.

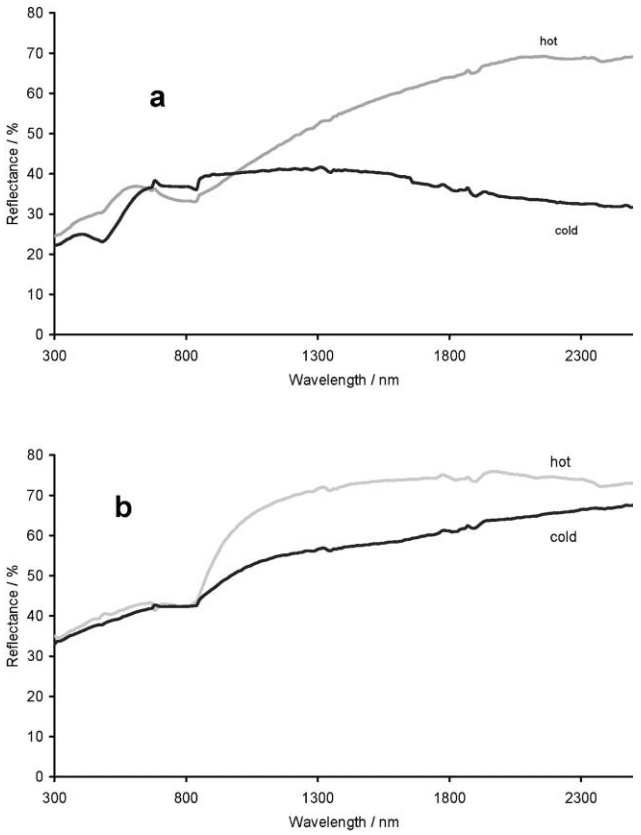

Fig. 10 The optical reflectance properties of a doped sample produced using a) the slow condition set and b) the fast condition set. Slow conditions used a [$VO(acac)_2$] bubbler flow rate of 5 L min^{-1} for a deposition time of 30 min, and fast 10 L min^{-1} for a deposition time of 2 min. In all cases the bubbler temperature was kept constant at 175 °C and the substrate temperature constant at 525 °C. The [WCl_6] bubbler flow rate was kept constant at 1 L min^{-1}, the bubbler temperature was varied to adjust the amount of tungsten doping. Both of the samples shown here contain 0.5 ± 0.1 atom% tungsten.

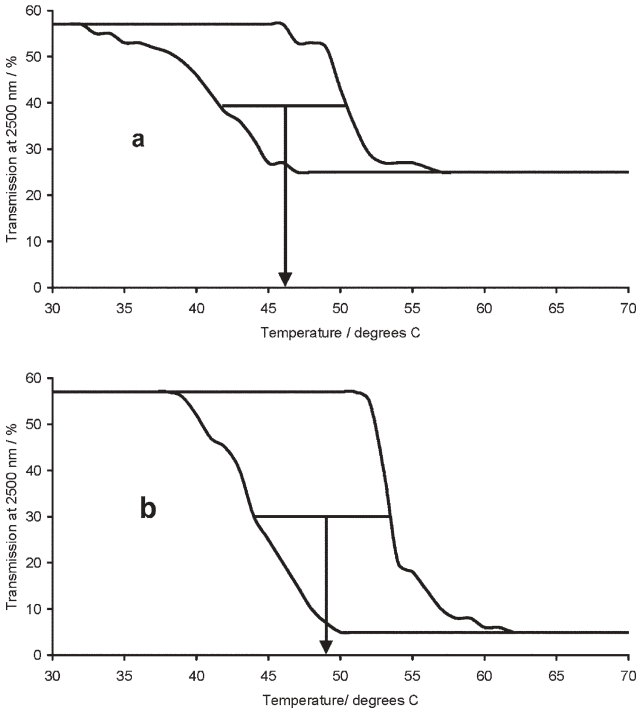

Fig. 11 Hysteresis loops for doped films grown with different conditions. Slow conditions (a) used a [$VO(acac)_2$] bubbler flow rate of 5 L min^{-1} for a deposition time of 30 min, and fast (b) 10 L min^{-1} for a deposition time of 2 min. In all cases the bubbler temperature was kept constant at 175 °C and the substrate temperature constant at 525 °C. The [WCl_6] bubbler flow rate was kept constant at 1 L min^{-1}, the bubbler temperature was varied to adjust the amount of tungsten doping. Both of the samples shown here contain 1.0 ± 0.1 atom% tungsten.

Doping has the effect of narrowing the hysteresis loop for those films grown using slow growth conditions. Tungsten doping decreases the transition temperature for all films irrespective of growth conditions (Fig. 11). Similarly to un-doped films the hysteresis properties are unaffected by film thickness. As reported previously incorporation of 1% tungsten reduces the transition temperature by 20 °C.[9]

Discussion

Tungsten doped and un-doped thin films of monoclinic vanadium dioxide have been produced from the atmospheric pressure chemical vapour deposition reaction of vanadyl acetylacetonate, tungsten hexachloride and 2% oxygen in nitrogen on glass substrates. The resulting optical and thermochromic properties of the films were investigated with respect to thickness and structure. The films were transparent and a dark brown/yellow in colour similar to previous work utilising vanadium tetrachloride and water;[9] the films produced in this work have the advantage of being less powdery, also the vanadyl acetylacetonate system does not suffer from the same problems of gas phase nucleation that is common with metal chloride precursors.[28]

Film thickness principally affects the amount of transmitted light through the coating. Thicker films were less transmissive. It also has some effect on the thermochromic transition. No thermochromic transition was detectable from films thinner than 40 nm. This is in contrast to results seen from films created from PVD methodologies where films as thin as 5 nm showed a transition.[26] Between 40 nm and 80 nm thickness the thermochromic transition was limited to an absolute change of 15–20% at 2500 nm. Above 80 nm thickness the thermochromic transition was in the region of 35–50% at 2500 nm; this appears to be independent of thickness above the 80 nm critical threshold. However, where films were thicker than 300 nm, transmission was very low at 2500 nm. A reduction in film thickness did not lead to a lowering of the transition temperature as has previously been reported by CVD and PVD methods.[18,25] This is most likely because the grain size and distribution are not significantly different between the samples prepared in this study.

Film morphology appears to play a significant role in determining the thermochromic properties of the films. Un-doped films, 100 nm thick, grown under slow growth conditions have typical island growth morphologies (Fig. 1a and b), the particles are relatively symmetrical, and there is

good size uniformity and even distribution across the substrate surface. The related thermochromic properties are wide hysteresis loops (35 °C) and a transition temperature at 66 °C. In contrast films grown at faster growth rates with a similar thickness (100 nm) have different morphologies (Fig. 1c and d), which consist of asymmetric or fused nucleation centres on the surface of the substrate. X-Ray diffraction and Rietveld analysis indicate a different type of preferred orientation in these films compared to those grown with the slow growth conditions. The thermochromic properties of these films, grown with fast conditions, are somewhat different as well: typically the hysteresis width is much smaller (10 °C) and the transition temperature reduced from 66 °C to 51 °C.

As previously reported tungsten doping lowers the transition temperature by *ca.* 20 °C per atom%.[9] The film morphologies of doped films grown under fast and slow growth conditions are similar to the un-doped films. In this study tungsten doping leads to a crystallographic reorientation of the films produced using the slow condition set. This is not apparent from electron microscopy investigation. The thermochromic properties are also affected. Doped films grown with the fast condition set have thin hysteresis loops, similar to the un-doped films grown under fast conditions. Doped films grown under slow conditions have similarly narrow hysteresis widths; this appears to be as a result of the aforementioned crystallographic reorientation. It is desirable to have thinner hysteresis loops as this will maximise the switching efficiency of the film and thus increase the effectiveness of the solar control properties, *i.e.*, the film responds more uniformly and with a sharper switch optimising room comfort. It has been suggested previously that a range of particle sizes leads to hysteresis broadening;[29] in the work presented here all samples have similar particle sizes but a large difference is observed in the hysteresis widths of the thermochromic transition for samples prepared using different growth conditions: this appears to be related to the crystallographic orientation. In all cases similar levels of tungsten doping led to similar transition temperatures; it was found that this was independent of film thickness, preferred orientation or growth conditions used.

The maximum change in IR transmittance (2500 nm^{-1}) observed was 50% on passing through the metal semiconductor transition for a 0.5 atom% tungsten doped monoclinic vanadium dioxide thin film grown using fast growth conditions (1 min deposition time) with a transition temperature of 55 °C, this is 5–10% better than seen previously.[9] The large changes in infrared transmittance observed on passing through the metal to semiconductor transition would affect the amount of sunlight passing through the window. The minimal change in the optical properties in the visible region of the spectrum indicates that the colour of the film remains constant and predictable. These are desirable properties for use in smart windows.

Previous studies indicate that decreasing film thickness leads to a reduction in transition temperature,[15,26] although this is not found to be the case in this study. A previous CVD study using vanadium acetylacetonate as a precursor for the production of monoclinic vanadium dioxide films found that an optimum decrease in transition temperature occurred at a film thickness of 300 nm on quartz substrates;[19] closer examination of these data, however, suggests a constant transition temperature of 65 °C with a large error in measurement of ±20 °C. In the same study films with thickness between 100 nm and 400 nm deposited on borosilicate, silicon and strontium titanate substrates had constant transition temperatures of 65 °C ± 5 °C.[19]

Epitaxial films of monoclinic vanadium dioxide deposited on sapphire substrates by PVD methodologies had a constant transition temperature of 67 °C at film thicknesses of 50 nm and above.[26] Below this thickness the transition temperature dropped; a film 5 nm thick was reported as having a transition temperature of 50 °C. The same trend was not observed here. Two explanations are presented for this phenomenon. Firstly film crystallinity: an increase in the number of grain boundaries and/or a large surface/interface ratio for very thin films may lead to the distortion of V–V pairs thus destabilising the low temperature phase and causing a drop in transition temperature.[15] The second postulated reason is stress.[30] It has been reported that reducing the intrinsic stress in a thin film of monoclinic vanadium dioxide by low energy argon ion bombardment lowers the transition temperature. This film processing was found to affect the morphology of the films, reducing surface roughness and altering the optical properties, decreasing transmission, increasing reflectance and absorption.

In both previous studies (CVD and PVD) film morphology is profoundly affected. In the former the thinner films (10 nm) have a smaller crystallite size, typically 20 nm, whereas thicker films (≥100 nm) have a crystallite size of the order of 100 nm. In the latter case processing leads to a less rough surface and a decrease in the number of grain boundaries. These two sets of results are seemingly contradictory. In one instance a decrease in grain size corresponding to an increase in the number of grain boundaries is correlated with a decrease in transition temperature, in the other case it is a decrease in the number of grain boundaries that is correlated to a decrease in the transition temperature. In this study crystallographic orientation changes; it is likely that different crystallographic orientations lead to different levels of stress in the resulting film and that this is a more dominant factor in determining stress and thus the transition temperature than particle size or the number of grain boundaries as reported in previous studies.[9,15,30] Unfortunately no crystallographic information is available from previous studies to allow comparison.

Comparison to previous work done on tungsten doped vanadium thin films created from the APCVD reaction of vanadium chloride, water and tungsten ethoxide[9] yields some interesting similarities. The samples show a large (011) reflection similar to the tungsten doped samples in this work. The samples show columnar type growth similar to the doped samples grown under slow growth conditions; indeed their optical properties are similar, though the thermochromic transition is not as pronounced as in the current work. One surprising difference is with the hysteresis behaviour of the samples. The hysteresis width of samples prepared from the APCVD reaction of vanadium chloride, water and tungsten ethoxide gets wider as more tungsten is doped into the films. This effect is absent in the current work: the hysteresis width is similar for the ranges of tungsten doping examined.

Unfortunately no direct comparison on the effect of thickness can be made as all of the films produced in the previous work were of a similar thickness (200–300 nm).

In our work films whose crystallites were preferentially orientated along the (001) plane, parallel to the substrate (with low March–Dollase *r* factors), had enhanced thermochromic properties compared to those with other preferential orientations. The best thermochromic properties were observed for a 0.5 atom% tungsten doped monoclinic vanadium dioxide thin film grown using fast growth conditions (1 min deposition time) with a transition temperature of 55 °C, which had a March–Dollase *r* factor of 0.6. This sample had a 50% drop in transmittance at 2500 nm^{-1} on passing through the metal to semiconductor transition, and a hysteresis width of 10 °C. The change in transmission of 50% is 5–10% better than has been seen previously.[9]

The effect of film thickness has been investigated and is found to have a less profound influence on thermochromic properties than previously thought. This study indicates, for the first time, that micro-structural phenomena, particularly crystallographic orientation, fundamentally affect the thermochromic properties of vanadium dioxide thin films. A change in orientation around the [001] axis has been demonstrated to decrease the transition temperature by as much as 15 °C and reduce hysteresis width by 20 °C.

Conclusions

Atmospheric pressure chemical vapour deposition reactions of vanadyl acetylacetonate, tungsten hexachloride and 2% oxygen led to the production of tungsten doped or un-doped vanadium(IV) oxide films on glass substrates. Film thickness had no discernable effect on the hysteresis width or temperature of transition but was found to influence the extent of the transition and visible light transmittance. The properties of the thermochromic transition were significantly influenced by the crystallographic orientation of the film. Films whose crystallites were preferentially orientated along the (001) plane, parallel to the substrate, had enhanced thermochromic properties compared to those with other preferential orientations investigated in this study. Variation of the growth rate and conditions was found to profoundly influence the preferential orientation of the crystals to the substrate and hence the resulting thermochromic properties of the films. A maximum change in transmittance at 2500 nm^{-1} of 50% was observed, 5% more than seen previously. Tungsten doping was found to decrease the transition temperature by 20 °C per 1% tungsten incorporated.

Acknowledgements

This was financially supported by the EU project Termoglaze. The authors would like to thank Pilkington Glass for providing glass substrates and Mr Kevin Reeves for the help with scanning electron microscopy. IPP thanks the Royal Society/Wolfson Trust for a merit award.

References

1 C. G. Granqvist, *Thin Solid Films*, 1990, **193**, 730.
2 C. G. Gramqvist, *Adv. Mater.*, 2003, **15**, 1789.
3 A. W. Smith, *Appl. Phys. Lett.*, 1973, **23**, 437.
4 W. R. Roach, *Appl. Phys. Lett.*, 1971, **19**, 453.
5 M. A. Richardson and J. A. Coath, *Opt. Laser Technol.*, 1998, **30**, 137.
6 K. D. Rogers, *Powder Diffr.*, 1993, **8**, 240.
7 T. E. Phillips, R. A. Murray and T. O. Poelher, *Mater. Res. Bull.*, 1997, **22**, 1113.
8 F. Beteille, R. Morineau, J. Livage and M. Nagano, *Mater. Res. Bull.*, 1997, **32**, 1109.
9 T. D. Manning, I. P. Parkin, M. E. Pemble, D. W. Sheel and D. Vernardou, *Chem. Mater.*, 2004, **16**, 744.
10 I. Takahashi, M. Hibino and T. Kudo, *Jpn. J. Appl. Phys.*, 2001, **40**, 1391.
11 W. Burkhardt, T. Christmann, B. K. Meyer, W. Niessner, D. Schalch and A. Scharmann, *Thin Solid Films*, 1999, **345**, 229.
12 C. Piccirillo, I. P. Parkin and R. Binions, *Chem. Vap. Deposition*, submitted.
13 T. D. Manning and I. P. Parkin, *Polyhedron*, 2004, **23**, 3087.
14 U. Qureshi, T. D. Manning and I. P. Parkin, *J. Mater. Chem.*, 2004, **14**, 1190.
15 Y. Takahshi, M. Kanamori, H. Hashimoto, Y. Moritani and Y. Masuda, *J. Mater. Sci.*, 1989, **24**, 192.
16 T. Maruyama and Y. Ikuta, *J. Mater. Sci.*, 1993, **28**, 5073.
17 J. B. MacChesney, J. F. Potter and H. J. Guggenheim, *J. Electrochem. Soc.*, 1968, **115**, 52.
18 M. B. Sahana, M. S. Dharmaprakash and S. A. Shivashankar, *J. Mater. Chem.*, 2002, **12**, 333.
19 M. B. Sahana, G. N. Subbanna and S. A. Shivashankar, *J. Appl. Phys.*, 2002, **92**, 6495.
20 D. Borreca, L. E. Depero, E. Franzato, G. A. Rizzi, L. Sangaletti, E. Tondello and U. Vettori, *J. Electrochem. Soc.*, 1999, **46**, 551.
21 T. D. Manning, I. P. Parkin, R. J. H. Clark, D. W. Sheel, M. E. Pemble and D. Vernardou, *J. Mater. Chem.*, 2002, **12**, 2936.
22 T. D. Manning and I. P. Parkin, *Proc.–Electrochem. Soc.*, EuroCVD 14, 2003, **2**, p. 777.
23 D. Vernardou, M. E. Pemble and D. W. Sheel, *Surf. Coat. Technol.*, 2004, **188–189**, 250.
24 T. D. Manning and I. P. Parkin, *J. Mater. Chem.*, 2004, **14**, 2554.
25 P. Dagur, A. U. Mane and S. A. Shivashankar, *J. Cryst. Growth*, 2005, **275**, e1223–e1228.
26 G. Xu, P. Jing, M. Tazawa and K. Yoshimura, *Appl. Surf. Sci.*, 2005, **244**, 449.
27 K. D. Rogers, *Powder Diffr.*, 1993, **8**, 240.
28 R. Binions, C. S. Blackman, C. J. Carmalt, S. A. O'Neill, I. P. Parkin, K. Molloy and L. Apostilco, *Polyhedron*, 2002, **21**, 1943.
29 F. Beteille, L. Mazerolles and J. Livage, *Mater. Res. Bull.*, 1999, **34**, 2177.
30 F. C. Case, *J. Vac. Sci. Technol., A*, 1984, **2**, 1509.

Chemical Vapor Deposition

DOI: 10.1002/cvde.200706641

Full Paper

Hybrid Aerosol Assisted and Atmospheric Pressure CVD of Gold-Doped Vanadium Dioxide**

By *Russell Binions*, *Clara Piccirillo*, *Robert G. Palgrave*, and *Ivan P. Parkin**

Hybrid aerosol-assisted (AA) and atmospheric pressure (AP) CVD methodology is utilized, for the first time, to produce thin films of gold nanoparticle-doped vanadium dioxide. Good surface coverage, comparable to that of APCVD processes, is observed, and a variety of different film thicknesses and dopant levels are easily produced. The films are analyzed by X-ray diffraction (XRD), scanning electron microscopy (SEM), and X-ray photoelectron spectroscopy (XPS). Their optical and thermochromic behaviors are also determined. Incorporation of gold nanoparticles in the films leads to significant changes in the color of the film due to the presence of a surface plasmon resonance (SPR) band.

Keywords: Aerosol, Nanoparticles, Thermochromism

1. Introduction

Vanadium dioxide is a material with great potential as an intelligent glazing material.[1,2] The technology is based on a metal to semiconductor transition (MST) where there is an associated structural change from the higher temperature rutile structure to the lower temperature monoclinic structure.[3] This structural transition results in significant changes in optical properties and electrical conductivity. The rutile material is metallic and reflects a wide range of solar radiation, whereas the monoclinic phase is a semiconductor and generally optically transparent. Work has been successfully conducted in recent years to reduce the transition temperature of VO_2 by adding dopants.[4,5] Tungsten has repeatedly proved to be the most successful dopant,[6] however the resulting films suffer from retaining an unpleasant brown/yellow color,[7] and this work has been conducted in an effort to improve upon this. We have focused on using gold nanoparticles as these have a surface plasmon resonance that is strongly absorbing, the frequency of which is strongly dependent on the dielectric properties of the host matrix and the size of the nanoparticles.[8,9] By using nanoparticles of the right size the color centre can effectively be tuned. Gold-doped vanadium dioxide composites, produced using reactive ion beam sputtering followed by annealing and laser ablation. have received attention as fast optical switches.[10,11]

Attempts to produce gold-doped vanadium dioxide films from a single-source AACVD reaction have proved futile as there appears to be an adduct reaction on mixing solutions of vanadium and gold precursors. Although there are no cheap and easily available gold precursors for use in APCVD, there is a potential abundance of precursors that can be used in AACVD as the precursor limitations of APCVD do not apply.[12,13] So far, only auric acid and colloidal gold suspensions have been reported.[14,15] A hybrid methodology has been used to deposit thin films of gold nanoparticle-doped vanadium dioxide from the CVD reaction of vanadyl acetylacetonate and auric acid in methanol. Here we report the first instance of this hybrid methodology being successfully used. This hybrid technique shows great potential as the film characteristics are similar to those produced by APCVD (good adhesion, uniformity, and coverage) but with the versatility afforded by AACVD. In principle this technique could be applied to any reaction system and take advantage of unusual precursors, leading to the deposition of new and interesting materials.

2. Results and Discussion

We have conducted experiments which combine the AA and AP CVD systems by adding the aerosol flow into the reaction chamber along with the atmospheric pressure reaction gas flow. This is illustrated schematically in Figure 1.

The APCVD reaction of vanadyl acetylacetonate to produce thin films of doped and undoped vanadium dioxide

[*] Prof. I. P. Parkin, Dr. R. Binions, Dr. C. Piccirillo, Dr. R G. Palgrave
Christopher Ingold Laboratories, Department of Chemistry,
University College London
20 Gordon Street, London, WC1H 0AJ, (U. K.)
E-mail: i.p.parkin@ucl.ac.uk

[**] This research was supported financially as part of the EU project TERMOGLAZE. Pilkington glass are thanked for the provision of glass substrates. IPP thanks the Wolfson trust for a merit award. Mr. Kevin Reeves is thanked for invaluable assistance with electron microscopy.

affords a great variety of growth rates.[16] It was felt that this would be the most suitable precursor to use in our experiments as the growth rate could be tailored to match that of the AACVD system. Previous work has shown that an AACVD system containing 25 mL of methanol with 40 mg of $HAuCl_4$ dissolved in it, with a flow rate of 2 L min^{-1} typically takes 15 min to exhaust, we therefore chose an APCVD system flow rate that led to the production of films of between 100 and 300 nm thickness over the same time period.[16] The flow conditions used in these experiments are summarized, with compositional and resultant film color data, in Table 1.

The aerosol flow is composed of liquid droplets transported, using a nitrogen gas flow, to the reaction chamber where the solvent evaporates and the precursor is able to take part in surface reactions. One of the challenges of AACVD is to prevent aerosol droplet condensation prior to introduction into the reactor. The two flows were introduced into the reaction chamber by means of a special manifold block containing two inputs, one for the APCVD flow and one for the AACVD. The routes through the block differed; the APCVD route had a baffle in the way of the flow, whereas the AACVD route did not, as it was felt that this might induce deposition in the manifold and lead to blockages. The vanadyl acetylacetonate and plain flows were mixed in the mixing chamber prior to the manifold block. The two flows were introduced separately into the reaction chamber to reduce the likelihood of prereaction or disruption of the aerosol droplets. The APCVD flow was introduced above the AACVD flow relative to the substrate to suppress the effects of thermophoresis that have been observed previously with AACVD systems.[17] Thermophoresis is undesirable as it leads to deposition on the top plate of the reaction chamber and powdery, non-adherent films. Use of a lower total flow, ~3 L min^{-1}, is not sufficient to negate the effects of thermophoresis, and impairs film growth rate. The use of a higher total flow rate (6 – 10 L min^{-1}) suppresses thermophoresis effects and leads to greater surface coverage, uniformity, and reproducibility. The flow rate used was relatively high, total flow of around 7 L min^{-1}, which, as well as suppressing the effects of thermophoresis, minimized the possibility of the aerosol droplets condensing or reacting anywhere before the reaction chamber.

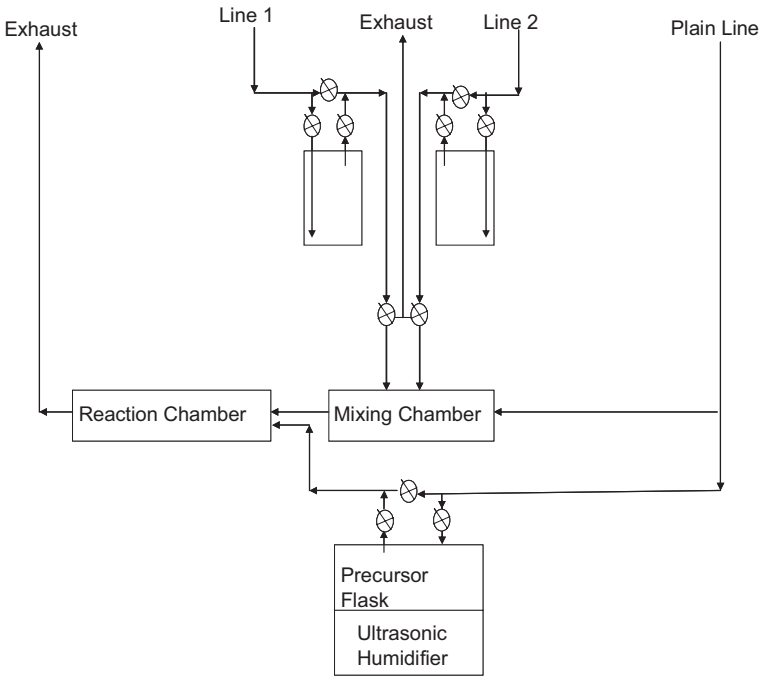

Fig. 1. Schematic of the AA/AP CVD set up.

The deposited films showed good surface coverage, uniformity, and reproducibility. Film thickness could easily be varied by increasing or decreasing the time of deposition. In all cases at least the first 75 % of the substrate is covered, similar to that observed previously with VO_2 films

Table 1. A summary of flow conditions and analytical data. All deposition experiments were conducted for 15 min with the substrate heated to 525 °C.

Sample	2% O_2 in N_2 flow rate [L min^{-1}]	$[VO(acac)_2]$ bubbler flow rate [L min^{-1}] {bubbler temperature [°C])	AACVD system flow rate [L min^{-1}] {$HAuCl_4$ concentration [M])	Phase observed with XRD	Au/V ratio as determined by EDAX	CIELAB transmission colour a*/b*/ dominant transmission wavelength [nm]	SPR centre [nm]
Un-doped VO_2	2	3 {175}	N/A	VO_2(m)	N/A	–4.83/40.39/568	N/A
1	4	1 {175}	2 {0.0047}	VO_2(m) + Au + V_2O_5	0.62	–6.67/0.73/495	620
2	1	2 {175}	2 {0.0047}	VO_2(m) + Au	1.00	–6.90/–2.99/484	620
3	2	3 {175}	2 {0.0047}	VO_2(m) + Au	0.16	–5.77/27.14/566	670
4	2	4 {175}	2 {0.0047}	VO_2(m) + Au	0.15	–11.81/11.86/551	720
5	2	3 {175}	2 {0.0059}	VO_2(m) + Au + V_2O_5	0.09	–7.97/1.46/498	640
6	2	3 {175}	2 {0.0071}	VO_2(m) + Au	0.30	–8.92/0.51/493	620
7	2	3 {175}	2 {0.011}	VO_2(m) +Au	0.36	–7.29/–13.5/476	590
8	2	3 {175}	2 {0.0024}	VO_2(m) + Au + V_2O_5	0.07	–4.14/16.44/566	590

produced from the APCVD reaction of vanadyl acetylacetonate, and with other APCVD systems such as those that produce metal oxide and metal phosphide materials.[18–22] Similarly, there are changes in thickness that correlate with the temperature gradient across the substrate surface, as seen previously,[18–22] and a highly uniform area 2 cm × 5 cm in the middle of the substrate. The color of the films (Table 1) could be substantially altered with a range of blues and greens being produced in contrast to the yellow/brown color normally associated with monoclinic vanadium dioxide; this is attributed to the inclusion of gold nanoparticles in the VO_2 matrix. UV-vis absorbance spectroscopy of the gold-doped films indicates that a plasmon resonance band is present (Table 1); however this is very broad due to significant variation in nanoparticle size. The strength of the band correlates strongly with the gold to vanadium ratio in the films. The position of this band determines the overall color and is dependent upon three factors: the inter-particle distance, particle size, and the refractive index of the host matrix.[8,9] The refractive index of the host matrix is assumed to be constant between samples; SEM (Fig. 2) suggests a wide distribution of particle sizes that is similar between samples. It is likely that the only significant difference between samples is the localized electronic environment. Where there is significant gold in the sample, each nanoparticle experiences a local environment that is influenced by other gold nanoparticles and not just vanadium dioxide, hence there is a significant change in the SPR centre where this occurs. There is wide variation (590 – 700 nm, Table 1) in the SPR centre between samples in the same region as the SPR band seen with nanocomposites produced by laser ablation (645 nm).[10] The higher the gold to vanadium ratio, the more blue-shifted the SPR, and the lower the dominant wavelength. The reason for this is likely to be twofold: the effect of the localized environment as described above, and the strength of the SPR. If only a small amount of gold is present in the film, then the effect on the film color of the SPR will be small, possibly negligible. Previous work conducted using sol-gel methodologies does not show a change in film color, most likely because of phase segregation as a result of the sol-gel process.[23]

The films were also more adherent than films of vanadium dioxide or gold produced using AACVD.[14,15] They passed the Scotch tape test and could not be wiped off with a piece of toweling. The films could, however, be marked with a brass or steel stylus in a similar way to films of VO_2 produced previously.[6,7,16] The films were found to be insulating, suggesting that the amount of gold in the films was not enough to exceed the percolation limit.

Analysis with energy dispersive X-ray (EDX) analysis indicated that the films contained gold and vanadium (summarized in Table 1) and no contaminant, at least to the limit of detection of the methodology (around 0.5 at.-%, depending on the element). The amount of gold in the film depended on the ratio of the precursor flows (Table 1), where the higher the ratio of $[HAuCl_4]$ to $[VO(acac)_2]$ the higher the gold to vanadium ratio in the resultant film. Secondary electron imaging (Fig. 2a) indicates that rod-like crystallites of VO_2, around 100 nm in width and up to 1.5 μm long, grow on the surface of the substrate, similar to morphologies previously seen in samples from the APCVD reaction of vanadyl acetylacetonate.[16] Backscattered electron images (Fig. 2b) indicate that gold is found amongst the crystallites on the surface rather than segregating as independent gold crystallites as seen as a result of the sol-gel process.[23]

XRD analysis (Fig. 3) indicates that, in all cases, cubic gold and monoclinic vanadium dioxide are formed. In some cases there is some evidence of the formation of V_2O_5. This is not entirely unexpected as, since XPS (Fig. 4) of the sample surface suggests a variety of vanadium environments, we believe V_2O_5 to be present only at the surface. Indeed, on etching, only a single vanadium environment is observed consistent with vanadium dioxide. Previous work on vanadium dioxide by APCVD has seen a similar phenomenon and has shown that surface V_2O_5 does not effect the thermochromic behavior of the bulk film.[6,7] XPS shows that the gold is found in a single metal environment, this indicates several things: There are no other detectable gold compounds present in the film; there is no unreacted precursor on the film surface; and the gold is present only as gold nanoparticles on the surface and in the bulk of the host film matrix. XPS and Raman spectroscopy were used to evaluate carbon contamination in the films. Carbon could not be detected in the bulk of the films using these methods, and although some carbon was detected on the surface of the films

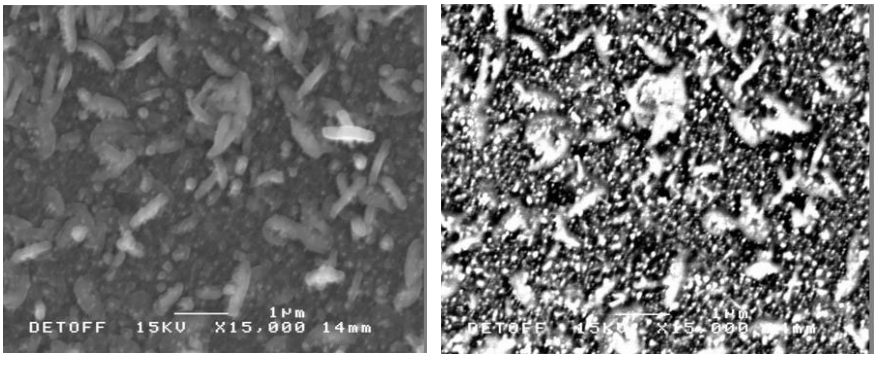

a b

Fig. 2. a) Secondary electron image, and b) Back scattered electron image of sample 4 typical of these gold-doped vanadium dioxide samples deposited using the combined system over 15 min at a temperature of 525 °C.

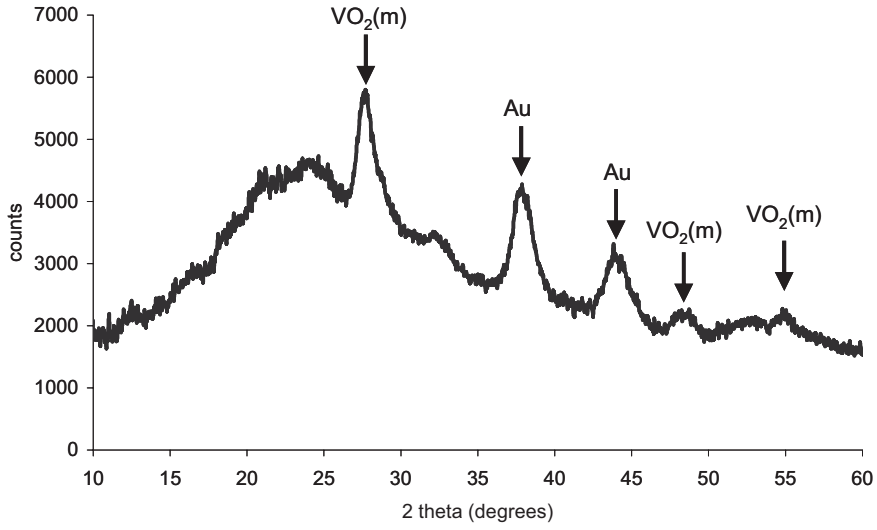

Fig. 3. XRD pattern of sample 7, typical of gold-doped vanadium dioxide samples deposited using the combined system over 15 min at a temperature of 525 °C.

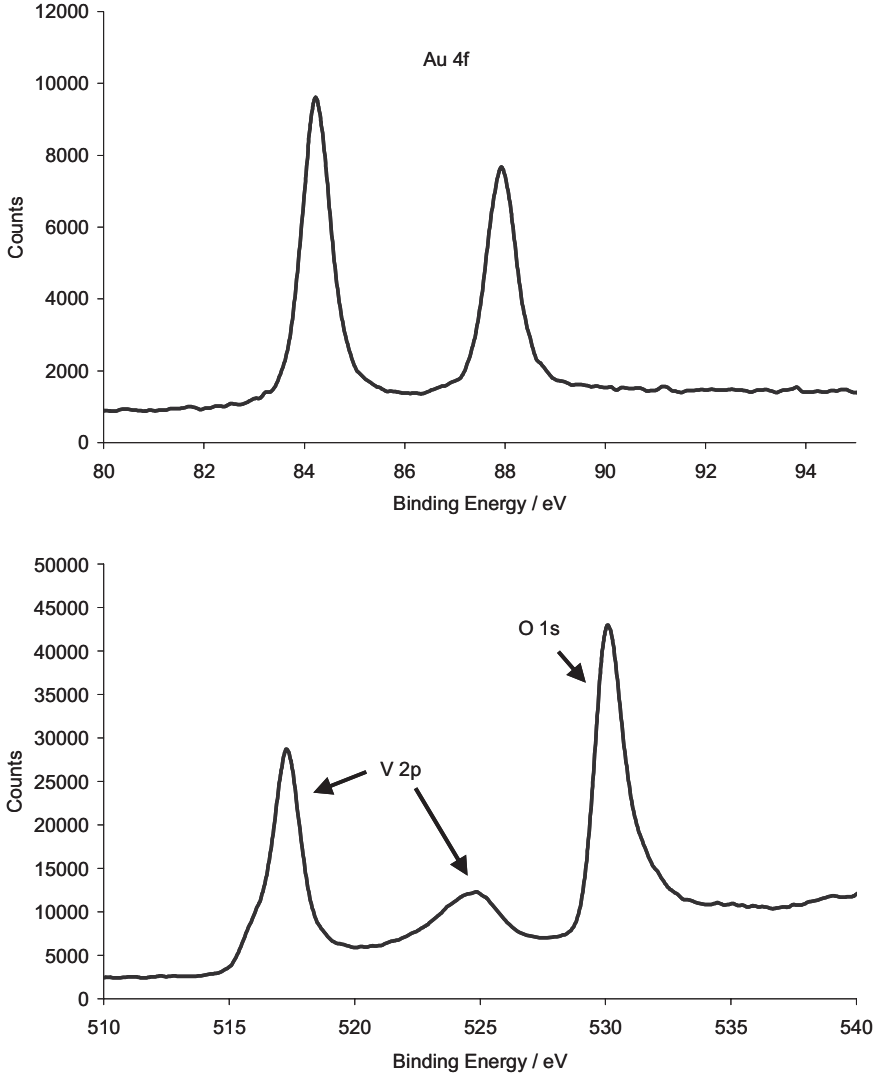

Fig. 4. XPS image of the surface of sample 4, typical of gold-doped vanadium dioxide samples deposited using the combined system over 15 min at a temperature of 525 °C.

using XPS, it is most likely to have come from an external source.

All of the films show thermochromic behavior with reduced transition temperatures. Typically the hysteresis width (Fig. 5) of gold-doped vanadium dioxide thin films is quite wide, in the range 15 – 20 °C compared to 10 °C as seen with some tungsten-doped samples produced by APCVD,[6,7,16] and 10 – 15 °C seen for films produced by sol-gel methods.[23] The hysteresis width seemed to be independent of the amount of gold present in the film. Ideally this hysteresis would be as small as possible to maximize the energy saving effect. The hysteresis width is attributable to several factors such as a variety of grain size,[24] and/or crystallographic orientation.[16] Indeed the transition temperature is reduced to ~50 °C, which is independent of the amount of gold in the films. It is likely that this reduction is caused by strain as a result of preferential orientation as observed previously,[16] indeed the XRD pattern has only one significant observable peak, the 011, suggesting a high degree of preferred orientation. We are unable to conduct a meaningful Reitveld analysis as we are only able to observe two peaks; two smaller peaks in the VO_2(m) diffraction pattern are obscured by the peaks due to gold. Similarly, films that were prepared by sol-gel gave transition temperatures of ~55 °C similar to undoped films prepared by the same method, indeed the XRD patterns of these films have a very strong 011 reflection.[23] By comparison, samples of gold-doped nanocomposites produced by laser ablation, and thin films prepared by reactive ion beam, sputtering have transition temperatures of around 68 °C, similar to undoped vanadium dioxide.[10,11] Unfortunately no XRD data is presented for comparison.

As seen with undoped and tungsten-doped samples prepared by CVD, a large change in transmission is observable at 2500 nm (Fig. 6a), typically 35–40 % comparable with previous literature values.[6,7,16] The

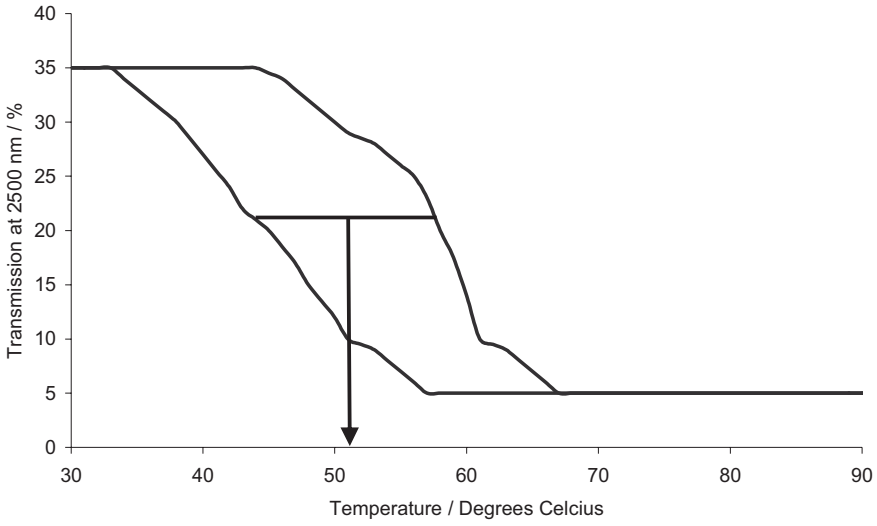

Fig. 5. Hysteresis behavior at 2500 nm of sample 5, typical of gold-doped vanadium dioxide samples deposited using the combined system over 15 min at a temperature of 525 °C.

reflectance spectrum is different (Fig. 6b) since there is only a small change of around 10 % on undergoing the transition. This is attributable to the higher reflectance of the films below the transition temperature, due to the metallic nature of the gold nanoparticles. Undoped or tungsten-doped films of monoclinic vanadium dioxide do not have as significant a metallic contribution to the reflectance, and the change at 2500 nm on undergoing the MST is around 35 %.[6,7,16]

Figure 7 details the temperature-dependent hysteresis of the SPR band. The SPR band changes with temperature as the rutile and monoclinic forms of vanadium dioxide provide different dielectric environments. The SPR hysteresis behavior is similar to the optical hysteresis – the hysteresis width is around 20 °C and it indicates a transition temperature of ~50 °C. In comparison to SPR hysteresis observed from gold-doped vanadium dioxide nanocomposites produced by laser ablation,[10] the hysteresis width is similar and there is a comparable change of SPR wavelength of 40 nm.

3. Conclusions

The use of hybrid AA and AP CVD methodology has afforded thin films of gold nanoparticle-doped monoclinic vanadium dioxide. The inclusion of gold nanoparticles into the thin film matrix has successfully and significantly altered the color of the films compared to the undoped films due to the presence of a SPR band. The use of preformed nanoparticles may offer greater control over the film color by changing the position of the SPR band. The thermochromic properties of these films are similar to those seen previously with vanadium dioxide films grown by APCVD; with an enhanced low-temperature reflectance. This methodology offers advantages over others such as sol-gel, as it is a one-step process that may possibly be incorporated into the online production of float glass. Good surface coverage, comparable to that of APCVD processes, is observed, and a variety of different film thicknesses and dopant levels can be easily produced. We believe this to be the first time that a hybrid AA/AP CVD system has been reported in the literature, and that the technique shows great promise as a generally applicable method.

4. Experimental

A 98 % nitrogen, 2 % oxygen mixture was obtained from the British Oxygen Company (BOC) and used, as supplied, in the plain line. Nitrogen (99.99 %) was obtained from BOC and used, as supplied, in the bubbler lines. Coatings were obtained on SiO_2-coated float glass. Combined AA/AP CVD experiments were conducted on 150 mm × 45 mm × 3 mm pieces of glass using a flat-bed, cold-wall CVD reactor. The glass was cleaned prior to use by washing with petroleum ether (60–80 °C) and isopropanol, and then dried in air. A graphite block containing a Whatman cartridge heater was used to heat the glass substrate. The temperature of the substrate was monitored by a Pt-Rh thermocouple. Independent thermocouple measurements indicated that temperature gradients of up to 50 °C cm^{-1} were observable at 600 °C across the surface of the glass. The rig was designed so that four independent gas lines could be used. All gas handling lines, regulators, and flow valves were made of stainless steel and were 6.5 mm in internal diameter, except for the inlet to the mixing chamber and the exhaust line from the apparatus that were 13 mm in diameter. In these experiments three gas lines were used. Gases came directly from a cylinder and were preheated by passing along 2 m lengths of stainless steel tubing, which were curled and inserted inside a tube furnace. The temperatures of all the gas inlet lines were monitored by Pt-Rh thermocouples and Eurotherm heat controllers.

Vanadyl acetylacetonate (99.99 %) which was obtained from Aldrich and used without further purification, was placed into a stainless steel bubbler. The bubbler was heated to 175 °C by a heating jacket, and vanadyl acetylacetonate introduced into the gas streams by passing hot nitrogen gas through the bubbler. 40 mg of $HAuCl_4$ (99.9 %, obtained from Aldrich and used without further purification) was dissolved in 25 mL methanol and placed into a glass flask. An aerosol was generated at room temperature by use of a PIFCO air humidifier. Nitrogen was passed through the aerosol mist thus forcing the aerosol particles, encapsulated with precursor, into the heated reaction chamber.

The two components of the system were transported using stainless steel pipes 13 mm in internal diameter. The pipes were attached directly to the reaction chamber of the coater. Gas flows were adjusted using suitable regulators and flow controllers. The exhaust from the reactor was vented directly into the extraction system of a fume cupboard. All of the apparatus was baked out with nitrogen at 150 °C for 30 min before use. Deposition experiments were conducted by heating the horizontal-bed reactor and the bubblers to the desired temperatures before diverting the nitrogen line through the bubbler and hence to the reactor. Deposition experiments were timed by use of a stopwatch and were conducted at periods of between 30 s and 30 min in order to vary the thickness of the samples. The maximum possible deposition temperature with this equipment was 600 °C. At the end of the deposition only nitrogen was allowed to flow over the glass substrate until the substrate had cooled sufficiently to handle (~60 °C). Samples were

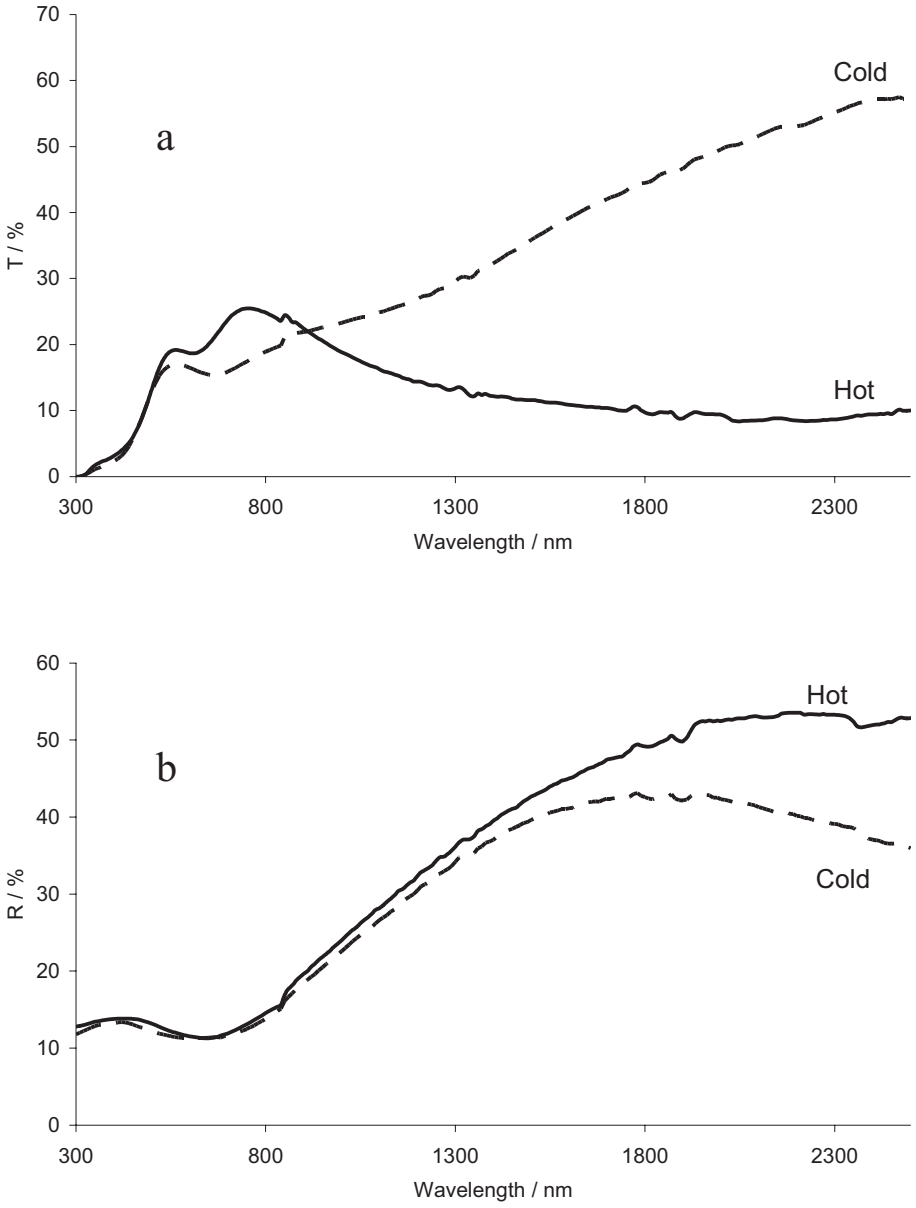

Fig. 6. a)Transmission, and b) reflectance spectra of sample 7, typical of gold doped vanadium dioxide samples deposited using the combined system over 15 min at a temperature of 525 °C.

handled and stored in air. The substrate temperature for deposition was kept constant at 525 °C as this has been found to be the optimal temperature to grow monoclinic vanadium dioxide thin films from vanadyl acetylacetonate. Due to the nature of the graphite heating block there are changes in thickness that correlate with the temperature gradient across the substrate, however, a highly uniform area 2 cm × 5 cm in the middle of the substrate was always used for observations; it is this area that is referred to when discussing the uniformity of the films.

Electron microprobe analysis was obtained on a JEOL EMA and referenced against vanadium and oxygen standards. Energy dispersive X-ray analysis (EDAX) and WDAX were conducted using a Phillips XL30 ESEM instrument. SEM images were acquired on a Jeol 6301F field emission instrument. XRD patterns were measured on a Bruker Gadds D8 diffractometer using monochromated (Cu Ka_{1+2}) radiation in the reflection mode using a glancing incident angle of 5°. Reflectance and transmission spectra were recorded between 300 and 2500 nm on a Perkin Elmer Lambda 950 UV-VIS spectrometer. UV-vis spectra were obtained using a Helios double beam instrument. Raman spectra were acquired on a Renishaw Raman system 1000 using a helium-neon laser of wavelength 632.8 nm. The Raman system was calibrated against the emission lines of neon. Transmittance-temperature studies were performed on a Perkin-Elmer 457 grating spectrometer set to 4000 cm^{-1}. An aluminum temperature cell controlled by RS resistive heaters, Eurotherm temperature controllers, and k-type thermocouples was used to manipulate sample temperature. Sample temperature was measured using a k-type thermocouple taped directly onto the film surface. Film thickness was measured directly by SEM then correlated with EDAX and optical transmission data.

Received: August 22, 2007
Revised: December 14, 2007

[1] C. G. Granqvist *Thin Solid Films* **1990**, *193*, 730.
[2] C. G Granqvist *Adv. Mater.* **2003**, *15*, 1789.
[3] K. D. Rogers *Powder Diffract.* **1993**, *8*, 240.
[4] T. E. Phillips, R. A. Murray, T. D. Poelher *Mater. Res. Bull.* **1997**, *22*, 1113.

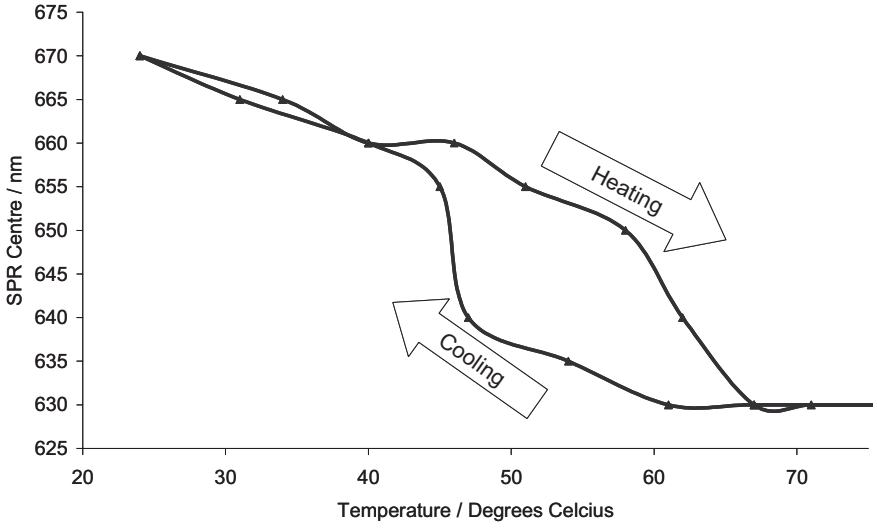

Fig. 7. SPR hysteresis of sample 4.

[5] F. Beteille, R. Morineau, J. Livage, M. Nagano *Mater. Res. Bull.* **1997**, *32*, 1109.
[6] T. D. Manning, I. P. Parkin , M. E. Pemble, D. W. Sheel, D. Vernardou *Chem. Mater.* **2004**, *16*, 744.
[7] T. D. Manning, I. P. Parkin *J. Mater. Chem.* **2004**, *14*, 2554.
[8] T. Ung, L. M. Liz-Marzan, P. Mulvaney *Colloids Surf. A* **2002**, *202*, 119.
[9] S. Link, M. El-Sayed in *Semiconductor and Metal Nanocrystals*; (Ed. V. I. Klimnov) Marcel Dekker, New York, **2004**, p45.
[10] M. Maaza, O. Nemravoui, C. Sella, A. C. Beye *Gold Bull.* **2005**, *38*, 100.
[11] S. Chen, H. Ma, X. Yi, H. Wang, X. Tao, M. Chem, X. Li, C. Ke *Infrared Phys. Technol.* **2004**, *45*, 239.
[12] W. B. Cross, I. P. Parkin, *Chem. Comm.* **2003**, *14*, 1696.
[13] R. Binions, C. J. Carmalt, I. P. Parkin, *Thin Solid Films* **2004**, *416*, 9469.
[14] R. G. Palgrave, I. P. Parkin *J. Am. Chem. Soc.* **2006**, *128*, 1587.
[15] R. G. Palgrave, I. P. Parkin *J. Mater. Chem.* **2007**, *19*, 4639.
[16] R. Binions, C. Piccirillo, G. Hyett, I. P. Parkin *J. Mater. Chem.* **2007**, *17*, 4652.
[17] L. Talbot, R. K. Cheng, R. W. Schefer, D. R. Wills *J. Fluid Mech.* **1980**, *101*, 737.
[18] R. Binions, C. S. Blackman, C. J. Carmalt, I. P. Parkin, S. A. O'Neill, K. C. Molloy, L. Apostolico *Polyhedron* **2002**, *21*, 1943.
[19] R. Binions, C. J. Carmalt, I. P. Parkin *Polyhedron* **2003**, *22*, 1683.
[20] R. Binions, C. J. Carmalt, I. P. Parkin *Polyhedron* **2006**, *25*, 3032.
[21] R. Binions, I. P. Parkin *Meas. Sci. Technol.* **2007**, *18*, 190.
[22] R. Binions, C. J. Carmalt, I. P. Parkin *Chem. Mater.* **2004**, *16*, 2489.
[23] E. Cavanna, J. P. Segaud, J. Livage *Mater. Res. Bull.* **1999**, *34*, 167.
[24] F. Beleille, L. Mazerolles, J. Livage *Mater. Res. Bull.* **1999**, *34*, 2177.

Journal of Nano Research Vol. 2 (2008) pp 1-20
Online available since 2008/Aug/07 at www.scientific.net

doi:10.4028/www.scientific.net/JNanoR.2.1

Thermochromic Coatings for Intelligent Architectural Glazing

Ivan P. Parkin[1, a], Russell Binions[1], Clara Piccirillo[1], Christopher S. Blackman[1] and Troy D. Manning[2].

[1] Department of Chemistry, University College London, 20 Gordon Street, London, WC1H OAJ , United Kingdom

[2] Current address: Pilkington plc, Pilkington Technical Centre, Hall Lane, Lathom, Ormskirk, Lancashire, England, L40 5UF, United Kingdom

[a] i.p.parkin@ucl.ac.uk

received paper 20.11.2007, received revised paper 15.01.2008, accepted date 20.01.2008

Keywords: Solid state chemistry, Materials Science, Thin Films, Chemical Vapour Deposition, Thermochromism, Vanadium Dioxide.

Abstract. Thermochromic glazing is a type of intelligent glazing; one where the properties of the glazing change according to some external stimulus. More particularly a thermochromic window is a device that changes its transmission and reflectance properties at a critical temperature (T_c). At this specific temperature the material undergoes a semi-conductor to metal transition. At temperatures lower than T_c the window lets all of the solar energy that hits it through. At temperatures above T_c the window reflects the infra-red portion of solar energy. In such a way thermochromic windows may help reduce air conditioning and heating costs leading to more energy efficient buildings. This review details the nature of the semi-conductor to metal transition and indicates how substitutional doping within a crystal lattice can be used to manipulate and fine tune the critical temperature. Also detailed is the underlying science and methodologies so far employed in the production of thermochromic thin films.

Solar control coatings.
The use of air-conditioning equipment in order to maintain comfortable conditions inside buildings during the summer months is ever increasing and consumes vast amounts of electricity [1]. There is a concurrent increase in carbon dioxide emissions and of various other atmospheric pollutants created during the power generation. The effect is a self propagating cycle: global warming increases necessitating the further use of air conditioning in the summer months leading to a further growth in carbon dioxide emissions. There is thus a requirement that this cycle is broken and carbon dioxide emissions limited.

Solar control coatings are a technology applicable to all types of glazing – commercial or residential, to play an active role in improving the energy efficiency of the building. The currently available products take an extreme approach to solar control. Current coatings consist of an all out approach that is applicable to constant climates. If an environment is consistently hot, tinted glass or thin metallic coatings can be used to reflect solar heat and prevent it from entering the building [2], limiting the need for internal cooling. In a consistently cold environment heat may be retained in a building by the use of a wavelength selective coating such as doped tin oxides such as ITO or K-glass; both of which are transparent in the visible part of the spectrum but highly reflective in the infra red [2]. This allows sunlight to enter into the building but prevents blackbody radiation and internally generated heat from escaping, consequently reducing heating requirements. [2]

However, coatings of either type typically produce only a marginal energy benefit in changeable climates such as northern and central Europe, the USA, Canada and Japan which have cold winters and hot summers. The use of thermochromic coatings [1-7], whose optical properties are dependant on temperature and are usually related to a structural phase change, may have potential application in these geographical areas.
Vanadium (IV) oxide is an example of a thermochromic material which shows great promise for use in glazing coatings. Figure 1 schematically indicates the manner in which thermochromic glazing coatings work.

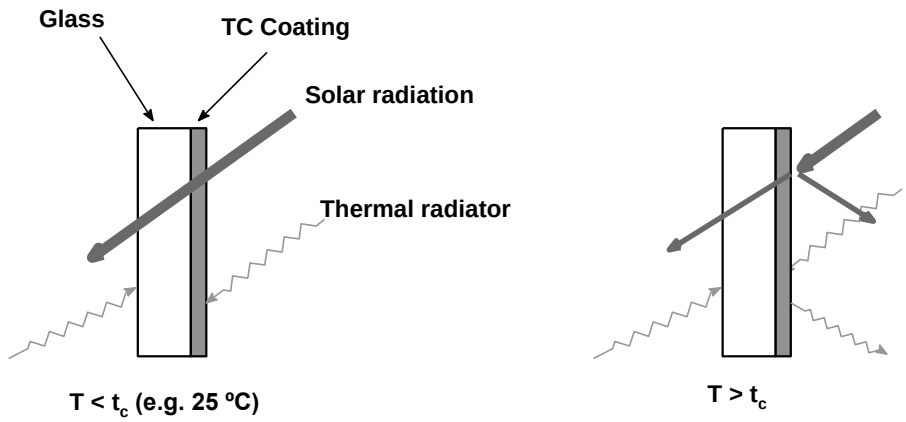

Figure 1 Schematic demonstration of the application of thermochromic materials to advanced window glazing [8].

The transition temperature (T_c) for a pure single crystal of vanadium (IV) oxide is 68 ºC. At temperatures below T_c the material is transparent in both the infra red and visible part of the spectrum, thus allowing solar radiation to pass through the window maximizing the heating effect of sunlight and black body radiation within the building. At temperatures above T_c the coating is transparent in the visible but becomes reflective in the infra red part of the spectrum. This prevents the thermal part of solar radiation from heating the building interior. This also allows for the

greatest use of natural light which is highly desirable as internal lighting contributes towards the buildings energy use and maintenance costs.

At 68 ºC the critical temperature of vanadium (IV) oxide is too high to be effective in maintaining a comfortable temperature (18 – 25 ºC). The use of dopants has been shown to affect the critical temperature. This may increase or decrease depending on factors such as dopant size [9], dopant charge [10] and changes in electron carrier density [11]. Tungsten has been shown to the most effective dopant to lower the Tc of vanadium (IV) oxide [9] with a 2 atom% tungsten loading reducing Tc to around 25 ºC in films prepared by physical vapour deposition [12] and sol-gel coating [13].

One significant challenge facing thermochromic coatings based on doped vanadium (IV) oxide is the balance of the extent of the transition and the visible transmittance. For larger changes in reflective properties visible transmission is low [12-15], this may require an increase in internal lighting, negating the energy benefit of having the coating in the first place. Two methods have been investigated to improve the visible transmittance of these films. Fluorine doping [4] into vanadium (IV) oxide thin films by r.f. sputtering formed films of VO_xF_y, transmittance properties were improved and also led to a decrease in T_c. Fluorine doping has however, also been reported [12] to decrease the sharpness of the thermochromic transition, potentially reducing their usefulness in glazing. A potentially more promising solution to this problem is the direct application of an antireflection coating to the thermochromic film. Silicon (IV) oxide over layers were found to greatly improve the visible transmittance below and above T_c without affecting the temperature that T_c occurs at [14]. Multifunctional window coatings have been prepared [15] using titanium (IV) oxide as and antireflection over layer. Improved transmittance and a reduced transition temperature were reported. It was proposed that such composite films would have multifunctional properties as titanium (IV) oxide is a well characterised photo-catalyst [16] that is used in self-cleaning glazing [17,18].

To enable the use of vanadium (IV) oxide as an intelligent window coating, a method is required to produce thin films on glass cheaply and efficiently ideally during the manufacturing process in the float-glass furnace [19]. Physical vapour deposition and sol-gel methods are processes that require the glass to be ready formed and cannot be integrated directly into a float-glass furnace making them off-line processes. The ideal process for applying thin films of material to glass substrates is atmospheric pressure chemical vapour deposition which has the advantage of not requiring a reduced pressure environment and has the high growth rates necessary for a high throughput process.

The structure and properties of vanadium (IV) oxide.
Since the thermo-conductive properties of several transition metal oxides was investigated in the late 1950's [20], much research has been undertaken to comprehend the nature of this transition. The transition was originally named a metal-to-insulator transition due to the changes in conductive properties of the materials, but other properties of these materials soon became apparent and has since been re-labelled a metal-to-semiconductor transition (MST). Their optical properties also showed large decreases in transmittance and increases in reflectance on passing through the transition temperature [21, 22].

The most promising of the transition metal oxides investigated by Morin for technological applications is vanadium (IV) oxide as this material has a metal-to-semiconductor transition temperature of 68 ºC, the closest to room temperature of the thermo-transitive metal oxides. This metal-to-semiconductor phase transition (MST) corresponds to a structural phase transformation from monoclinic to tetragonal (Figure 2, ref 23). The low temperature, monoclinic phase has unit

cell parameters a = 5.75 Å, b = 4.52 Å, c = 5.38 Å and β = 122.60º. The structure involves $V4^+$ – $V4^+$ pairing with alternate shorter (0.265 nm) and longer (0.312 nm) $V4^+$ – $V4^+$ distances along the monoclinic a axis. The high temperature phase has a tetragonal rutile type structure, cell parameters a = 4.55 Å and c = 2.85 Å, with equidistant vanadium atoms (0.288 nm) in chains of edge sharing [VO6] octahedra. On passing through the MST, the (100) planes of vanadium atoms in the monoclinic phase shift by 0.043 nm parallel to (001). This shift is sufficient to break the $V4^+$ – $V4^+$ pairs to form a tetragonal phase allowing metallic conductivity [23]. Figure 2 shows representations of the two phases of vanadium (IV) oxide. The diagram of the monoclinic phase displays the alternate $V4^+$ – $V4^+$ pairs and the distortion of the vanadium atoms along the a-axis.

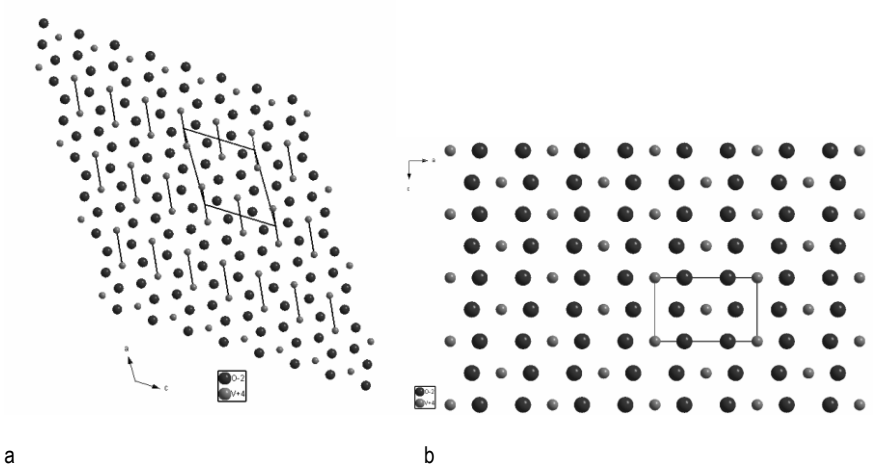

Figure 2. Representations of the structures of (a) monoclinic VO_2, with V-V pairs indicated, and (b) tetragonal VO_2, viewed along the b-axis of the unit cell. Oxygen atoms are the larger dots.

On passing through the transition temperature, electrical conductivity and infrared reflectivity increase dramatically but there is virtually no change in the visible region. This has lead to vanadium (IV) oxide being investigated as a potential data storage media [1, 3], an optical switch [24], and as an infrared modulator for missile guidance systems [5]. It is as an intelligent window coatings that vanadium (IV) oxide may find its most beneficial application.

The nature of the metal-to-semiconductor transition in vanadium (IV) oxide.

A larger number of computational studies have been undertaken to investigate the details of the metal-to-semiconductor transitions in transition metal oxides and vanadium (IV) oxide in particular [25-30]. Despite these studies, the metal-to-semiconductor transition is still not completely understood. Goodenough [26], produced a useful explanation describing the band structure of the two phases of vanadium (IV) oxide in terms of molecular orbitals.

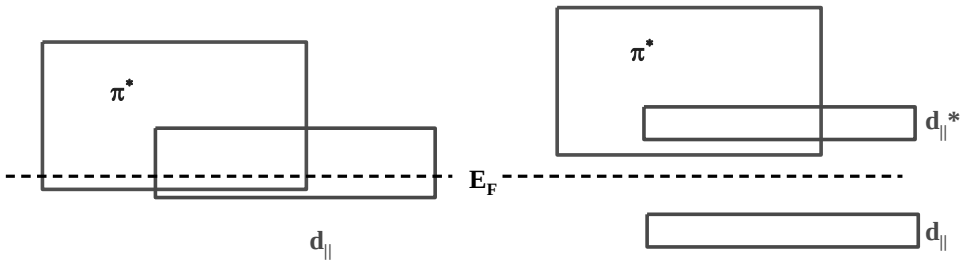

(a) Tetragonal **(b) Monoclinic**

Figure 3. Band structure scheme for (a) tetragonal and (b) monoclinic VO_2 at the Fermi level (EF) (adapted from Ref 29). d‖ orbitals are due to V-V pairs resulting from overlap of dx2- y2 atomic orbitals.

Goodenough discussed the possibility of an anti-ferroelectric transition being the driving force for the metal to semiconductor transition in vanadium (IV) oxide. He initially constructed an energy level diagram for tetragonal vanadium (IV) oxide (Figure 3a) and then argued that V-V pairing becomes energetically stable on cooling after the rearrangement of the band structure in forming the monoclinic phase (Figure 3b). In this way, he argued that there are two transition temperatures, T_c due to the anti-ferroelectric distortion and T_c', due to the crystallographic distortion, which happen to be coincident for vanadium (IV) oxide. Goodenough concluded that the driving force for low-temperature distortion in vanadium (IV) oxide is the anti-ferroelectric component of the distortion and that the transition temperature T_c is controlled by the entropy of the lattice vibrational modes and not by the thermal excitation of electrons into the anti-bonding bands.

A more recent paper by Eyert [31], uses density functional theory and the local density approximation, corroborates Goodenough's model as a Peierls-like instability. The MST of vanadium (IV) oxide, when cycled between the low and high temperature phases, displays hysteresis behaviour. This indicates a first-order transition whereby some regions of the material have completed the transition and others have not. First-order transitions involve a latent heat and the energy of the transition cannot be instantaneously transferred between the material and the surroundings.

Doping of vanadium (IV) oxide.
The introduction of dopants at low levels may influence the temperature (T_c) at which the metal-to-semiconductor transition occurs. The way dopants introduced into the vanadium (IV) oxide lattice give rise to this effect is less well understood than the nature of the metal to semiconductor itself. There are various theories on the action of doping in vanadium (IV) oxide that result from experiments and theoretical calculations.

It has been observed that high valence metal ions, such as tungsten (VI) or niobium (V), when doped into vanadium (IV) oxide, decrease the metal to semiconductor (MST) temperature of vanadium (IV) oxide, room temperature with 2 atom % tungsten (VI). Low valence ions, such as aluminium (III) or chromium (III), were shown to increase the MST temperature. It has been observed that dopant ions with an ionic radius smaller than V^{4+}, or that created V^{5+} defects (which were smaller than V^{4+}) increased the MST temperature, while dopant ions with a larger ionic radius than V^{4+} caused a decrease in the MST temperature [9].

A more involved discussion (by Goodenough) builds on X-ray diffraction observations that a second semi-conducting phase is present in doped samples between the low-temperature monoclinic phase and the high-temperature tetragonal phase [11, 26]. For low-valence dopant ions, this second semi-conducting phase has an orthorhombic structure and for high-valence ions it has a rutile

structure. Goodenough then explains various scenarios of doped vanadium (IV) oxide in accordance to his description of the MST [26].

Cations that cannot contribute to homopolar bonds but can participate through π bonding, such as titanium (IV) d0, decrease the crystallographic transition temperature T_c'. Dopants that introduce electrons to the vanadium d bands, such as cations with a higher valence state than vanadium (IV) (e.g. tungsten (VI) or niobium (V)) or anions with a lower valence state than vanadium (IV) (such as F^-), reduce the anti-ferroelectric stabilisation of the low-temperature phase by introducing π* electrons into the anti-ferroelectric state. This then reduces the anti-ferroelectric transition temperature, T_c. The additional electrons may be localised as discrete vanadium (III) ions.

Low valence cations, introduced into the vanadium(IV) oxide lattice stabilise the anti-ferroelectric distortion as they are relatively more stable in lower anion co-ordination sites, such as those in monoclinic vanadium(IV) oxide with its distorted lattice, than high valence cations,. Chromium (III) would be expected to show the smallest effect due to having a high preference for octahedral co-ordination.

The work of Goodenough has been further confirmed by Tang et al [32] who investigated the oxidation states of vanadium and tungsten in $W_{0.05}V_{0.95}O_2$ and $W_{0.08}V_{0.92}O_2$ by EXAFS and magnetic susceptibility studies. They suggest the formation of V^{3+}-W^{6+} and V^{3+}-V^{4+} pairs in vanadium (IV) oxide with tungsten doping, in accordance with Goodenough's theories on the stability of the anti-ferroelectric distortion.

Tungsten Doping.

Of the dopants investigated so far in single crystals and PVD or sol-gel prepared thin films, tungsten [33-38] has been found to reduce the transition temperature of vanadium (IV) oxide by the greatest extent per atom % and as such is the dopant that been the focus of the majority of research. For all reported methods of preparation, vanadium (IV) oxide films containing ~2 atom % tungsten have been shown to have a thermochromic transition temperature of about 25 ºC, suggested as the ideal transition temperature for intelligent window coatings.

Other Dopants.

In addition to tungsten, other metal ions, when introduced into the vanadium (IV) oxide lattice, have been shown to affect the metal-to-semiconductor transition temperature of vanadium (IV) oxide. The direction and magnitude of the change in the transition temperature is related to a number of factors such as dopant ion charge and size. Sol-gel methods for the formation of thin films of vanadium (IV) oxide have seen the greatest variety of dopant ions used with most of the first row transition metals having been used [37-40]. Other metal ions have also been doped into the vanadium (IV) oxide lattice by sol-gel methods, including gold [41], molybdenum [42], niobium [43], and aluminium [37]. The co-doping of molybdenum and tungsten, or tungsten and titanium into the vanadium (IV) oxide lattice has also been shown to give very low thermochromic transition temperatures. Tungsten and titanium co-doping of vanadium (IV) oxide displayed almost no hysteresis width for the infrared switching [44].

The range of metal ions that have been doped into the vanadium(IV) oxide lattice using PVD methods is not quite as extensive as those investigated with sol-gel and is mostly limited to those that are known to induce the largest decrease in the metal-to-semiconductor transition temperature, namely tungsten [12, 34, 35], and molybdenum [45-46]. Iron doping of vanadium (IV) oxide by PVD showed a minimum thermochromic transition temperature with 1.4 atom% Fe at 59 ºC on the heating cycle [10].

Vanadium (IV) oxide film doped with 1.2 atom% fluorine (fluorine replacing oxygen atoms) has been shown to reduce T_c to 20 ºC, but also causes the hysteresis width of the thermochromic transition to broaden appreciably making fluorine doping less suitable for use in window coatings [10]. The co-doping of tungsten and fluorine by PVD into vanadium (IV) oxide gave thin films with reduced thermochromic transition temperature and with improved visible transmittance over tungsten doped vanadium (IV) oxide [47].

Film stresses and their effect on the thermochromic transition of vanadium (IV) oxide.
Pure, crystalline vanadium (IV) oxide displays a metal-to-semiconductor transition at 68 ºC. Most thin films of the material also display the transition at the same or slightly reduced (66 ºC) temperature. There have been reports in the literature where very thin films (ca 200 nm) of pure vanadium (IV) oxide grown by various methods have shown transition temperatures lower than 68 ºC.[41,48,49] Maruyama et al [47] link the variations in the thermochromic transition temperature to the thickness of the thin film, but does not suggest a mechanism for the effect, and indeed closer inspection of their data suggests that this is not a reasonable conclusion. Case [49] however, investigates the effects of mismatches in substrate-film expansion co-efficients that cause extrinsic stresses in the film crystallites. Low-energy ion bombardment is utilised to cause intrinsic stresses in the thin film. Both effects are shown to decrease the temperature at which the MST occurs. Rakotoniaina et al [50] also discuss the effects of strain on the MST of vanadium (IV) oxide caused by pressure and tungsten doping, showing that stress along the square plane of the rutile cell can result in a decrease in the thermochromic transition temperature.

Methods of preparing pure and doped vanadium (IV) oxide films.

Single crystals of vanadium (IV) oxide are unsuitable for many of the technological applications mentioned and thin films of the material are required. Thin films also survive the stresses resulting from cycling between the two polymorphs of vanadium (IV) oxide involved in the MST, which causes single crystals to crack and disintegrate after only a small number of cycles [9]. Guzman et al [51] showed that a vanadium (IV) oxide thin film prepared by sol-gel methods could be cycled 108 times without any degradation in electrical contrast. The preparation of vanadium (IV) oxide thin films has preceded using three routes, sol-gel spin and dip coating; physical vapour deposition (PVD) and chemical vapour deposition (CVD). Of these CVD has attracted less interest due to the inherent difficulty in achieving controllable stoichiometry using this method and the relatively few volatile precursors available. Thin films of vanadium (IV) oxide prepared by PVD methods are generally used for fundamental studies of the properties of the thin films, whereas sol-gel spin or dip coated takes a more application based approach. Chemical vapour deposition studies also fall into the latter category as this methodology has the most potential for large scale industrial process integration. Preparation of thin films of vanadium (IV) oxide for commercial applications is often the focus of the research.

The sol-gel method.
The sol-gel method involves the formation of thin films by dip or spin coating substrates with solutions of metal alkoxides, and then suitably treating them to form a thin film of the required metal oxide. The sol-gel methods are thus multi-stage, off-line processes. For the formation of vanadium (IV) oxide this involves partially hydrolysing the initial coating and then heating it in a reducing atmosphere to form crystalline vanadium (IV) oxide. Dopants are readily introduced by the addition of salts or additional alkoxides to the precursor solution in the necessary proportions. Due to the simplistic nature of the method, sol-gel has been used extensively to prepare vanadium (IV) oxide thin films in a pure and doped form. The most widely used precursors for the sol-gel preparation of vanadium (IV) oxide are vanadyl tri(iso-propoxide) and vanadyl tri(tert-amyloxide).

The alkoxide is dissolved in a parent alcohol to form the sol. Different alcohols cause different transesterifications reactions and the formation of different alkoxides. The whole of the first row d-block elements and much of the second and third row d-block elements have been doped into vanadium (IV) oxide using this method.

A new method using polyvanadate sols was reported by Takahashi et al [38] that used metallic vanadium dissolved in 30% H_2O_2 and then heated to form a hydrosol. The hydrosol could then be spin coated onto a suitable substrate and reduced in a hydrogen atmosphere. Tungsten and molybdenum could be introduced in metallic form at the initial dissolution stage [38, 44].

Physical vapour deposition methods.
The second general method discussed here involves physical vapour deposition (PVD) techniques [52]. These involve energetically removing atoms or molecules from a target under reduced pressure conditions. The species can then react with any seed gases present in the deposition chamber to form a thin film of the desired compound by condensing onto a substrate. The composition of the thin film can be accurately controlled by the amount of material removed from the target and the amount of reactive gas present in the deposition chamber. There are numerous ways to energetically remove atoms from a metal target and most have been used to prepare vanadium (IV) oxide thin films. These include laser ablation, RF magnetron sputtering, DC magnetron sputtering and ion beam sputtering. Doping is also readily achieved by placing another target in the deposition chamber. The amount of doping can be easily controlled by the relative sizes of the targets.

Chemical vapour deposition methods.
The final method used to prepare thin films of VO_2 is chemical vapour deposition. In particular APCVD is the ideal method for producing thin films on high throughput glass substrates.

Doped vanadium (IV) oxide thin films prepared by CVD methods have to our knowledge and prior to our work not been reported in the literature. Pure vanadium (IV) oxide films have been produced by chemical vapour deposition onto glass substrates [43]. Vanadyl tri(iso-propoxide) or vanadyl tri(iso-butoxide) [53] have been used as single source precursors for the CVD of vanadium(IV) oxide films, usually by reducing the resultant vanadium(V) oxide thin films. Vanadium oxides can also be deposited using VCl_4 or $VOCl_3$ and an oxygen source such as water or ethanol [54] or with carbon dioxide [55]. These films can then be reduced to vanadium (IV) oxide in a suitable atmosphere. Vanadium (IV) oxide thin films have also been prepared from vanadium(III) acetylacetonate, $[V(acac)_3]$, by an APCVD method followed by slow post-deposition cooling [48], and from vanadium(IV) acetylacetonate, $[V(acac)_4]$, by a pyrolysis method in a controlled atmosphere [56]. Vanadyl acetylacetonate, $[VO(acac)_2]$, has been used to prepare the meta-stable VO_2(B), which can be converted to the tetragonal phase by annealing in argon at 500 ºC [57-58]. Vanadyl precursors have also been used in a CVD method to prepare various vanadium oxide thin films including vanadium (IV) oxide [59]. The precursors used in these studies are generally expensive and require a post-deposition reduction process to form vanadium (IV) oxide thin films. Ideally a process is required that utilises inexpensive, readily available precursors that will produce vanadium (IV) oxide directly without the need for a reduction step.

Comparison of the different production methods.

Sol-gel methods are simple to use, with readily available, though expensive precursors and give films with complete coverage of the substrate and reasonably even thickness. They are not, however, suitable for integrating into the industrial float-glass process as sol-gel techniques often involve spin coating the substrate, a process that is difficult with very large areas of glass.

PVD methods require reduced pressure or vacuum conditions and expensive evaporation/sputtering/ablation equipment. This would increase production costs, limiting the commercial applications due to economic factors. Growth rates are also often low with PVD techniques making them additionally unsuitable for integration into modern float glass processes.

Glass manufacturers currently use sol-gel and PVD methods to prepare coated-glass products but the extra cost of these off-line processes can often make them prohibitively expensive for widespread, consumer use.

Atmospheric pressure CVD equipment can be easily integrated into the float-glass production process, the coaters are easily constructed and no expensive vacuum systems are required. The precursors are often readily available and relatively inexpensive, especially when films of only a few hundred nanometers may be required. Growth rates are also high compared to PVD techniques and are sufficiently fast to be suitable for float-glass production lines. These factors make APCVD methods the most attractive when wishing to prepare coated float-glass; indeed APCVD finds use in the production of K glass and Activ [19].

Atmospheric pressure chemical vapour deposition.
Chemical vapour deposition (CVD) is a process whereby a thin solid film is synthesized from a gaseous phase by a chemical reaction. It is this reactive process that distinguishes CVD from a physical vapour deposition processes. The APCVD process is shown schematically in figure 4. There are several steps associated with the CVD process (not always in this order [60])

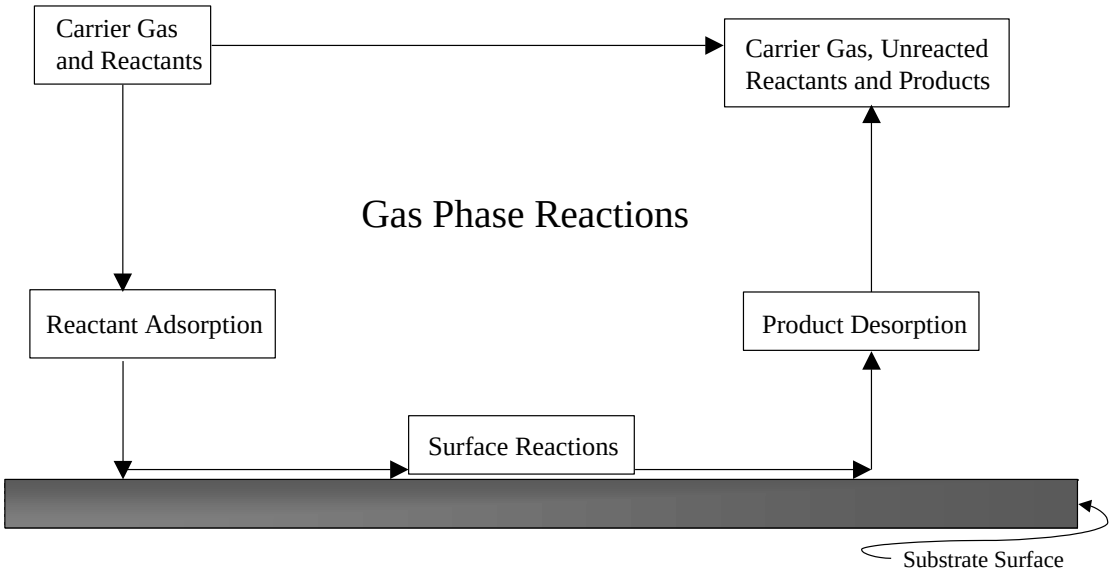

Figure 4. Schematic representation of the atmospheric pressure chemical vapour deposition process.

Transport of the reactive species to the reaction site.
Gas phase reaction.
Adsorption onto the substrate surface
Nucleation on the substrate surface / Surface reaction

Reaction and desorption of by-products

Film growth.
In the APCVD experiment the reaction chamber is at or close to atmospheric pressure. The precursors therefore need to be low-melting solids or volatile liquids and are transported to the reaction site via hot, inert carrier gas. At the very least, precursors must have enough vapour pressure to allow sufficient material to transport to the reaction chamber in the gas phase. The substrate temperature also needs to be relatively high to initiate the deposition.

Reaction sites in the APCVD process.
In the reaction chamber two types of reaction may occur; homogeneous reactions occurring entirely in the vapour phase and heterogeneous reactions that occur at the vapour - solid surface interface [61]. In cold wall reactors such as those used at UCL the homogeneous reactions and heterogeneous reactions at the reactor walls are suppressed due to the lower heat input to the system. Vapour - substrate reactions are therefore dominant [61]. Little is known about these types of reaction due to the difficulties in determining the exact nature of the surface species and the influence of the electronic structure of the solid surface on the kinetics of the reaction.

Recent work conducted using APCVD.
Four precursor systems have received the most attention in the preparation of thin films of tungsten doped vanadium (IV) oxide via APCVD [62-64]. Some work has been conducted using aerosol assisted chemical vapour deposition (AACVD) to produce thin films of tungsten or niobium doped vanadium (IV) oxide [68, 69, 71].

APCVD
The four precursor systems used in APCVD were:

A) $VCl_4 + W(OEt)_6 + H_2O$ deposition at 600 ºC
B) $VOCl_3 + WCl_6 + H_2O$ deposition at 650 ºC
C) $VCl_4 + WCl_6 + H_2O$ deposition at 550 ºC
D) $VO(acac)_2 + WCl_6 + 2\%\ O_2$ in N_2 deposition at 525 ºC

The four precursor systems will be referred to as A, B, C or D accordingly.

Physical Properties.

Films deposited from APCVD reactions A and B were similar in appearance to un-doped vanadium (IV) oxide being a dark yellow / brown in colour, they were opaque in appearance. The majority of films had poor adhesion qualities; they could be scratched with a brass stylus and wiped off with a tissue. However, the majority did pass the Scotch tape test. Films deposited from the APCVD reactions C and D were also similar in appearance to un-doped vanadium (IV) oxide being a dark yellow / brown colour in transmission. They however differed with a blue / silver colour in reflection; they appeared transparent and quite glassy in appearance. All of these films had better adhesion qualities; they could not be scratched with a brass stylus or wiped off with a tissue and all of the films passed the Scotch tape test.

X-ray diffraction (XRD) was used to characterise the films from all reactions and indicated the production of monoclinic vanadium (IV) oxide in all cases (Figure 5). As can be seen in the figure, in all cases the 011 reflection is the strongest. X-ray photoelectron spectroscopy (XPS) and energy

dispersive analysis of X-rays (EDAX) were conducted to evaluate the tungsten dopant level present in all of the films. The two methods gave consistent results and indicated it was possible to introduce up to 1.2 atom % into the vanadium (IV) oxide lattice from the APCVD reaction A; 3.5 or 3.0 atom % in sample from APCVD reactions B and D respectively, and up to 8 atom % in samples prepared from APCVD reaction C. Because [$W(OEt)_6$] is a solid it has a relatively low vapour pressure and it was difficult to incorporate more than about one atom % into the vanadium (IV) oxide matrix as seen with samples prepared from APCVD reaction A. Using higher bubbler temperatures or higher flow rates led to condensation problems in the CVD rigs gas lines and ultimately blockages. [WCl_6] is a solid but has better vapour pressure and vapour transport characteristics (less condensation and less blockages) than [$W(OEt)_6$] and correspondingly a higher W atom % was incorporated into the vanadium (IV) oxide matrix as seen in samples prepared from the APCVD reactions of B, C and D. Additionally the range of temperatures at which this precursor can be used at is wider allowing for a greater level of control. Subsequently [WCl_6] is preferred as a tungsten precursor.

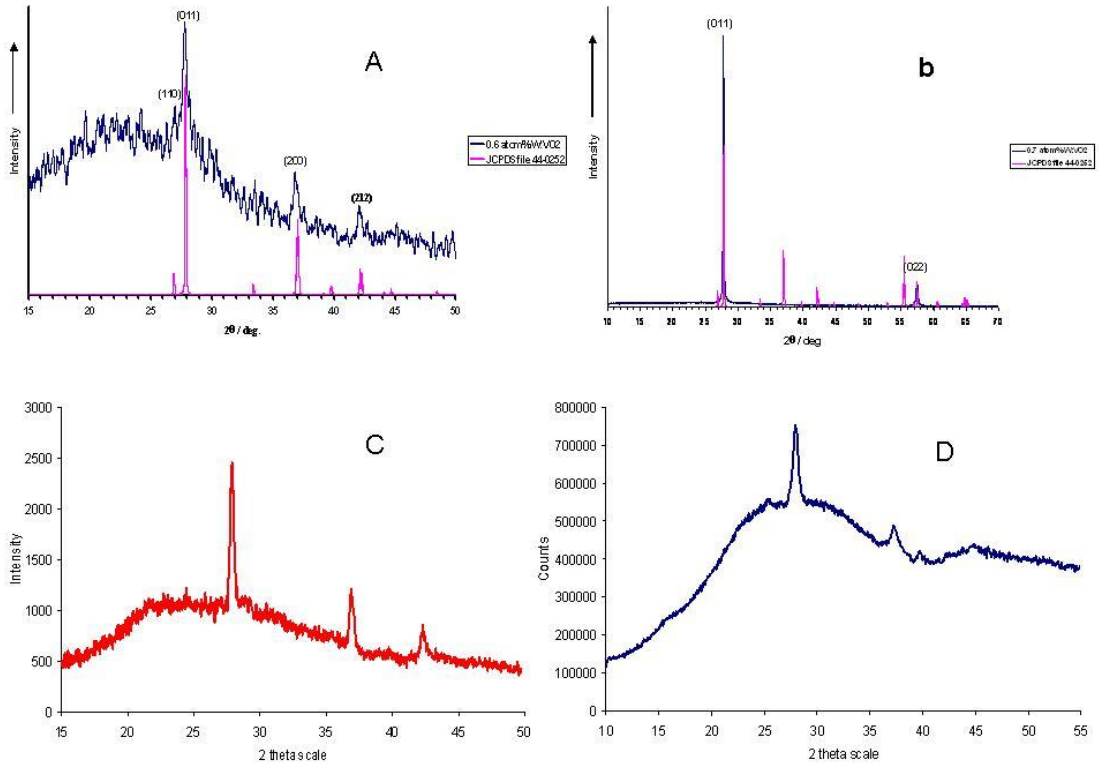

Figure 5. X-ray diffraction patterns of films made from APCVD reactions A, B, C and D. In all cases the 011 peak is dominant indicating preferred orientation with this plane. Some amorphous character due to the glass substrate is observed in C and D as these films are particularly thin (100-150 nm).

Electron microscopy (plan view and side on view) was used to evaluate the surface morphology, film thickness and growth mechanism in each of these reactions. Films prepared from the APCVD reactions A and D had similar morphologies (figure 6A and 6D) of agglomerated particles on the substrate surface. Typically particles were 100 nm in diameter. Side on view micrographs (figure 7A and 7D) indicated a high degree of columnar growth. Both observations are consistent with a Volmer-Webber type island growth mechanism, typical of highly nucleating substrates.

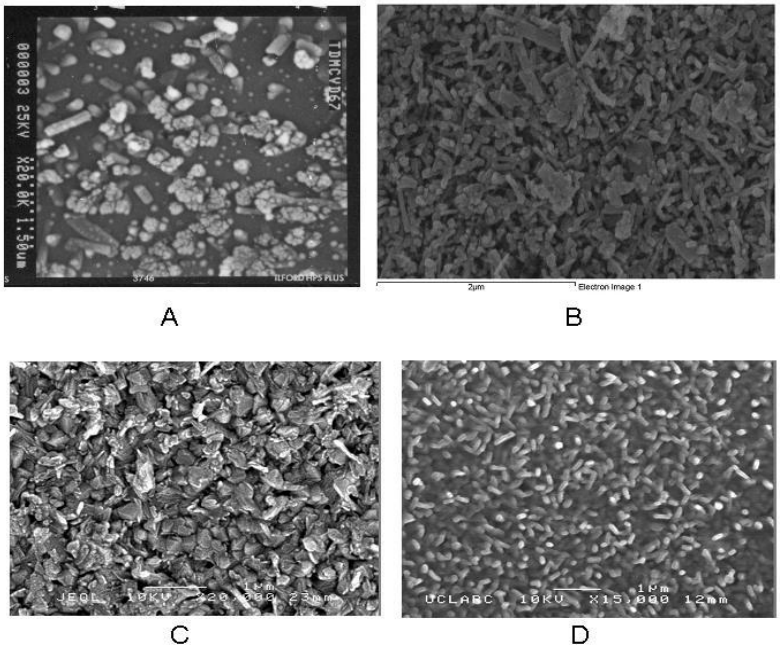

Figure 6. Plan view electron micrographs of thin films prepared from APCVD reactions A, B, C and D.

Films prepared from the APCVD reaction B and C were somewhat different. The surface was covered with thin worm like structures with a width of around 10 nm and lengths between 100 and 800 nm (figure 6B and 6C, and 7B and 7C respectively), almost perpendicular to the substrate. This is an unusual morphology and is an extreme form of the Volmer-Webber island growth mechanism.

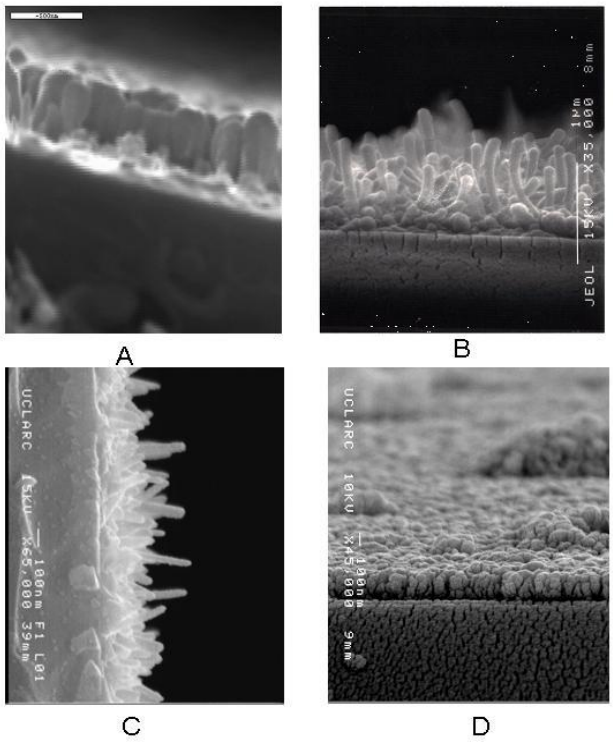

Figure 7. Side view electron micrographs of thin films prepared from APCVD reactions A, B, C and D.

Film thickness and growth rates are summarised in Table 1. As is expected films grown from the metal chloride precursors have faster growth rates than those from [$VO(acac)_2$].

Table 1. Table indicating film thickness and nominal growth rates.

Reaction	Thickness / nm	Deposition Time / minutes	Nominal Growth Rate / $nm.min^{-1}$
A	400 - 500	1	450
B	100 – 800	1	400
C	100 – 300	1	200
D	100 – 120	3	35

Thermochromic properties.

The thermochromic properties of these films were assessed by measuring the optical properties (transmission and reflectance spectroscopy and hysteresis at 2500 nm) of the films above and below the transition temperature.

To give an indication of the effectiveness of the tungsten doped vanadium (IV) oxide thin films as intelligent window coatings the transmittance and reflectance spectra of the films were measured below and above the metal-to-semiconductor transition. In all cases when the temperature of the films was increased there was no appreciable change in the transmittance in the visible region but a dramatic change in the near infrared region was observed (figure 8). The same is true to a lesser extent with reflectance behaviour.

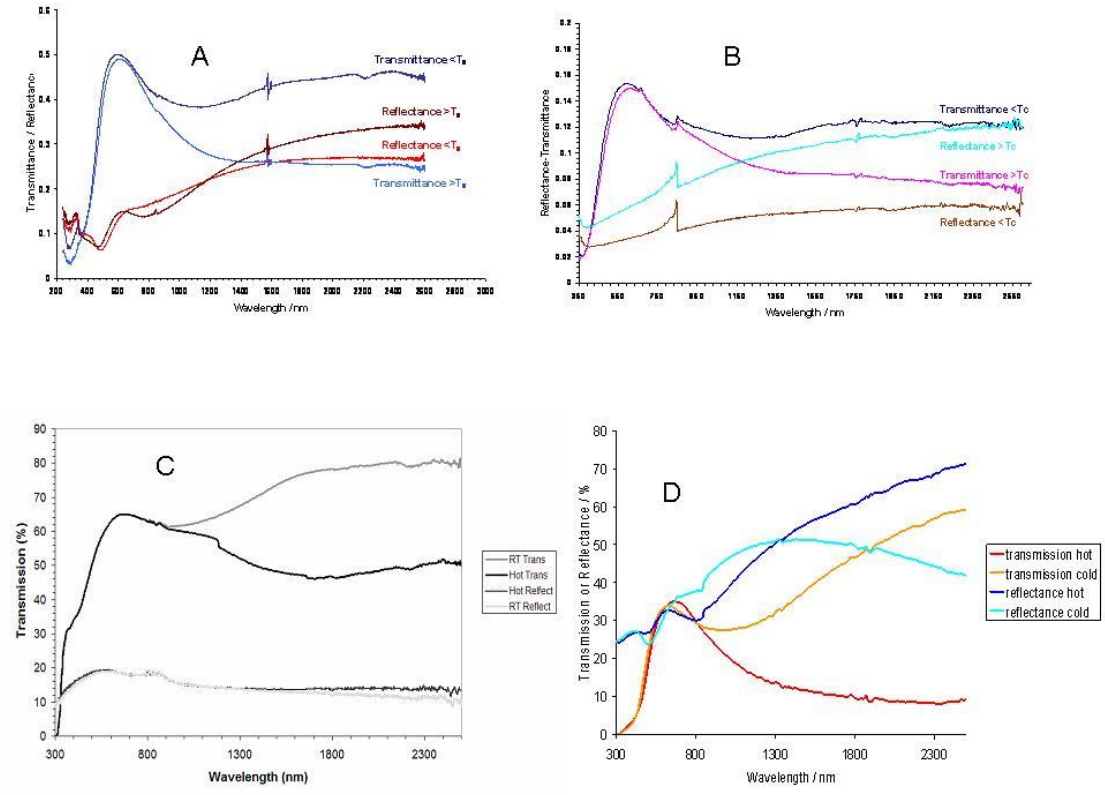

Figure 8. Transmission and reflectance spectra of typical films produced from the APCVD reactions A, B, C and D. In all cases there is a large change in transmission at 2500 nm on undergoing the transition, ideal behaviour for an intelligent thermochromic window product.

Films prepared from APCVD reaction B seem to be anomalous in that there is a small change (1%) in the visible part of the reflectance spectrum upon heating. It is likely that this results from the greater film thickness of this sample. This is the desired behaviour for an intelligent window material. The extent of the transition (ΔT and ΔR) at 2500 nm is given in table 2.

Table 2. Table showing a summary of changes in transmission and reflectance at 2500 nm on undergoing the transition for typical films made from the APCVD reactions A, B, C and D.

Reaction	ΔT / % at 2500 nm	ΔR / % at 2500 nm
A	20	8
B	5	6
C	32	3
D	50	25

As anticipated, thinner films have higher transmittance in the visible part of the spectrum and show a larger change on moving through the transition temperature. Ideally a glazing product will have a visible transmittance of at least 55% [59].

To determine the thermochromic transition switching temperature, the transmittance of the films at 2500 nm was measured while the temperature was cycled through the metal-to-semiconductor transition. The results of some of these measurements are shown in figure 9.

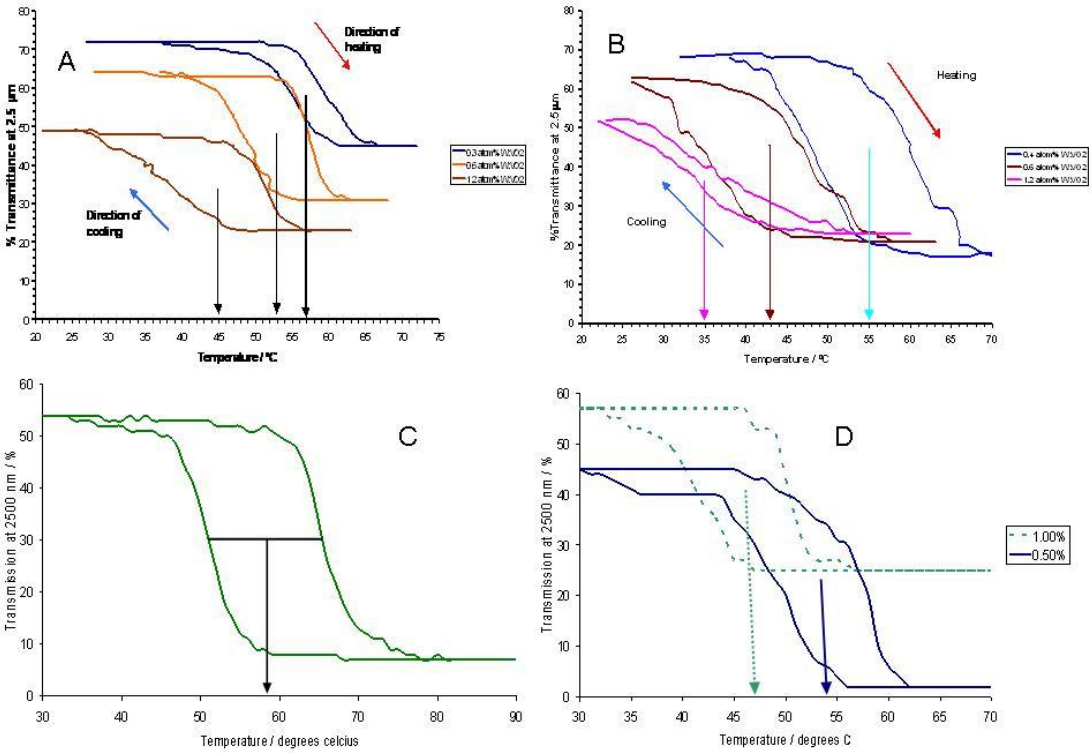

Figure 9. Hysteresis loops of typical films prepared from the APCVD reactions A, B, C and D.

In all cases, as the temperature was increased and the thermochromic transition temperature was approached, the transmittance of the films decreased dramatically. The thermochromic transition temperature decreased to as low as 45 ºC for a vanadium (IV) oxide thin film doped with approximately 1-atom % tungsten (prepared from APCVD reaction A). As the amount of tungsten in the films increased the hysteresis width was also found to increase, possibly due to a greater number of defects in the vanadium (IV) oxide lattice which would cause a greater variation in the

temperatures at which different regions of the film would undergo the transition. In all cases the hysteresis width was found to be between 10 and 12 ºC. Ideally this would be as small as possible to maximise the energy benefit of having this type of thermochromic coating.

Comparison of APCVD reactions.

In all cases the films show promise as intelligent window coatings with reduced transition temperatures and the typical change in optical properties associated with un-doped vanadium (IV) oxide. In all cases thermochromic behaviour and the associated optical properties were maintained after repeated heating and cooling cycles.

AACVD of $VO(acac)_2$ + $W(OEt)_6$.
In Aerosol Assisted Chemical Vapour Deposition (AACVD) the precursor is dissolved into a suitable solvent and then an aerosol is generated ultrasonically. A flow of inert gas, generally N_2, transports the aerosol droplets to the deposition substrate, where the deposition takes place.

An advantage of AACVD is that the precursor does not need to be volatile (as in APCVD) but just soluble in the solvent; this allows the use of more unconventional precursors not usable with APCVD [65,66]. The solvent used, however, must have the right physical and chemical properties to form an aerosol [67]. Another advantage of AACVD is that it is easier to use when more than one precursor is used, for instance for the deposition of doped films. In fact it is simpler to control the precursor proportions in the solution than in the gas phase.

Undoped VO_2
To our knowledge, AACVD has never been employed before to deposit VO_2 (M) thin films. For this reason, a series of depositions was carried out to optimise the experimental conditions for the deposition of VO_2 (M) only, with no other vanadium oxide phase present.

It was shown that experimental parameters such as the vanadium precursor, the nature of the solvent and the carrier gas flow rate affected the nature of the deposited phase [68]. The optimised conditions subsequently used to deposit doped VO_2 are listed in table 3.

Table 3. Experimental conditions for the deposition of VO_2(M).

Vanadium precursor	$VO(acac)_2$
Precursor concentration	0.075 mol L^{-1}
Solvent	Ethanol
N_2 flow rate	1.5 L min^{-1}
Temperature	500-550^oC
Substrate	SiO_2 coated glass

The deposited VO_2 thin films had good optical properties and a transition temperature of about 58^{o}C; this value is about 10^{o}C lower than what has been previously reported for single crystals, most likely due to strain in the coating lattice.

W-doped VO_2
The first metal employed as dopant was tungsten; in fact, as mentioned previously, tungsten proved to be the most effective metal to decrease the value of the transition temperature T_c [33-38]. $W(OC_2H_5)_5$ was used as tungsten precursor, dissolved in ethanol together with $VO(acac)_2$; several

depositions were carried out using different tungsten concentrations, to study the effect of the tungsten concentration on the transition temperature [69].

The deposition solutions used had a W/V atom ratio between 1 and 6 %; EDAX measurements of the deposited thin films showed that about one third of the tungsten of the solution was incorporated into the coatings. A good linear correlation was observed between the W/V ratio in solution and in the deposited films.

The coatings were analysed with different techniques such as XRD and Raman spectroscopy; both showed the presence of VO_2 (M) phase only, with no W and/or V-W mixed phases. This indicates the formation of a solid solution between tungsten and vanadium oxide, with no phase separation.

An example of the optical properties of W-doped VO_2 thin films is shown in Figure 10, where the transmittance and reflectance are reported at different temperatures – below and above the transition temperature. It can be seen how the behaviour is that expected from an intelligent window material: in fact the transmittance decreases while the reflectance increases for values of T above the transition temperature T_c (Figure 10a and 10b respectively).

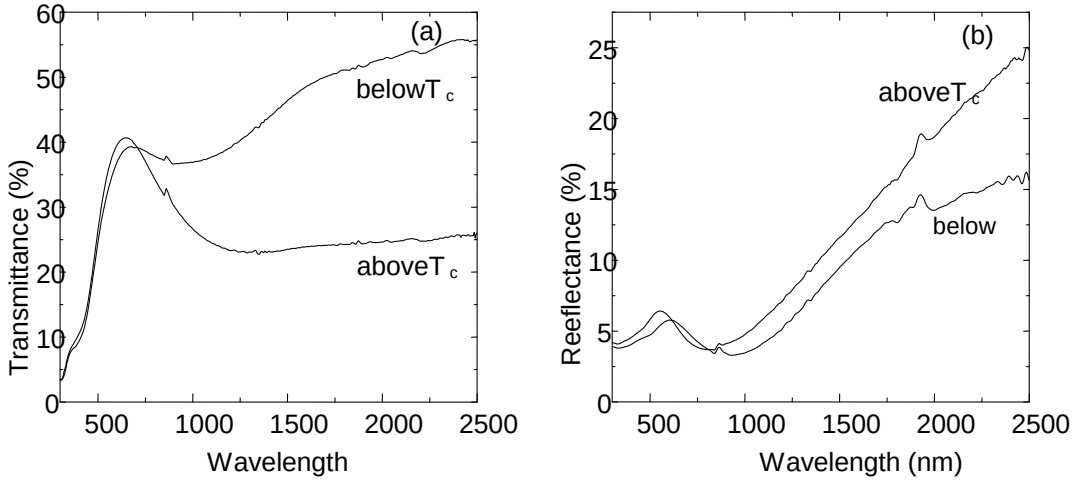

Figure 10. Transmission and reflectance spectra of a typical tungsten doped monoclinic vanadium (IV) ocide thin film produced via AACVD.

Figure 11 shows a comparison of the transition temperature for an un-doped and a W-doped VO_2 coatings. The temperature was determined by measuring the change in the transmittance at 2500 nm as a function of the temperature. It can be seen that for the W-doped sample there is a net decrease in the T_c value; furthermore, the width of the hysteresis loop is smaller, making the material even more suitable for an intelligent material coating.

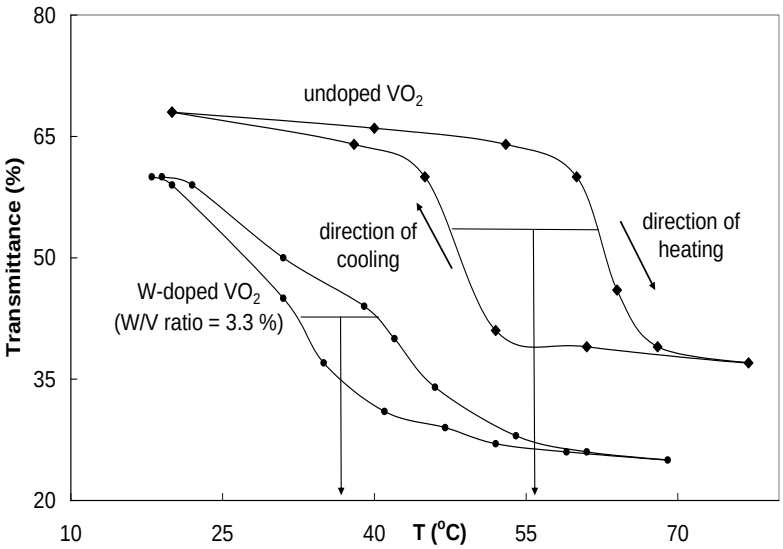

Figure 11. Hysteresis behaviour of thin films of doped and un-doped vanadium (IV) oxide prepared by AACVD.

The transition temperature was determined for every sample; these measurements showed a linear correlation between the tungsten amount in the film and the T_c value. It was seen that an amount of dopant of 1% reduces the transition temperature of about 22°C; therefore thin films with a concentration of about 2 % have a T_c value close to room temperature (28°C).

Nb-doped VO_2

The use of niobium as dopant was considered as well; in fact, previous results obtained with APCVD methodology showed that Nb-doped VO_2 samples have a remarkable decrease in the transmittance in the infrared region, fulfilling the requirement for intelligent window coatings [70]. There were, however, difficulties to incorporate high concentration of niobium into the VO_2 lattice; consequently the observed T_c values were not close enough to room temperature.

In recent work, $[Nb(OC_2H_5)_5]$ was used as niobium precursor, following the same experiemtnal procedure described above for tungsten. The Nb/V molar ratio in the films, measured by EDAX analysis, reached values up to about 3.7 % [71]; these concentrations are much higher than the ones obtained by APCVD (0.4 %), confirming the suitability of AACVD for the deposition of doped thin films.

However, differently from what was observed with tungsten, the correlation between the solutions and film concentrations was not linear; in fact a progressive increase was observed for the Nb/V ratio in the films, until when a plateau was reached. These results confirm the difficulties of incorporating niobium into VO_2 films, as previously experienced by APCVD.

The characterisation of these films showed that only VO_2 (M) was present, with no Nb-V mixed phases; the optical properties such as transmittance and reflectance showed features similar to the ones of W-doped VO_2 and reported in Figure 2.

A linear decrease in the transition temperature with increasing niobium concentration was observed as well, indicating the effect of niobium as dopant. However, a niobium concentration of about 2 % lowered the value of T_c of about 15°C; therefore it can be stated that niobium is less effective if compared with tungsten. However, it is still possible to reach T_c values close to room temperature; therefore Nb-doped VO_2 thin films can be used as intelligent window materials.

Conclusions and Future Challenges.

Intelligent thermochromic glass can be made which can switch at temperatures that are practically important: 25-30 °C and that the precise switching temperature could be chosen by the level of tungsten doping. These coatings were made by a process compatible with and currently used in commercial glass manufacture – APCVD.

The challenges to be overcome in producing a commercial product include:

Colour - the films are yellow / brown in transmission an undesirable colour for glazing. This could be improved by coating the films on a coloured glass, by use of refractive index matched over/under layers or mixtures of dopants.

Scale-up – will the precursor chemistry work on an industrial scale? Some important glazing products such as K-glass and Activ were initially developed on equipment similar to that used in these experiments. It is certainly within the realms of possibility that this process can be scaled up successfully.

Weathering – will the coating survive environmental conditions? This is not necessarily an issue as in a double glazed unit the film could be on an internal surface.

Thermal cycling – will the coating survive repeated temperature cycles? CVD films are generally robust and to date have shown no deterioration in film properties after hundreds of thermal cycles.

There is no doubt that a large market will be available for a commercial thermochromic glass. This will include both household, office and factory window applications through to automotive applications and even for space exploration – a material that can switch its infra-red reflection properties with temperature is very desirable in order to keep space craft components at the correct temperature. It also has potential in fire retardant clothing and in security devices.

Acknowledgements.

The EU and EPSRC are thanked for financial support. Pilkington Glass are thanked for a supply of substrates and useful discussions. The authors would like to thank Mr. Kevin Reeves for the help with Scanning Electron Microscopy. IPP thanks the Royal Society/ Wolfson Trust for a merit award.

References

1. Roach, W. Appl. Phys. Lett., 1971, 19, 453.
2. Granqvist, C. G. Advanced Mater., 2003, 15, 1789.
3. Smith, A. W. Appl. Phys. Lett., 1973, 23, 437-438.
4. Granqvist, C. G. Thin Solid Films, 1990, 193/194, 730-741.
5. Richardson M. A.; Coath, J. A. Optics and Laser Technol., 1998, 30, 137-140.
6. Hårsta, A. Chem. Vapor Deposition, 1999, 5, 191-193.
7. Nicholls, J. Mater. World, 1996, 4, 19-21.

8. Jin. P. "Demonstration of Thermochromic Coating." http://www.aist.go.jp/NIRIN/People/pjin/GIF/tc.gif . 2000.
9. MacChesney J. B.; Guggenheim, H. J. J. Phys. Chem. Solids, 1969, 30, 225-234.
10. Phillips, T. E.; Murray, R. A.; Poehler, T. O. Mater. Res. Bull., 1987, 22, 1113-1123.
11. Pierce, J. W.; Goodenough, J. B. Phys. Rev. B, 1972, 5, 4104-4111.
12. Burkhardt, W.; Christmann, T.; Meyer, B. K.; Niessner, W.; Schalch, D.; Scharmann, A. Thin Solid Films, 1999, 345, 229-235.
13. Livage, J. Coord. Chem. Rev., 1999, 190-192, 391-403.
14. Lee, M. H.; Cho, J. S. Thin Solid Films, 2000, 365, 5-6.
15. Jin, P.; Xu, G.; Tazawa, M.; Yoshimura, M. Jap. J. Appl. Phys., 2002, 41, L278-L280.
16. Mills, A.; Le Hunte, S. J. Photochem. Photobiol. A, 1997, 108, 1-35.
17. O'Neill, S. A.; Parkin, I. P.; Clark, R. J. H. C.; Mills, A.; Elliott, N. J. Mater. Chem., 2003, 13, 56-60.
18. Pilkington ActivTM glass. www.pilkington.com. 2004.
19. http://www.pilkington.com/pilkington/Corporate/English/company+briefing/glass+manufacturing/floatprocess.htm; "At the heart of the world's glass industry is the float glass process - invented by Sir Alastair Pilkington in 1952 - which manufactures clear, tinted and coated glass for buildings, and clear and tinted glass for vehicles. The process, originally able to make only 6mm thick glass, now makes it as thin as 0.4 mm and as thick as 25 mm. Around 260 float plants are in operation, under construction or planned worldwide. Molten glass, at approximately 1000ºC, is poured continuously from a furnace onto a shallow bath of molten tin. It floats on the tin, spreads out and forms a level surface. Thickness is controlled by the speed at which the solidifying glass ribbon is drawn off from the bath. After annealing (controlled cooling) the glass emerges as a 'fire' polished product with virtually parallel surfaces. A float plant, which operates non-stop for between 10-15 years, makes around 6000 kilometres of glass a year in thicknesses of 0.4mm to 25mm and in widths up to 3 metres. The float process has been licensed to more than 40 manufacturers in 30 countries. There are around 260 float plants worldwide with a combined output of about 800,000 tonnes of glass a week – over 90% of glass is manufactured from this process".
20. Morin, F. J. Phys. Rev. Lett., 1959, 3, 34-36.
21. Barker, A. S.; Verleur, W. H.; Guggenheim, H. J. Phys. Rev. Lett., 1966, 17, 1286-1289.
22. Verleur, W. H.; Barker, A. S.; Berglund, C. N. Phys. Rev., 1968, 172, 788-798.
23. Rogers, K. D. Powder Diffraction, 1993, 8, 240-244.
24. Becker, M. F.; Buckman, A. B.; Walser, R. M.; Lepine, T.; Georges, P.; Brun, A. Appl. Phys. Lett., 1994, 65, 1507-1509.
25. Mott, N. F. Rev. Modern Phys., 1968, 40, 677-683.
26. Goodenough, J. B. J. Solid State Chem., 1971, 3, 490-500.
27. Hyland, G. J. Rev. Modern Phys., 1968, 40, 739-743.
28. Adler, D.; Brooks, H. Phys. Rev., 1967, 155, 826-840.
29. Adler, D.; Feinleib, J.; Brooks, H.; Paul, W. Phys. Rev., 1967, 155, 851-860.
30. Adler, D. Rev. Modern Phys., 1968, 40, 714-736.
31. Eyert, V. Annalen Der Physik, 2002, 11, 650-702.
32. Tang, C.; Georgopoulos, P.; Fine, M. E.; Cohen, J. B.; Nygren, M.; Knapp, G. S.; Aldred, A Phys. Rev. B, 1985, 31, 1000-1011.
33. Nygren, M.; Israelsson, M. Mater. Res. Bull., 1969, 4, 881-886.
34. Jin, P.; Nakao, S.; Tanemura, S. Thin Solid Films, 1998, 324, 151-158.
35. Jin, P.; Tanemura, S. Jap. J. Appl. Phys., 1995, 34, 2459-2460.
36. Sobhan, M. A.; Kivaisi, R. T.; Stjerna, B.; Granqvist, C. G. Solar Energy Mater. Solar Cells, 1996, 44, 451-455.

37. Béteille, F.; Livage, J. J. Sol-Gel Sci. Technol., 1998, 13, 915-921.
38. Takahashi, I.; Hibino, M.; Kudo, T. Jap. J. Appl. Phys., 1996, 35, L438-L440.
39. Béteille, F.; Morineau, R.; Livage, J. Mater. Res. Bull., 1997, 32, 1109-1117.
40. Lu, S. W.; Hou, L. S.; Gan, F. X. J. Mater. Sci. Lett., 1996, 15, 856-857.
41. Cavanna, E.; Segaud, J. P.; Livage, J. Mater. Res. Bull., 1999, 34, 167-177.
42. Hanlon, T. J.; Coath, J. A.; Richardson, M. A. Thin Solid Films, 2003, 436, 269-272.
43. Greenberg, C. B. Thin Solid Films, 1983, 110, 73-82.
44. Takahashi, I.; Hibino, M.; Tetsuichi, K., Jap. J. Appl. Phys., 2001, 40, 1391-1395.
45. Jin, P.; Tanemura, S. Thin Solid Films, 1996, 281-282, 239-242.
46. Wu, Z. P.; Miyashita, A.; Yamamoto, S.; Abe, H.; Nashiyama, I.; Narumi, K.; Naramoto, H. J. Appl. Phys., 1999, 86, 5311-5313.
47. Burkhardt, W.; Christmann, T.; Franke, S.; Kriegseis, W.; Meister, D.; Meyer, B. K.; Niessner, W.; Schalch, D.; Scharmann, A. Thin Solid Films, 2002, 402, 226-231.
48. Maruyama, T.; Ikuta, Y; J. Mater. Sci., 1993, 28, 5073-5078.
49. Case, F. C. J. Vac. Sci. Technol. A, 1984, 2, 1509-1512.
50. Rakotoniaina, J. C.; Mokrani-Tamellin, R.; Gavarri, J. R.; Vacquier, G.; Casalot, A.; Calvarin, G. J. Solid State Chem., 1993, 103, 81-94.
51. Guzman, G.; Béteille, F.; Morineau, R.; Livage, J. J. Mater. Chem., 1996, 6, 505-506.
52. Hai-Ning Cui, Vasco Teixeira, Li-Jian Meng, Rong Wang, Jin-Yue Gao, Elvira Fortunato, Thin Solid Films 516 (2008) 1484.
53. Takahshi, Y.; Kanamori, M.; Hashimoto, H.; Moritani, Y.; Masuda, Y. J. Mater. Sci., 1989, 24, 192.
54. Field, M. N.; Parkin, I. P. J. Mater. Chem., 2000, 10, 1863-1866.
55. MacChesney, J. B.; Potter, J. F.; Guggenheim, H. J. J. Electrochem. Soc. Solid State Sci., 1968, 115, 52-55.
56. Ryabova, L. A.; Serbinov, A.; Darevsky, A. S. J. Electrochem. Soc., 1972, 119, 427-429.
57. Sahana, M. B.; Dharmaprakash, M. S.; Shivashankar, S. A. J. Mater. Chem., 2002, 12, 333-338.
58. Sahana, M. B.; Subbanna, G. N.; Shivashankar, S. A. J. Appl. Phys., 2002, 92, 6495-6504.
59. Barreca, D.; Depero, L. E.; Rizzi, G. A.; Sangaletti, L.; Tondello, E.; Vettori, U. J. Electrochem. Soc., 1999, 146, 551-558.
60. Hitchman, M. L. and Jensen, K. F. Chemical Vapor Deposition, Academic Press, New York, 1993.
61. Rees, W. S.; CVD of Non-Metals, VCH, Weinheim, 1996.
62. Manning, T. D.; Parkin, I. P.; Clark, R. J. H.; Sheel, D.; Pemble, M. E.; Vernadou, D. J. Mater. Chem., 2002, 12, 2936-2939.
63. Manning, T. D.; Parkin, I. P. J. Mater. Chem., 2004, 2554-2559.
64. Manning, T. D.; Parkin, I. P.; Pemble, M. E.; Sheel, D.; Vernardou, D.; Chem. Mater.; 2004; 16(4); 744-749.
65. Cross, W. B.; Parkin, I.P. Chem. Comm., 2003, 14, 1696.
66. Binions, R.; Carmalt, C. J.; Parkin, I. P.; Thin Sol. Films, 2004, 469-470, 416.
67. Choy, K.L.; Progr. Mater. Sci., 2003, 48, 57-170.
68. Piccirillo, C.; Binions, R.; Parkin, I. P.; Chem. Vap. Dep., 2007, 13 (4), 145.
69. Piccirillo, C.; Binions, R.; Parkin, I. P.; Thin Sol. Films, in press.
70. Manning, T.D.; PhD thesis, London, 2004.
71. Piccirillo, C.; Binions, R.; Parkin, I. P.; Europ. J. Inorg. 2007, 25 4050.

Journal of Nano Research Vol. 2
doi:10.4028/www.scientific.net/JNanoR.2

Thermochromic Coatings for Intelligent Architectural Glazing
doi:10.4028/www.scientific.net/JNanoR.2.1

References

1. Roach, W. Appl. Phys. Lett., 1971, 19, 453.
doi:10.1063/1.1653769

2. Granqvist, C. G. Advanced Mater., 2003, 15, 1789.
doi:10.1002/adma.200300378

3. Smith, A. W. Appl. Phys. Lett., 1973, 23, 437-438.
doi:10.1063/1.1654949

4. Granqvist, C. G. Thin Solid Films, 1990, 193/194, 730-741.
doi:10.1016/0040-6090(90)90225-3

5. Richardson M. A.; Coath, J. A. Optics and Laser Technol., 1998, 30, 137-140.
doi:10.1016/S0030-3992(98)00035-8

6. Hårsta, A. Chem. Vapor Deposition, 1999, 5, 191-193.
doi:10.1002/(SICI)1521-3862(199908)5:4<191::AID-CVDE191>3.0.CO;2-U

7. Nicholls, J. Mater. World, 1996, 4, 19-21.

8. Jin. P. “Demonstration of Thermochromic Coating.”
http://www.aist.go.jp/NIRIN/People/pjin/GIF/tc.gif . 2000.

9. MacChesney J. B.; Guggenheim, H. J. J. Phys. Chem. Solids, 1969, 30, 225-234.
doi:10.1016/0022-3697(69)90303-5

10. Phillips, T. E.; Murray, R. A.; Poehler, T. O. Mater. Res. Bull., 1987, 22, 1113-1123.
doi:10.1016/0025-5408(87)90241-8

11. Pierce, J. W.; Goodenough, J. B. Phys. Rev. B, 1972, 5, 4104-4111.
doi:10.1103/PhysRevB.5.4104

12. Burkhardt, W.; Christmann, T.; Meyer, B. K.; Niessner, W.; Schalch, D.; Scharmann, A. Thin Solid Films, 1999, 345, 229-235.
doi:10.1016/S0040-6090(98)01406-0

13. Livage, J. Coord. Chem. Rev., 1999, 190-192, 391-403.
doi:10.1016/S0010-8545(99)00096-X

14. Lee, M. H.; Cho, J. S. Thin Solid Films, 2000, 365, 5-6.
doi:10.1016/S0040-6090(99)01112-8

15. Jin, P.; Xu, G.; Tazawa, M.; Yoshimura, M. Jap. J. Appl. Phys., 2002, 41, L278-L280.
doi:10.1143/JJAP.41.L278

16. Mills, A.; Le Hunte, S. J. Photochem. Photobiol. A, 1997, 108, 1-35.
doi:10.1016/S1010-6030(97)00118-4

17. O'Neill, S. A.; Parkin, I. P.; Clark, R. J. H. C.; Mills, A.; Elliott, N. J. Mater. Chem., 2003, 13, 56-60.
doi:10.1039/b206080a

18. Pilkington ActivTM glass. www.pilkington.com. 2004. 19. http://www.pilkington.com/pilkington/Corporate/English/company+briefing/glass+manufacturing/floatprocess.htm; “At the heart of the world’s glass industry is the float glass process - invented by Sir Alastair Pilkington in 1952 - which manufactures clear, tinted and coated glass for buildings, and clear and tinted glass for vehicles. The process, originally able to make only 6mm thick glass, now makes it as thin as 0.4 mm and as thick as 25 mm. Around 260 float plants are in operation, under construction or planned worldwide. Molten glass, at approximately 1000ºC, is poured continuously from a furnace onto a shallow bath of molten tin. It floats on the tin, spreads out and forms a level surface. Thickness is controlled by the speed at which the solidifying glass ribbon is drawn off from the bath. After annealing (controlled cooling) the glass emerges as a ‘fire’ polished product with virtually parallel surfaces. A float plant, which operates non-stop for between 10-15 years, makes around 6000 kilometres of glass a year in thicknesses of 0.4mm to 25mm and in widths up to 3 metres. The float process has been licensed to more than 40 manufacturers in 30 countries. There are around 260 float plants worldwide with a combined output of about 800,000 tonnes of glass a week – over 90% of glass is manufactured from this process”.

20. Morin, F. J. Phys. Rev. Lett., 1959, 3, 34-36.
doi:10.1103/PhysRevLett.3.34

21. Barker, A. S.; Verleur, W. H.; Guggenheim, H. J. Phys. Rev. Lett., 1966, 17, 1286-1289.
doi:10.1103/PhysRevLett.17.1286

22. Verleur, W. H.; Barker, A. S.; Berglund, C. N. Phys. Rev., 1968, 172, 788-798.
doi:10.1103/PhysRev.172.788

23. Rogers, K. D. Powder Diffraction, 1993, 8, 240-244.

24. Becker, M. F.; Buckman, A. B.; Walser, R. M.; Lepine, T.; Georges, P.; Brun, A. Appl. Phys. Lett., 1994, 65, 1507-1509.
doi:10.1063/1.112974

25. Mott, N. F. Rev. Modern Phys., 1968, 40, 677-683.
doi:10.1103/RevModPhys.40.677

26. Goodenough, J. B. J. Solid State Chem., 1971, 3, 490-500.
doi:10.1016/0022-4596(71)90091-0

27. Hyland, G. J. Rev. Modern Phys., 1968, 40, 739-743.
doi:10.1103/RevModPhys.40.739

28. Adler, D.; Brooks, H. Phys. Rev., 1967, 155, 826-840.
doi:10.1103/PhysRev.155.826

29. Adler, D.; Feinleib, J.; Brooks, H.; Paul, W. Phys. Rev., 1967, 155, 851-860.
doi:10.1103/PhysRev.155.851

30. Adler, D. Rev. Modern Phys., 1968, 40, 714-736.
doi:10.1103/RevModPhys.40.714

31. Eyert, V. Annalen Der Physik, 2002, 11, 650-702.
doi:10.1002/1521-3889(200210)11:9<650::AID-ANDP650>3.0.CO;2-K

32. Tang, C.; Georgopoulos, P.; Fine, M. E.; Cohen, J. B.; Nygren, M.; Knapp, G. S.; Aldred, A Phys. Rev. B, 1985, 31, 1000-1011.
doi:10.1103/PhysRevB.31.1000

33. Nygren, M.; Israelsson, M. Mater. Res. Bull., 1969, 4, 881-886.
doi:10.1016/0025-5408(69)90044-0

34. Jin, P.; Nakao, S.; Tanemura, S. Thin Solid Films, 1998, 324, 151-158.
doi:10.1016/S0040-6090(98)00362-9

35. Jin, P.; Tanemura, S. Jap. J. Appl. Phys., 1995, 34, 2459-2460.
doi:10.1143/JJAP.34.2459

36. Sobhan, M. A.; Kivaisi, R. T.; Stjerna, B.; Granqvist, C. G. Solar Energy Mater. Solar Cells, 1996, 44, 451-455.
doi:10.1016/S0927-0248(95)00051-8

37. Béteille, F.; Livage, J. J. Sol-Gel Sci. Technol., 1998, 13, 915-921.

38. Takahashi, I.; Hibino, M.; Kudo, T. Jap. J. Appl. Phys., 1996, 35, L438-L440.
doi:10.1143/JJAP.35.L438

39. Béteille, F.; Morineau, R.; Livage, J. Mater. Res. Bull., 1997, 32, 1109-1117.
doi:10.1016/S0025-5408(97)00084-6

40. Lu, S. W.; Hou, L. S.; Gan, F. X. J. Mater. Sci. Lett., 1996, 15, 856-857. doi:10.1007/BF00592709

41. Cavanna, E.; Segaud, J. P.; Livage, J. Mater. Res. Bull., 1999, 34, 167-177. doi:10.1016/S0025-5408(99)00017-3

42. Hanlon, T. J.; Coath, J. A.; Richardson, M. A. Thin Solid Films, 2003, 436, 269-272. doi:10.1016/S0040-6090(03)00602-3

43. Greenberg, C. B. Thin Solid Films, 1983, 110, 73-82. doi:10.1016/0040-6090(83)90175-X

44. Takahashi, I.; Hibino, M.; Tetsuichi, K., Jap. J. Appl. Phys., 2001, 40, 1391-1395. doi:10.1143/JJAP.40.1391

45. Jin, P.; Tanemura, S. Thin Solid Films, 1996, 281-282, 239-242. doi:10.1016/0040-6090(96)08641-5

46. Wu, Z. P.; Miyashita, A.; Yamamoto, S.; Abe, H.; Nashiyama, I.; Narumi, K.; Naramoto, H. J. Appl. Phys., 1999, 86, 5311-5313.

47. Burkhardt, W.; Christmann, T.; Franke, S.; Kriegseis, W.; Meister, D.; Meyer, B. K.; Niessner, W.; Schalch, D.; Scharmann, A. Thin Solid Films, 2002, 402, 226-231. doi:10.1016/S0040-6090(01)01603-0

48. Maruyama, T.; Ikuta, Y; J. Mater. Sci., 1993, 28, 5073-5078. doi:10.1007/BF00361182

49. Case, F. C. J. Vac. Sci. Technol. A, 1984, 2, 1509-1512. doi:10.1116/1.572462

50. Rakotoniaina, J. C.; Mokrani-Tamellin, R.; Gavarri, J. R.; Vacquier, G.; Casalot, A.; Calvarin, G. J. Solid State Chem., 1993, 103, 81-94. doi:10.1006/jssc.1993.1081

51. Guzman, G.; Béteille, F.; Morineau, R.; Livage, J. J. Mater. Chem., 1996, 6, 505-506. doi:10.1039/jm9960600505

52. Hai-Ning Cui, Vasco Teixeira, Li-Jian Meng, Rong Wang, Jin-Yue Gao, Elvira Fortunato, Thin Solid Films 516 (2008) 1484.

53. Takahshi, Y.; Kanamori, M.; Hashimoto, H.; Moritani, Y.; Masuda, Y. J. Mater. Sci., 1989, 24, 192. doi:10.1007/BF00660953

54. Field, M. N.; Parkin, I. P. J. Mater. Chem., 2000, 10, 1863-1866.
doi:10.1039/b002132f

55. MacChesney, J. B.; Potter, J. F.; Guggenheim, H. J. J. Electrochem. Soc. Solid State Sci., 1968, 115, 52-55.

56. Ryabova, L. A.; Serbinov, A.; Darevsky, A. S. J. Electrochem. Soc., 1972, 119, 427-429.
doi:10.1149/1.2404222

57. Sahana, M. B.; Dharmaprakash, M. S.; Shivashankar, S. A. J. Mater. Chem., 2002, 12, 333-338.
doi:10.1039/b106563g

58. Sahana, M. B.; Subbanna, G. N.; Shivashankar, S. A. J. Appl. Phys., 2002, 92, 6495-6504.

59. Barreca, D.; Depero, L. E.; Rizzi, G. A.; Sangaletti, L.; Tondello, E.; Vettori, U. J. Electrochem. Soc., 1999, 146, 551-558.
doi:10.1149/1.1391642

60. Hitchman, M. L. and Jensen, K. F. Chemical Vapor Deposition, Academic Press, New York, 1993.

61. Rees, W. S.; CVD of Non-Metals, VCH, Weinheim, 1996.
doi:10.1002/9783527614813
PMid:AMBIGUOUS (195 citations) PMCid:AMBIGUOUS (20 citations)

62. Manning, T. D.; Parkin, I. P.; Clark, R. J. H.; Sheel, D.; Pemble, M. E.; Vernadou, D. J. Mater. Chem., 2002, 12, 2936-2939.
doi:10.1039/b205427m

63. Manning, T. D.; Parkin, I. P. J. Mater. Chem., 2004, 2554-2559.

64. Manning, T. D.; Parkin, I. P.; Pemble, M. E.; Sheel, D.; Vernardou, D.; Chem. Mater.; 2004; 16(4); 744-749.
doi:10.1021/cm034905y

65. Cross, W. B.; Parkin, I.P. Chem. Comm., 2003, 14, 1696.
doi:10.1039/b303800a
PMid:12877508

66. Binions, R.; Carmalt, C. J.; Parkin, I. P.; Thin Sol. Films, 2004, 469-470, 416.
doi:10.1016/j.tsf.2004.06.178

67. Choy, K.L.; Progr. Mater. Sci., 2003, 48, 57-170.

doi:10.1016/S0079-6425(01)00009-3

68. Piccirillo, C.; Binions, R.; Parkin, I. P.; Chem. Vap. Dep., 2007, 13 (4), 145. doi:10.1002/cvde.200606540

69. Piccirillo, C.; Binions, R.; Parkin, I. P.; Thin Sol. Films, in press.

70. Manning, T.D.; PhD thesis, London, 2004.

71. Piccirillo, C.; Binions, R.; Parkin, I. P.; Europ. J. Inorg. 2007, 25 4050. doi:10.1002/ejic.200700284